

MODIFIED SUBSTITUTE STRUCTURE METHOD FOR
ANALYSIS OF EXISTING R/C STRUCTURES

by

SUMIO YOSHIDA

B. A. Sc., University of British Columbia, 1976

A THESIS SUBMITTED IN PARTIAL FULFILLMENT OF
THE REQUIREMENTS FOR THE DEGREE OF
MASTER OF APPLIED SCIENCE

in

THE FACULTY OF GRADUATE STUDIES
(Department of Civil Engineering)

We accept this thesis as conforming to
the required standard

THE UNIVERSITY OF BRITISH COLUMBIA

March, 1979

© Sumio Yoshida, 1979

In presenting this thesis in partial fulfilment of the requirements for an advanced degree at the University of British Columbia, I agree that the Library shall make it freely available for reference and study. I further agree that permission for extensive copying of this thesis for scholarly purposes may be granted by the Head of my Department or by his representatives. It is understood that copying or publication of this thesis for financial gain shall not be allowed without my written permission.

Department of Civil Engineering

The University of British Columbia
2075 Wesbrook Place
Vancouver, Canada
V6T 1W5

Date March, 1979

ABSTRACT

The modified substitute structure method is developed for the earthquake hazard evaluation of existing reinforced concrete buildings constructed before the most recent advances in seismic design codes. The main characteristic of the proposed method is the use of modified linear analysis for predicting the behaviour, including inelastic response, of existing structures when subjected to a given type and intensity of earthquake motion, represented by a linear response spectrum. The procedure involves an extension of the substitute structure method, which was originally proposed by Shibata and Sozen as a design procedure. With properties and strengths of a structure known, the modified substitute structure method computes ductility demand of each member via an elastic modal analysis, in which reduced flexural stiffness and substitute damping factors are used iteratively. As a result of the analysis, it is possible to describe, in general terms, the location and extent of damage that would occur in a structure subjected to earthquakes of different intensity.

Several reinforced concrete structures of different sizes and strengths were tested by the proposed method and the results compared with a nonlinear dynamic analysis. In general, a small number of iterations was required to obtain an estimate of damage

ratios. The method appears to work well for structures in which yielding is not extensive and widespread. Furthermore, it appears to work better for those in which yielding occurs mainly in beams and the effect of higher modes is not predominant. Though further research is necessary, the modified substitute structure method can constitute an integral part of the rational retrofit procedure.

TABLE OF CONTENTS

	Page
ABSTRACT.....	ii
TABLE OF CONTENTS.....	iv
LIST OF TABLES.....	vii
LIST OF FIGURES.....	ix
ACKNOWLEDGEMENTS.....	xii
CHAPTER	
1. INTRODUCTION	
1.1 Background.....	1
1.2 Literature Survey.....	4
(a) ATC Report.....	4
(b) Okada and Bresler.....	6
(c) Freeman, Nicoletti, and Tyrrell...	9
1.3 Purpose and Scope.....	11
2. SUBSTITUTE STRUCTURE METHOD	
2.1 Modal Analysis.....	14
(a) Equation of Motion.....	14
(b) Periods and Mode Shapes.....	15
(c) Response Spectra.....	16
(d) Modal Forces.....	17
(e) Combination of Forces and Displacements.....	18
2.2 Substitute Structure Method	
(a) Development.....	20
(b) Substitute Structure Method.....	23
(c) Computer Program.....	29

CHAPTER	Page
2.3 Examples and Observations	
(a) Frames with Flexible Beams.....	31
(b) Soft-Story Frame.....	33
(c) 2-Bay, 3-Story Frame.....	35
2.4 Equal-Area Stiffness Method	
(a) Observation.....	37
(b) Equal-Area Stiffness.....	38
(c) Examples.....	39
(d) Area for Further Studies.....	40
3. MODIFIED SUBSTITUTE STRUCTURE METHOD	
3.1 Modified Substitute Structure Method.....	42
3.2 Computer Program.....	51
3.3 Convergence.....	54
3.4 Accelerated Convergence.....	60
4. EXAMPLES	
4.1 Assumptions and Comments.....	65
4.2 Examples	
(a) 2-Bay, 2-Story Frame.....	69
(b) 3-Bay, 3-Story Frame.....	72
(c) 1-Bay, 6-Story Frame.....	76
(d) 3-Bay, 6-Story Frame.....	79
(e) Observations.....	83
5. FACTORS AFFECTING MODIFIED SUBSTITUTE STRUCTURE METHOD	
5.1 Effect of Higher Modes.....	86
5.2 Spectrum.....	91
5.3 Guidelines for Use of Method.....	96

CHAPTER	Page
5.4 Further Studies.....	99
6. CONCLUSION.....	101
BIBLIOGRAPHY.....	167
APPENDIX	
A. Modification of Damage Ratio - Strain Hardening Case.....	169
B. Computer Program.....	173

LIST OF TABLES

Table		Page
2.1	Natural Periods and Smeared Damping Ratios for 3-, 5-, and 10-Story Frames.....	103
2.2	Computed Damage Ratios for 3-, 5-, and 10-Story Frames.....	104
2.3	Comparison of Damage Ratios for 3-, 5-, and 10-Story Frames.....	105
2.4	Computed Natural Periods for 3-, 5-, and 10-Story Frames.....	106
3.1	Natural Periods for 2-Bay, 3-Story Frame A.....	106
3.2	Damage Ratios for 2-Bay, 3-Story Frame A.....	107
3.3	Natural Periods for 2-Bay, 3-Story Frame B.....	108
3.4	Number of Iterations - 2-Bay, 3-Story Frame B....	108
3.5	Damage Ratios for 2-Bay, 3-Story Frame B.....	109
4.1	Natural Periods for 2-Bay, 2-Story Frame.....	109
4.2	Displacements for 2-Bay, 2-Story Frame.....	110
4.3	Natural Periods for 3-Bay, 3-Story Frame.....	110
4.4	Displacements for 3-Bay, 3-Story Frame.....	110
4.5	Natural Periods for 1-Bay, 6-Story Frame.....	111
4.6	Displacements for 1-Bay, 6-Story Frame.....	111
4.7	Natural Periods for 3-Bay, 6-Story Frame.....	111
4.8	Displacements for 3-Bay, 6-Story Frame.....	112
5.1	Natural Periods for 3-Bay, 6-Story Frame A - Spectrum B.....	112
5.2	Displacements for 3-Bay, 6-Story Frame A - Spectrum B.....	112

Table		Page
5.3	Natural Periods for 3-Bay, 6-Story Frame B - Spectrum B.....	113
5.4	Displacements for 3-Bay, 6-Story Frame B - Spectrum B.....	113
5.5	Natural Periods for 3-Bay, 6-Story Frame B - Spectrum A.....	113
5.6	Displacements for 3-Bay, 6-Story Frame B - Spectrum A.....	114
5.7	Natural Periods for 3-Bay, 6-Story Frame B - El Centro EW Spectrum and Taft S69E Spectrum.....	114
5.8	Displacements for 3-Bay, 6-Story Frame B - El Centro EW Spectrum.....	115
5.9	Displacements for 3-Bay, 6-Story Frame B - Taft S69E Spectrum.....	115
5.10	Natural Periods for 3-Bay, 6-Story Frame A - El Centro EW Spectrum and Taft S69E Spectrum.....	116
5.11	Displacements for 3-Bay, 6-Story Frame A - El Centro EW Spectrum.....	116
5.12	Displacements for 3-Bay, 6-Story Frame A - Taft S69E Spectrum.....	117

LIST OF FIGURES

Figure		Page
1.1	Load-Deflection Curve for Elastic and Elastoplastic Structure.....	118
2.1	Idealized Hysteresis Loop for Reinforced Concrete System.....	118
2.2	Force-Displacement Curve - Definition of Damage Ratio.....	119
2.3	Flow Diagram for Substitute Structure Method.....	120
2.4	Member Properties and Design Moments for 3-, 5-, 10-Story Frames.....	123
2.5	Smoothed Response Spectrum - Design Spectrum A...	124
2.6	Soft Story Frame A - Member Properties and Yield Moments.....	125
2.7	Soft Story Frame A - Damage Ratios for Individual Earthquakes.....	126
2.8	Soft Story Frame B - Member Properties and Yield Moments.....	127
2.9	Soft Story Frame B - Damage Ratios for Individual Earthquakes.....	128
2.10	2-Bay, 3-Story Frame - Member Properties and Yield Moments.....	129
2.11	2-Bay, 3-Story Frame - Damage Ratios for Individual Earthquakes.....	130
2.12	Force-Displacement Curve - Definition of Equal-Area Stiffness.....	131
3.1	Moment-Rotation Curve - Modification of Damage Ratio.....	132

Figure		Page
3.2	Flow Diagram for Modified Substitute Structure Method.....	133
3.3	2-Bay, 3-Story Frame A - Member Properties and Yield Moments.....	136
3.4	2-Bay, 3-Story Frame A - Plot of Periods vs. Number of Iterations.....	137
3.5	2-Bay, 3-Story Frame A - Plot of Damage Ratios vs. Number of Iterations.....	138
3.6	2-Bay, 3-Story Frame B - Member Properties and Yield Moments.....	139
3.7	2-Bay, 3-Story Frame B - Plot of Periods vs. Number of Iterations.....	140
3.8	2-Bay, 3-Story Frame B - Damage Ratios Computed at the End of 4, 12, 20, and 200 Iterations.....	141
3.9	2-Bay, 3-Story Frame B - Plot of Damage Ratios vs. Number of Iterations.....	142
4.1	2-Bay, 2-Story Frame - Member Properties and Yield Moments.....	143
4.2	2-Bay, 2-Story Frame - Damage Ratios.....	143
4.3	2-Bay, 2-Story Frame - Damage Ratios for Individual Earthquakes.....	144
4.4	3-Bay, 3-Story Frame - Member Properties and Yield Moments.....	145
4.5	3-Bay, 3-Story Frame - Damage Ratios.....	146
4.6	3-Bay, 3-Story Frame - Damage Ratios for Individual Earthquakes.....	147

Figure		Page
4.7	1-Bay, 6-Story Frame - Member Properties and Yield Moments.....	148
4.8	1-Bay, 6-Story Frame - Damage Ratios.....	149
4.9	1-Bay, 6-Story Frame - Damage Ratios for Individual Earthquakes.....	150
4.10	3-Bay, 6-Story Frame - Member Properties and Yield Moments.....	151
4.11	3-Bay, 6-Story Frame - Damage Ratios.....	152
4.12	3-Bay, 6-Story Frame - Damage Ratios for Individual Earthquakes.....	153
5.1	Smoothed Response Spectrum - Design Spectrum B...	154
5.2	3-Bay, 6-Story Frame A - Damage Ratios.....	155
5.3	3-Bay, 6-Story Frame A - Plot of Damage Ratios for Beams in the Exterior Bay.....	156
5.4	3-Bay, 6-Story Frame B - Damage Ratios.....	157
5.5	3-Bay, 6-Story Frame B - Plot of Damage Ratios for Beams in the Exterior Bay.....	158
5.6	3-Bay, 6-Story Frame B - Damage Ratios.....	159
5.7	3-Bay, 6-Story Frame B - Damage Ratios for Individual Earthquakes.....	160
5.8	El Centro EW Spectrum and Design Spectrum A.....	161
5.9	Taft S69E Spectrum and Design Spectrum A.....	162
5.10	3-Bay, 6-Story Frame B - Damage Ratios.....	163
5.11	3-Bay, 6-Story Frame B - Damage Ratios.....	164
5.12	3-Bay, 6-Story Frame A - Damage Ratios.....	165
5.13	3-Bay, 6-Story Frame A - Damage Ratios.....	166
A.1	Moment-Rotation Curve.....	172

ACKNOWLEDGEMENTS

The author wishes to express his sincere gratitude to his supervisors, Dr. N. D. Nathan, Dr. D. L. Anderson, and Dr. S. Cherry for their advice and guidance during the research and preparation of this thesis. Thanks are also due to Mr. R. Grigg, the Civil Engineering Department program librarian, for his advice and assistance.

The financial support of the National Research Council of Canada in the form of Postgraduate Scholarship is gratefully acknowledged.

March, 1979

Vancouver, British Columbia

CHAPTER 1 INTRODUCTION

1.1 Background

During the last two decades a great deal of progress has been made in understanding the behaviour of buildings during major earthquake motions. The new knowledge resulting from research and observation has been incorporated in building codes. It is not reasonable to expect the majority of newly designed buildings to be able to survive a major earthquake motion with tolerable damage.

Unfortunately, in any large city there exist many buildings which were designed and constructed before the recent advances in seismic codes. The performance of these buildings are at best uncertain if and when a sizable earthquake strikes the area. The city authorities must assess the seismic risks involved in such buildings from time to time. This point arises most often when an owner of an old building wishes to change the occupancy or do a structural alteration. Before issuing a new building permit, the authorities must make a decision on how well it complies with current codes. Unless the building is judged to be safe, they must decide on the modifications that have to be made in order to upgrade it to a satisfactory level. Upon their recommendations the owner can decide whether it is feasible to

carry on with his plan or whether it is more economical to replace the building with a new one.

It is, therefore, necessary to develop a methodology to screen and evaluate existing buildings against seismic hazards. Many issues are involved here, but the most difficult one is how to assess the degree of compliance with the current seismic codes. It is appropriate here to describe briefly the philosophy behind the current codes, which should be borne in mind when the evaluation of existing buildings is discussed later.

The current code procedure for the design of new buildings is based on the assumption that a structure will yield in a major earthquake, but that its ultimate displacement will be approximately equal to the displacement of the same structure if it remained elastic during the earthquake as illustrated in Fig. 1.1. It should be noted that the stiffness of the structure is usually predetermined by the layout and the design for gravity loads. The combination of ductility and strength must be chosen such that the structure reaches its maximum load-maximum displacement relationship with only a tolerable level of damage.

The code, such as the National Building Code of Canada,¹ achieves this combination of strength and ductility by estimating the available ductility for the particular structural system selected for the design of the building, and the load level is set accordingly. Thus a ductile system may be designed for a lower load level than a more brittle system. The code also specifies the detailed design requirements to ensure that this ductile failure mode occurs before the brittle failure

modes associated with shear, bond or detail failure.

The code actually gives a quasi-static force such that the structure is satisfactory if it can resist that force, provided that it is detailed properly to ensure the anticipated ductility and that it is also detailed correctly to ensure the desirable flexure failure mode.

It should now be clear that without the philosophy described above the code static force is meaningless. It is not the actual force which a structure is expected to receive during a major earthquake if it is designed and detailed differently from the current codes. The existing buildings were obviously designed with a different philosophy from the one implied in the current codes, and merely applying the quasi-static load is a questionable approach.

The best way to analyze existing buildings is to subject them to a nonlinear time-step analysis. Recent advances in computer technology have made this approach possible. But the cost involved in such analysis is still prohibitively high and it requires very accurate modelling of the entire structure. The high cost and tediousness make this analysis impractical except in very few cases.

Several proposals have been made to find a more practical way to treat the problem of analyzing the existing buildings, which is becoming known by the somewhat infelicitious term, "retrofit."

1.2 Literature Survey

The literature survey in this section is intended to be an introduction to the approaches that must be followed in order to identify the potentially hazardous buildings and to estimate an extent of hazards and an associated damage. Three papers are discussed.

(a) ATC Report

The Applied Technology Council in the United States made a first attempt at a comprehensive procedure for the seismic hazard evaluation of existing buildings.² The relevant section of ATC III, the report of the council, is briefly discussed here.

ATC III points out that there are probably thousands of buildings in the United States which are potentially earthquake hazardous. Since a thorough study of all buildings is economically impossible, they suggest a graduated procedure. They are,

- (1) Selection to identify potentially hazardous buildings
- (2) Evaluation to establish the possible extent of hazards
- (3) Correction to ensure the elimination of unacceptable hazards.

The first step is to screen the potentially hazardous buildings. The seismic hazard is related to the severity of the ground motion and the usage of buildings. The severity of the ground motion is indicated by the Seismic Hazard Index SHI correlated with ground motion. SHI ranges from 1 to 4, with the higher number indicating greater severity. The usage of

the buildings is indexed by the Seismic Hazard Exposure Group SHE. SHE ranges from I to III, with the higher number indicating less usage.

The buildings in the area where the Seismic Hazard Index is less than or equal to 3 are excluded from analysis. In the area where SHI is 4, the newer buildings and SHE-II and SHE-III buildings with low occupancy are also exempt. The buildings with historical values are subjected to the alternate procedure.

The evaluation procedure may be qualitative or quantitative. A qualitative evaluation is required for SHE-II and -III groups. The procedure is prescribed in the report. It involves a judgement on the adequacy of the primary structural system and nonstructural elements, and it can be carried out very rapidly.

SHE-I buildings and those judged uncertain in the previous analysis are subject to more thorough analytical studies. The aseismic design procedure for new constructions are stipulated. The procedure involves the determination of an earthquake capacity ratio, R_c , which is a ratio of actual lateral seismic force capacity of an existing system or element to the capacity required to meet the prevailing seismic code provisions for the design of new buildings. The occupancy potential are also used to assess building hazards.

The total lateral seismic force is distributed over the building height and the resulting applied member moment, shear, and axial forces are evaluated at particular sections. The member capacities can be calculated from the known section and material properties. The earthquake capacity ratio is computed by dividing the section capacity available for earthquake loading

by the seismically induced load. The ratios are computed for moments, shear, axial forces, and drift. The smallest ratio governs the earthquake capacity of the building. In the author's opinion, a distinction should be made in failure modes. A failure in bending is much more preferable to a failure in shear and it is not proper to treat them equally in choosing the governing earthquake capacity ratio.

Unless the earthquake capacity ratio is greater than or equal to one, there is a hazard which is a function of the building and the occupancy potential. ATC sets the minimum acceptable earthquake capacity ratios and those which fail to meet the requirements must be strengthened or demolished according to the schedule outlined in the report.

(b) Okada and Bresler

Okada and Bresler in "Strength and Ductility Evaluation of Existing Low-Rise Reinforced Concrete Buildings - Screening Method"³ describes a procedure for evaluating the seismic safety of low-rise reinforced concrete structures. Their method consists of series of steps which are repeated in successive cycles with more refined modeling. Each cycle represents a "screening". Three screening cycles are proposed and the first screening cycle, the first execution of the basic procedure, is described in detail in their paper. It also shows how this procedure can be applied to existing school buildings.

The first screening is based on approximate evaluation of the load-deflection characteristics of the first or weakest story. The second involves a more precise estimate of overall

structural behaviour, and in the third screening nonlinearity of each member is modeled.

In describing the first screening procedure, the authors point out that the criteria which define the permissible damage resulting from a specified earthquake are the most important factors which determine structural adequacy. Two grades of earthquake motions and two corresponding degrees of building damage are chosen. Three types of failure modes, bending, shear and shear bending are considered.

The procedure consists of five major steps, namely,

- (1) structural modeling
- (2) analytical modeling
- (3) strength safety evaluation
- (4) ductility safety evaluation
- (5) synthesis evaluation of safety.

The structural modeling is initiated by identifying the load transmission system of the building from examining drawings, design calculations and field investigations. The main items to be determined are structural system, load intensity, properties of materials, design method, and other special structural features. Several models may have to be considered.

The analytical modeling is done to evaluate structural response under lateral forces. The shear cracking strength, C_{sc1} , ultimate shear strength, C_{su1} , and bending strength, C_{by1} , in terms of base shear coefficients are computed. The comparison of the three identifies the type of failure. The strength is evaluated with respect to shear cracking, ultimate shear strength, and bending strength. The capacity with respect to

each of these three failure modes and their relative values are weighed heavily in evaluating the structure. The fundamental period and the modal participation factor are computed in an approximate manner.

The strength safety evaluation determines the adequacy of lateral strength. For this purpose a linear earthquake response analysis is used with a standardized response spectrum. In calculating the linear response in terms of base shear coefficient, C_E , the building assumed to be a story-level-lumped-mass system with the number of stories equal to the number of degrees of freedom. Only the first mode shape is considered.

The ductility safety evaluation estimates the first story displacement using nonlinear displacement response spectra and modified modal participation factor to idealize the nonlinear behaviour of the building. The response ductility of the building, which is modeled as the equivalent one-mass system, is compared with the specified limit value.

The final step is the synthesis evaluation of safety. The assumptions and unknowns incorporated into the screening process and the need for modification of the existing building are carefully analyzed. Those buildings which failed to pass the first screening are classified uncertain and must go through the second and subsequent screening procedure.

The procedure set forth by Okada and Bresler represents a rational approach to the problem of evaluating existing buildings, and the present method of analysis could be fitted into their screening process.

(c) Freeman, Nicoletti, and Tyrrell

The procedure described in "Evaluation of Existing Buildings for Seismic Risk -- A Case Study of Puget Sound Naval Shipyard, Bremerton, Washington," by Freeman et al.⁴ is intended to fill the gap between statistical procedures for large areas, and detailed structural dynamic analysis of individual buildings. Its main feature is a very rapid screening process and a simple analysis with minimum of calculation. The structure at the Puget Sound Naval Shipyard at Bremerton, Washington, was studied and the findings were reported. A total of 96 buildings of different size, age, materials, type of construction and occupancy is evaluated for the overall vulnerability to earthquake damage.

The study is performed in six phases, namely,

- (1) a visual survey of 96 buildings
- (2) investigation of two representative buildings
- (3) determination of the seismicity of the area
- (4) estimation of probable damage for 80 buildings
- (5) detailed investigation of five critical buildings
- (6) estimation of the average annual costs of expected earthquake damage for 40 buildings.

Phases (1) to (3) need little explanation. The findings in the second phase are used for the next phases of study. In the third phase response acceleration spectra are constructed from the seismic records in the area and are used for the phase four of the study.

The fourth phase is the most relevant to this report. In analyzing the structures emphasis was placed on minimization of the man-hours spent. The lateral force strength capacities were

roughly approximated and the non-structural materials were also looked at. The base shear capacities were used to establish the yield limit and the ultimate limit. The former is defined as the base shear represented by the force required to reach the capacity of the most rigid lateral force-resisting system. The latter is defined as the base shear required to cause the most flexible lateral force-resisting system to yield after the collapse or yield of the more rigid ones. These were converted to spectral acceleration capacities by dividing by the weight of structure. The dynamic response characteristics and the periods were estimated by approximate methods.

Assumptions were made to simplify the evaluation of damage. The damage level was assumed to vary linearly from 0% at yield limit to 100% at the ultimate limit. In the inelastic range nonlinear effects were taken into account by linearly varying the damping between the two limits. The procedure used for estimating damage was based on reconciliation of the demand spectral acceleration and the capacity of the structure in relation to periods and damping. A graphical solution for estimating percentage damage was developed. The analysis was done in two directions and a weighted average was computed.

Sets of response spectra were chosen to represent the earthquake motions with different return periods. From the damage levels associated with those return periods the annual costs were computed for the 80 buildings.

The authors claim that the result of the procedure can be used to decide which buildings are most susceptible to earthquake damage and that the effects of modification on existing structures can be found.

1.3 Purpose and Scope

The three papers discussed in the previous section illustrate the type of approach that must be taken in order to analyze a large number of existing buildings which are potential seismic hazards. They all set up screening procedures to select potentially hazardous buildings and then subject them to seismic analysis. It is beyond the scope of this thesis to comment on the screening procedure; the structural analysis, however, deserves a few comments.

The ATC-III report² suggests the use of the quasi-static seismic forces in the current codes for the analysis. As was explained in the first section of this chapter, these forces are meaningless unless the structures were designed with the ductile properties and the proper detailing implied by the code recommendations. Even if a structure can carry only a fraction of the quasi-static forces, collapse or major damage may not occur, because in actual earthquakes the forces will be redistributed and the building will respond differently depending on its ductile properties.

Bresler's methods³ takes nonlinearity into account by modelling the structure as a one-mass system and through the use of nonlinear response spectra. The analysis is intended for low-rise structures and, for this purpose, the assumptions and simplifications that the authors made are satisfactory. An extension of the method to the analysis of medium- to high-rise buildings will, however, involve major modifications to their method.

Freeman's method⁴ is at best approximate. Their approach to inclusion of nonlinearity in their analysis has many assumptions and simplifications. The method is probably effective for screening many one- to two-story, single-bay buildings, but the extension of this method to larger buildings is of questionable value.

It is clear that a procedure for analysis of existing buildings against seismic hazards must be developed, especially for those buildings which are judged uncertain after the initial screening process. The procedure must be capable of handling medium- to high-rise structures without major assumptions and simplifications. It is desirable that different earthquake motions can be used to obtain a good estimate of behaviour of the structure and that the analysis should include the effects of nonlinearity after the yield of some of the members. At the same time the procedure must be simple and reasonably economical to use.

Such a procedure is developed and described in the subsequent chapters. The modified substitute structure method is intended to fill the gap between simplified structural analysis and the full-scale, nonlinear time-step analysis. The proposed method is suitable for reinforced concrete frame structures, but it is hoped that it can be used for shear-wall type buildings and steel structures. The procedure is a modified elastic modal analysis, which is developed from a design concept proposed by Shibata and Sozen.⁵

The design procedure proposed by Shibata and Sozen⁵ is described first in order to discuss the theory and assumptions

which are essential in understanding the proposed method. A brief discussion modal analysis is included. Examples of the design procedure are also presented. An alternate approach is described and the findings are discussed.

Then the modified substitute structure method is presented in the next chapter. The theory behind this procedure is discussed as well as the development of the computer program. Since it is an iterative procedure, convergence criteria are discussed. A method to achieve faster convergence is introduced.

In order to test the validity of the modified substitute structure method, frames of different type and height are analyzed. A comparison of results with those of nonlinear dynamic analysis is presented. All the assumptions are presented and described in this section.

In the final chapter factors which affect the results of the analysis are discussed, and a preliminary guideline is presented for successful applications of the method. The areas where further research is necessary are mentioned.

CHAPTER 2 SUBSTITUTE STRUCTURE METHOD

2.1 Modal Analysis

Modal analysis is an approximate dynamic analysis to solve the response of a multi-degrees-of-freedom system to a given earthquake motion. Although it is intended for analysis of elastic systems, a thorough knowledge of this method is essential for the discussion of the subsequent sections. Since it is not the intention of this paper to explain the dynamics of structures subjected to the earthquake motion, the discussion is kept very brief. The subject is covered in Clough and Penzien.⁶

(a) Equation of Motion

The basic equation of motion for a multi-degrees-of-freedom system is given by

$$[m](\ddot{u}) + [c](\dot{u}) + [k](u) = -\ddot{x}[m](I) \quad (2.1)$$

where $[m]$ = mass matrix
 $[c]$ = damping matrix
 $[k]$ = stiffness matrix
 (\ddot{u}) , (\dot{u}) , (u) = acceleration, velocity, and
displacement corresponding
to each degree of freedom.

\ddot{x} = ground acceleration

(I) = identity vector where every entry
is a unity

The mass of the system is usually lumped at the nodes for simplicity in computation. If such an assumption is made, the mass matrix becomes diagonal.

Discussion of the damping matrix is beyond the scope of this paper. Modal analysis does not require an evaluation of this matrix, although the damping value in each mode is required for synthesis of the results.

The stiffness matrix is formed by assembling the member stiffness matrices. The procedure is identical to that of frame analysis. The full member matrix with three degrees of freedom at each member end is 6×6 . If only bending deformation is of interest, its size is reduced to 4×4 .

(b) Periods and Mode Shapes

Solution of the free, undamped system yields mode shapes and natural frequencies. The equation of motion becomes,

$$[m](\ddot{u}) + [k](u) = (0) \quad (2.2)$$

The solution to this equation is of the form,

$$(u) = (A) \sin \omega t \quad (2.3)$$

with $(\ddot{u}) = -\omega^2(A) \sin \omega t \quad (2.4)$

Substitute equations (2.3) and (2.4) into (2.2),

$$-\omega^2 [m] (A) + [k] (A) = (0) \quad (2.5)$$

For a nontrivial solution,

$$|[k] - \omega^2 [m]| = 0 \quad (2.6)$$

This is an eigenvalue problem of the form,

$$[B] = \lambda [C] \quad (2.7)$$

in which $[B]$ is a symmetric, banded matrix and $[C]$ is a diagonal matrix. Eigenvalues associated with equation (2.6) correspond to the squares of the angular frequencies, ω^2 . Associated eigenvectors correspond to the mode shapes. If n is the rank of the mass matrix, $[m]$, there are n natural frequencies and n mode shapes.

(c) Response Spectra

Given an earthquake record, it is relatively simple to compute the response spectra. The peak acceleration, velocity, or displacement of a single-degree-of-freedom system with a given value can be determined from the response spectra. In the modal analysis of multi-degree-of-freedom systems, with the assumption that a damping ratio for each mode is known, a peak response for each mode can be read from the response spectra when natural periods are known. When a damping ratio is small,

with little error the peak acceleration, velocity, and displacement are related in the following manner,⁷

$$S_v = \frac{1}{\omega} S_a \quad (2.8)$$

$$S_d = \frac{1}{\omega} S_v = \frac{1}{\omega^2} S_a \quad (2.9)$$

Where S_a = peak acceleration corresponding to the natural frequency, ω .

S_v = peak velocity

S_d = peak displacement.

The choice of a damping ratio leaves some room for a debate. It is generally taken to be 5 to 10% of critical for concrete and 2 to 5% of critical for steel.

Strictly speaking, the response spectra are valid for one earthquake of known peak ground acceleration, but they can be scaled up or down depending on the peak ground acceleration which is appropriate for a particular site with certain assumptions on magnitude and probability of occurrence.

(d) Modal Forces

Suppose that the acceleration spectrum is given and that the damping ratios for all the modes are known or estimated; then, it is relatively simple to set up a force vector corresponding to each mode. Modal participation factors, α , must first be computed. Let r denote the r th mode and T the transpose of a vector. The modal participation factor for the r th mode can be computed as follows,

$$\alpha_r = \frac{(A^r)^T [m] (I)}{(A^r)^T [m] (A^r)} \quad (2.10)$$

where (A^r) = a vector representing the mode shape for the r th mode

$[m]$ = mass matrix

(I) = identity vector whose elements are all unity.

Then the force vector for the r th mode becomes

$$(F^r) = (A^r) \alpha_r S_a^r [m] \quad (2.11)$$

where (F^r) = force vector

S_a^r = peak acceleration corresponding to r th mode natural frequency and damping.

The modal displacements and response forces can be computed in the identical manner to that used in the stiffness method in a plane frame analysis. That is,

$$(F^r) = [k] (\Delta^r) \quad (2.12)$$

where $[k]$ = structure stiffness matrix

(Δ^r) = modal displacements in global coordinates.

With (F^r) known, (Δ^r) can be computed by simply inverting the stiffness matrix, $[k]$. The member forces can be calculated from the displacement vector, (Δ^r) .

(e) Combination of Forces and Displacements

These forces and displacements for each mode correspond to the peak response. It is not likely that these individual maxima

occur at the same time; therefore, summing up the absolute values of these forces and displacements may result in over-estimating the response. It is found that the root-sum-square (RSS) approach gives a more reasonable estimate. The individual modal responses are combined by taking the square root of the sum of the squares of the responses.

Contributions from the higher modes diminish very rapidly. For this reason it is usually sufficient to take the first three or four modes for computation. For low-rise structures only the first mode is sufficient for all the practical purposes. For high-rise structures higher modes play more dominant roles, and, hence, cannot be neglected.

2.2 Substitute Structure Method

(a) Development

Gulkan and Sozen performed a series of experiments to test the response of reinforced concrete structures to seismic motions.⁸ The tests were restricted to the single-degree-of-freedom system. They found that the basic characteristics of reinforced concrete structure which determine the response to earthquakes are a change in stiffness and a change in energy dissipation capacity, both of which are related to the maximum displacement. During strong motions the stiffness of reinforced concrete decreases because of cracking of concrete, spalling of concrete, and slipping and reduction in effective modulus of steel. The result of this is that the period of the structure increases as it undergoes inelastic deformation. The area within a cycle of the force-displacement curve is a measure of the energy dissipated by the system. They found that the area within the hysteretic loop increases with increase in displacement into the inelastic range of response.

The effect of the hysteresis loop and the change in stiffness is said to lead to a quantitative relationship between linear response analysis and inelastic analysis. A concept of substitute damping and effective stiffness are then introduced in order to interpret the inelastic response in terms of a linear response analysis, using a spectral response curve.

Consider an idealized symmetrical hysteresis loop as shown in Fig. 2.1. It follows Takeda's hysteresis loop which was used as an analytical model in the experiment by Takeda et al.⁹

It is assumed that the structure has already undergone several cycles of inelastic deformation. Let γ be the original stiffness; then the slope of the unloading curve BC, is $\gamma \left(\frac{1}{\eta}\right)^a$ where η is the ductility and a is a constant. The shape of the hysteresis curve is such that it is approximately represented by a linearly vibrating system with equivalent viscous damping.¹⁰ It is assumed that the energy input is entirely dissipated by an imaginary viscous damper associated with the horizontal velocity of the mass. Using this idea, the substitute damping ratio, β_s is given by,

$$\beta_s \quad 2m\omega_o \int_0^T (\dot{u})^2 dt = -m \int_0^T \ddot{x} \dot{u} dt \quad (2.13)$$

where m = mass
 \dot{u} = velocity
 \ddot{x} = ground acceleration
 T = period of vibration
 $\omega_o^2 = \frac{\text{measured absolute acceleration}}{\text{measured absolute displacement}}$

The left-hand side of the equation represents the energy dissipated per cycle and the right-hand side represents the energy input per cycle. On the hysteresis loop diagram it can be seen that

$$\beta_s \propto \frac{\text{area EBC}}{\text{area ABF}} = \frac{1/2 (\text{hysteresis loop area})}{1/2 (\text{energy input})} \quad (2.14)$$

a is taken as 0.5, then it can be shown that

$$\beta_s \propto (1 - 1/\sqrt{\eta}) \quad (2.15)$$

where η = ductility.

From the experimental data Gulkan and Sozen⁸ gave the following expression for the substitute damping ratio, β_s ,

$$\beta_s = [1 + 10(1 - 1/\sqrt{\eta})]/50 \quad (2.16)$$

It is assumed in equation (2.16) that β_s has a threshold value of 0.02 at $\eta=1.0$. The slope of the line AB is the effective stiffness and is equal to γ/η . The natural period corresponding to the effective stiffness is $T\sqrt{\eta}$.

Gulkan and Sozen⁸ proposed a design procedure for a reinforced concrete structure which can be idealized as a single-degree-of-freedom system. The design base shear can be calculated as follows:

- (1) assume an admissible value of ductility, η ,
- (2) calculate the stiffness based on the cracked section,
- (3) determine the natural period, T ,
- (4) calculate the substitute damping ratio, β_s , corresponding to the assumed value of ductility, η ,
- (5) obtain base shear and maximum displacement by entering a spectral response diagram with an increased natural period of $T\sqrt{\eta}$ and a damping ratio equal to β_s .

Even though this design procedure is intended for a single-degree-of-freedom system, the basic concepts are directly transferred to the substitute structure method, which is a design method for multi-story reinforced concrete frames.

(b) Substitute Structure Method

The substitute structure method was conceived by Shbata and Sozen.⁵ It is an extension of the method by Gulkan and Sozen⁸ which was described in the previous section. The method is intended for multi-story reinforced concrete frames and is a design procedure to establish the minimum strengths that the components must have so that a tolerable response displacement is not likely to be exceeded. The main characteristics of the substitute structure method are the definition of a substitute frame, which is a fictitious frame with its stiffness and damping differing from the actual frame, and the calculation of the design forces from modal analysis of the substitute frame using a linear response spectrum. These characteristics are chosen such that the forces and the deformations from the analysis agree with these from the nonlinear dynamic analysis.

Shibata and Sozen⁵ list the following conditions which must be satisfied in order to use the substitute structure method.

- (1) The system can be analyzed in one vertical plane.
- (2) There are no abrupt changes in geometry or mass along the height of the system.
- (3) Columns, beams and walls may be designed with different limits of inelastic response, but the limit should be the same for all beams in a given bay and all columns on a given axis.
- (4) All structural elements and joints are reinforced to avoid significant strength decay as a result of repeated reversals of the anticipated inelastic displacements.
- (5) Nonstructural components do not interfere with structural response.

The first condition implies that the method is subject to the limitations of plane frame analysis. Such effects as torsion and biaxial bending must be neglected. The second condition restricts the use of this method to structures of regular shapes with uniform distribution of mass and stiffness. The third condition deserves the most attention. The fact that the beams and columns may have different inelastic deformation limits is a big step forward from the conventional method in which the ductility of the entire structure must be chosen to be uniform. This point is perhaps the biggest advantage in using the substitute structure method. It is usually desirable to allow the beams to yield and absorb the bulk of energy while the columns remain elastic. The third condition does, however, exclude the possibility that this method may be used for the design of soft story frames. The conditions (4) and (5) need little explanation.

Before the design procedure is presented, terms particular to this method must be explained. As mentioned previously, a substitute frame is a fictitious frame with its stiffness and damping related but not identical to the actual frame. A damage ratio, μ , is used instead of ductility, η . Consider a force-displacement curve or a moment-rotation curve as in Fig. 2.2. Ductility is usually defined as the ratio of ultimate displacement to yield displacement, or

$$\eta = \frac{\Delta u}{\Delta_y} \quad (2.17)$$

The damage ratio on the other hand is the ratio of the initial stiffness of the substitute frame, or

$$\mu = \frac{\text{slope AB}}{\text{slope AC}} \quad (2.18)$$

They are identical for the elasto-plastic case, but if the stiffness after yield has a positive slope, the damage ratio is always smaller than ductility. Suppose s is the ratio of the stiffness after yield to the initial stiffness; that is, the ratio of the slope of BC to the slope of AB in Fig. 2.2. Then the relation between the damage ratio and ductility is

$$\mu = \frac{\eta}{1 + (\eta - 1)s} \quad (2.19)$$

where μ = damage ratio

η = ductility

s = ratio of stiffness after yield to initial stiffness

A substitute damping ratio is defined and computed in an identical manner to that described in the previous section. The damage ratio, however, is used instead of ductility; hence,

$$\beta_s = 0.2(1 - 1/\sqrt{\mu}) + 0.02 \quad (2.20)$$

where β_s = substitute damping ratio

μ = damage ratio.

The design procedure will now be described. A necessary assumption is that the preliminary member sizes of the actual structure are known from gravity loads and other functional requirements. Then the following steps are involved.

- (1) Assume an acceptable value of damage ratio, μ , for each group of members.

- (2) Define the flexural stiffness of substitute-frame elements as

$$(EI)_{si} = \frac{(EI)_{ai}}{\mu_i} \quad (2.21)$$

where $(EI)_{si}$ = flexural stiffness of i th substitute-frame element

$(EI)_{ai}$ = flexural stiffness of i th element in the actual frame

μ_i = tolerable damage ratio for i th element.

- (3) Compute natural periods, mode shapes and modal forces for the undamped substitute structure.
- (4) Compute an average or a "smeared" damping ratio for each mode.

$$\beta_{si} = 0.2(1 - 1/\sqrt{\mu_i}) + 0.02 \quad (2.22)$$

$$\beta_m = \sum_i \frac{P_i}{\sum_i P_i} \beta_{si} \quad (2.23)$$

where $P_i = \frac{L_i}{6(EI)_{si}} (M_{ai}^2 + M_{bi}^2 + M_{ai}M_{bi})$ (2.24)

and β_{si} = substitute damping ratio of i th member

β_m = smeared substitute damping for m th mode

P_i = flexural strain energy in i th element in the m th mode

L_i = length of frame element i

$(EI)_{si}$ = assumed stiffness of substitute frame element i

M_{ai}, M_{bi} = end moments of substitute frame element i
for m th mode.

- (5) Repeat the modal analysis using the smeared damping ratios and compute the root-sum-square (RSS) forces.
- (6) Compute the design forces,

$$F_i = F_{i \text{ rss}} \frac{v_{\text{rss}} + v_{\text{abs}}}{2v_{\text{rss}}}$$

where F_i = design force for i th element
 $F_{i \text{ rss}}$ = root-sum-square forces for i th element
 v_{rss} = RSS base shear
 v_{abs} = maximum value for absolute sum of any two
of the modal base shears.

- (7) To avoid the risk of excessive inelastic action in the columns increase the design moments of the columns by 20%.

In the first step a designer can choose how much inelastic deformation can be allowed in each element group. Since the target damage ratios are always greater than or equal to one, it is clear in the second step that the natural periods of the substitute frame are always greater than these of the actual frame. Steps 3 and 4 are necessary, because substitute damping ratios may be different for each element group. A smeared damping ratio is computed for each mode by assuming that each element contributes to modal damping in proportion to its relative flexural strain energy associated with the mode shape. Elements with complex stiffness can be used to compute the smeared damping ratios, but the flexural energy approach is easier to use and has more physical meaning. The sixth step is an extra factor of

safety in case any combination of two modes produces undesirable results. The last step is desirable in a design procedure, because failure in a column prior to failure in adjoining beams may lead to catastrophic failure of a structure. A linear response spectrum is used in the analysis; the authors suggest that a smoothed spectrum be used. It is mentioned as a critical feature of this method that it becomes plausible only with the understanding that the force response decreases as the structure becomes more flexible; therefore, the smoothed spectrum, in relation to the natural periods of the substitute structure, should have a shape such that the spectral acceleration response decreases with an increase in period.

Implicit assumptions and limitation of the substitute structure method are now discussed. It is implicitly assumed that the moment distribution in all the members are linear and that the points of inflection are placed at or near the mid-points of the member spans. With these assumptions, it becomes clear that the shape of force-displacement curve is identical to that of the moment-rotation curve. Otherwise dividing the actual flexural stiffness by the damage ratio greater than one may not be a correct approach. These assumptions are reasonable in beams which are more likely to receive inelastic deformations, but they may not be so valid in columns as shown by Blume et al.¹¹ This point, however, is not an important factor as long as columns are designed with a target damage ratio of one, which is desirable in most practical applications.

In practice, unless the design moments are known, the stiffness of a fully cracked section that must be used to

calculate the stiffness of the substitute frame cannot be determined. An educated guess is required and at the end of the calculations, it must be checked that the guess was indeed reasonable. The design moments correspond to extra moment capacities required over the capacities for the gravity loads. Two ends of a member must be capable of handling the same design moment both in positive and negative directions. This requirement again is reasonable for beams, but may not be so for columns.

The authors designed the test frames using the substitute structure method. These test frames were subjected to nonlinear time-step analysis, and they state that the frames behaved well and that inelastic deformation occurred at the prescribed locations.

(c) Computer Program

Use of a computer is almost as essential in the substitute structure method, as it is in the case of regular modal analysis. A flow diagram is shown in Fig. 2.3. Only minor modifications are required to convert an existing modal analysis program to be used for the substitute structure method.

A target damage ratio for each member must be read in and stored when structural data are read in. At this stage it may be advantageous to compute and store a substitute damping ratio for each member. When the structure stiffness matrix is assembled from member stiffness matrices, flexural components of the member stiffness matrix must be divided by the appropriate target damage ratio. The structure stiffness matrix becomes

that of the substitute frame, and this matrix is used to compute natural periods and associated mode shapes.

Calculations of modal responses are performed twice: on the first cycle modal forces are computed for the undamped substitute structure; flexural strain energy for each member is computed and stored for each mode. A smeared damping ratio for each mode is computed according to equation (2.23). With the smeared damping known the computation of modal forces and displacements are repeated. Root-sum-square forces and displacements are computed on the second cycle, but strain energy calculations are not required. From the modal base shears RSS base shear and the maximum value of the absolute sum of any two of the modal base shears must be computed. To compute the design forces the RSS forces are multiplied by the factor in equation (2.25). Furthermore, the column moments must be increased by 20%.

If a linear response spectrum is chosen as was suggested by Shibata and Sozen,⁵ only one inversion of the structure stiffness matrix is necessary. The program is a very efficient one that requires small storage and little CPU time. If a regular plane frame analysis program is to be converted, subroutines for setup of mass matrix, response spectrum, and computation of natural periods, mode shapes, and modal participation factors must be added.

2.3 Examples and Observations

(a) Frames with Flexible Beams

In order to test the computer program for the substitute structure method, sample frames from Shibata and Sozen's paper⁵ were chosen and the results were compared with theirs. The frames are 3-, 5-, and 10-stories high and they consist of stiff columns and flexible beams.

The data for the three frames are shown in Fig. 2.4. The width in each case was 24 feet and the story height was uniform at 11 feet with a weight of 72 kips concentrated at each story. The target damage ratios were one for columns and six for beams in all three frames. Since the moments of inertia of the cracked sections were not known, the assumptions made by Shibata and Sozen⁵ were repeated; that is, 1/3 of moment of inertia of the gross section was used for beams and 1/2 for the columns. The design spectrum A in their paper⁵ was used (Fig. 2.5). It is an acceleration spectrum derived from linear response spectra of six earthquake motions; namely, two components of El Centro 1940, two components of Taft 1952, and two components of Managua 1972. The peak ground acceleration was normalized at 0.5 g. It was assumed that the design response acceleration for any damping factor, β , could be related to the response for $\beta = 0.02$ by using,

$$\frac{\text{Response acceleration for } \beta}{\text{Response acceleration for } \beta = 0.02} = \frac{8}{6 + 100 \beta} \quad (2.26)$$

The natural periods and smeared damping factors of the

three frames are listed in Table 2.1 along with Shibata and Sozen's results.⁵ The design moments are shown on Fig. 2.4. The design moments for the 3-story frame agreed with those given by Shibata and Sozen.⁵ The design moments for 5- and 10-story frames were not shown in the paper. One may conclude that the program was capable of reproducing the results shown in Shibata and Sozen's paper.⁵

The three frames were then tested in a similar fashion to that employed by Shibata and Sozen.⁵ An inelastic dynamic program, SAKE,¹² was used to compute the response history of each frame to earthquake motions. This program was selected, because it was written exclusively for concrete frames. Its effectiveness was reported by Otani and Sozen.¹³ A record of Managua 1972 earthquake was not available; therefore, two components of El Centro 1940 and two components of Taft 1952 were used. These acceleration records were normalized so that the peak ground acceleration was 0.5 g in all four records. The yield moments were set at the design moments. Stiffness beyond yield was taken as 3% of the initial stiffness. The damping was taken to be proportional to stiffness, corresponding to 2% damping for the first mode. Computed damage ratios of three frames are shown in Table 2.2. Comparison of some of the results with those by Shibata and Sozen⁵ is shown in Table 2.3.

The three-story frame behaved very well. None of the columns yielded and the beam damage ratios were six or less in all four earthquakes. Thus the structure designed by the substitute structure method behaved as expected. In the five-story frame, El Centro EW record produced the worst result. The columns

yielded at three locations and the damage ratios of the beams, except the first-floor beam, were about seven. The frame, however, behaved very well in the other three earthquake motions. The columns remained in the elastic range and the beam damage ratios were less than five. The ten-story frame produced the worst results of the three frames. Like the five-story frame El Centro EW motion produced the most unfavorable results. The columns yielded at many locations. The fifth story column exhibited a damage ratio of about seven. All the beams exceeded the target damage ratio of six and some reached a damage ratio of about ten. The results were much better in the other three earthquakes. Although the columns yielded at a few locations in two earthquakes, inelastic deformations were not excessive. The beam damage ratios were all less than six.

These results agreed qualitatively with those by Shibata and Sozen,⁵ but not quantitatively (Table 2.3). The quantitative difference was the smallest for the three-story frame. The biggest discrepancy occurred in the ten-story frame, especially in El Centro EW motion. The difference may be due to modeling of elements in the nonlinear dynamic program, duration of earthquake motion, or difference in earthquake records caused by digitization of the records or filtering.

(b) Soft-Story Frame

Shibata and Sozen⁵ restricted a choice of a target damage ratio for each element in order that the substitute structure method may be used successfully. They stated that columns, beams, and walls may be designed with different target damage ratios, but

that the target damage ratios should be the same for all beams in a given bay and all columns on a given axis. This condition implies that a soft-story frame may not be designed properly by the substitute structure method. Two examples were tested in order to check the necessity for this restriction.

Two three-story frames similar to the one used in the previous section were used. Data for the first example are shown in Fig. 2.6. The ground floor was designed as a "soft story". A target damage ratio of two was assigned to the first-story columns and one to the rest of columns. A target damage ratio of six was given to the first-floor beam and one to the other beams. The frame consists of one 24-foot bay with 11 foot story heights. The floor weight is 72 kips for each level. The moment of inertia of the first story columns was $3/4$ of that of the columns above. The beams had constant moment of inertia. The design moments were computed by the substitute structure method and are shown in Fig. 2.6. The design spectra shown in Fig. 2.5 were used. The frames were then subjected to four earthquake motions, using the nonlinear dynamic analysis program, SAKE.¹² Each earthquake record was normalized so that the maximum ground acceleration was 0.5 g. The design moments were used as the yield moments. Two per cent stiffness-proportional damping and 3% strain hardening were assumed in the nonlinear analysis. The results of four runs are shown in Fig. 2.7. The frame tried to behave in the way it was designed to: the first-story columns yielded in all four cases. El Centro EW motion produced the worst result; the damage ratio reached 2.8. Taft S69E motion produced the smallest damage ratio, which was 1.2. The rest of the columns remained elastic. The

first-floor beam yielded in every case and the damage ratio ranged from 3.7 to 6.1. The second-floor beam remained more or less elastic except for one case. The third-floor beam did not behave as well as the other beams. It yielded in all four cases, but the damage ratios were less than 1.5 except in El Centro EW motion. Although the test frame did not perform very well during El Centro EW motion, the results from other motions seem to indicate that the substitute structure method produced a successful design of a soft story frame in this example.

In the second example the soft story was moved from the first story to the second story. The data are shown in Fig. 2.8. The same design spectrum was used and the substitute structure method was used to compute the design moments. Those design moments are shown in Fig. 2.8. The frame was again subjected to the four earthquake motions in an identical manner, with the same assumptions being made in the nonlinear dynamic analysis. The results are shown in Fig. 2.9. They were not as good as the first example, since the second-story columns remained elastic in all four cases, although they were designed to yield. The other columns remained essentially elastic. The beams behaved better than the columns. The second floor beam did yield in every earthquake; with the damage ratio ranging from 2.6 to 4.4 which is less than the target damage ratio of six. The other beams essentially remained in the elastic range.

(c) 2-Bay, 3-Story Frame

The results of the soft-story frames were inconclusive. The method worked well in the first example, but only a fair

result was obtained in the second example. A two-bay, three-story frame was used to test whether the substitute structure method could be used for a frame with randomly assigned target damage ratios. The data for the structure are shown in Fig. 2.10. The design spectrum was the same one used in the previous examples. The target damage ratios were randomly assigned. The substitute structure was used to compute the design moments, but the column moments were not increased by 20%, because they could yield before the beams.

The nonlinear dynamic analysis was carried out in an identical manner as in the previous examples. The same four earthquake records were used. The results of four runs are shown in Fig. 2.11. The structure behaved quite well when the average damage ratios of four earthquakes are compared with the target damage ratios. El Centro EW motion produced the biggest damage while Taft motions produced the least. In general, the bottom-story columns received more damage than they were expected to take, but the damage ratios of the second-story columns were very close to the target damage ratios. The third-story columns were damaged less severely than they were designed for. The same trend is found in the beams, but none of the average damage ratios were higher than the target damage ratios.

The results of this example seem to indicate that the substitute structure method can be used to design a structure in which different target damage ratios are assigned for beams in the same bay and for columns on the same axis. It appears that beams work better than columns.

2.4 Equal-Area Stiffness Method

(a) Observation

As was discussed in the section 2.3(a), three frames were designed using the substitute structure method and they were subjected to nonlinear dynamic analysis. When the dynamic analysis program was run, time-history plots of displacements and moments were obtained as a part of the output. Upon observation of these plots it was possible to pick up the periods of the most dominant vibration, and it was found that these periods were peculiar to the frames, not to the earthquake motions. Furthermore, these periods were different from the natural periods of the actual frames and from those of the substitute frames.

Table 2.4 lists the natural periods of the actual frames and substitute frames for the first mode as well as the observed periods from the dynamic analyses. In all three cases the observed periods were longer than the natural periods of the actual frames, but shorter than the natural periods of the substitute frames. This seemed to imply that the substitute structure method did not give the correct natural periods of a structure when it underwent inelastic deformation.

Some effort was made to find a method which would give a better estimate of the natural periods of a structure which would be subjected to inelastic deformation. This was felt to be important, since modal analysis was to be used, in which the response is read against the period.

(b) Equal-Area Stiffness

The preceding observation supports the theory that the stiffness of a system is reduced when it is subjected to strong motions such that its deformations exceed the elastic limit. At the same time it seems to indicate that the stiffness used in the substitute structure method is too small: true effective stiffness lies somewhere between the elastic stiffness and the stiffness of the substitute structure.

Consider the load-deflection curve in Fig. 2.12. Assume that it is an elasto-plastic case so that the damage ratio and ductility are the same. When a target damage ratio is chosen, the maximum displacement is implicitly selected. The system is allowed to undergo a deformation on the loading curve up to the point C. The area under the curve is equal to the area of the trapezoid ABCD. It is possible to make up a fictitious elastic system which reaches the same ultimate displacement and has the same area under its linear load-deflection curve AED as the area of the bilinear curve ABCD, while both systems reach the same ultimate displacement, Δ_u , and absorb the same energy of deformation in doing so, the elasto-plastic system has the yield force, F_y , as maximum force and the fictitious elastic system reaches F_1 , which is greater than the yield force. The slope of the line AE is the stiffness of this elastic system, which the author calls an "equal-area stiffness". By equating the two areas, the equal-area stiffness can be expressed in terms of the initial stiffness and the target damage ratio,

$$K_1 = k \left(\frac{2\mu - 1}{\mu^2} \right) \quad (2.27)$$

where k_1 = equal-area stiffness
 k = initial stiffness
 μ = target damage ratio.

The yield force is unknown, but it is expressed in terms of the maximum force, F_1 ,

$$F_Y = F_1 \left(\frac{\mu}{2\mu - 1} \right) \quad (2.28)$$

where F_Y = yield force
 F_1 = maximum force
 and μ = target damage ratio.

If the moment-curvature curve of an element has the same shape as that of the load-deflection curve, the flexural stiffness of the element can be reduced according to equation (2.26). This stiffness can be used to solve for the natural periods of the system. This approach is, of course, very hypothetical and there is no experimental data to support it. The concept of substitute damping loses much of its meaning, because it was derived from the simplified hysteresis loop of degraded reinforced concrete. But this hypothesis can be tested analytically by modifying the stiffness part of the substitute structure program.

(c) Examples

The same three frames used in section 2.2(a) were used to test the equal-area stiffness method. The target damage ratios were set at one for the columns and six for the beams. When the flexural components of the member stiffnesses were assembled, they

were reduced according to the equation (2.27); that is,

$$(EI)_{ei} = (EI)_{ai} \left(\frac{2\mu_i - 1}{\mu_i^2} \right) \quad (2.29)$$

where $(EI)_{ei}$ = equal-area stiffness of element i
 $(EI)_{ai}$ = stiffness of i th element of actual frame
 μ_i = target damage ratio of i th element.

The natural periods of the three frames were computed using the equal-area stiffness. The periods corresponding to the first mode are listed on Table 2.4. Those periods agreed very well with the dominant periods observed in the nonlinear analysis. Therefore, as far as the natural periods are concerned, this approach gives a more realistic estimate.

(d) Area for Further Studies

The design forces computed by the substitute structure method were used as the yield moments in the nonlinear dynamic analysis. If a method to obtain the same design forces could be developed, this equal-area stiffness method would become more attractive. An effort was made to find a way to compute design forces that are similar to those from the substitute structure method, but it was not possible to obtain a satisfactory result.

Further studies may be worthwhile, because the agreement in periods is too good to ignore. Any further research should be started with a single-degree-of freedom system. A theory to support this hypothesis needs to be established along with

experimental data. If a linear response spectrum is to be used, a new method of computing suitable damping properties must be developed.

CHAPTER 3 MODIFIED SUBSTITUTE STRUCTURE METHOD

3.1 Modified Substitute Structure Method

The term, "retrofit", is defined in the first chapter. It describes the problem of evaluating the performance of existing buildings against seismic hazards. A retrofit procedure is, then, a procedure for analyzing existing buildings. It is inevitable that almost all the structures yield and suffer inelastic deformation under a strong earthquake motion; such a procedure, therefore, must perform some sort of inelastic analysis. It must be capable of identifying the locations and extent of damage associated with a particular earthquake motion. If a structure is to fail, the mode of failure must be identified. It is desirable that a method be flexible enough to handle earthquakes of different nature and magnitude. At the same time it must be reasonably economical and easy to use in order to become a practical tool for average engineers. The use of a computer is probably inevitable because of the nature of the problem, but a program to run such an analysis must be easy to write and economical to operate.

The modified substitute structure method fulfills the aforementioned requirements. As the name suggests, it was developed from the substitute structure method by Shibata and Sozen.⁵ At present its use is restricted to reinforced concrete structures

as is the case for the substitute structure method itself, but with proper modifications the method may be used for analysis of steel and other structures. It is a modified elastic analysis in which the stiffness and damping properties are changed for use with modal analysis so that the forces and deformations agree with nonlinear dynamic analysis. A linear response spectrum is used to compute the inelastic response. The concepts of substitute damping, damage ratio, and substitute stiffness are borrowed from the substitute structure method.

The difference between a design procedure and a retrofit procedure is worth noting. In a seismic design procedure the initial stiffness of the structure is known approximately from other requirements. A designer can choose and specify the amount of inelastic deformation each element is allowed to undergo in a given earthquake motion. It is the design forces or yield forces that must be determined. In the substitute structure method, the stiffness of the actual frame is known or it can be estimated fairly precisely. Target damage ratios are selected for elements by a designer. Hence, the substitute stiffness and substitute damping ratios of the elements are prescribed. Natural periods, associated mode shapes, and modal participation factors need to be computed only once. After computation of a smeared damping ratio for each mode, modal forces are calculated and combined as specified. No iteration is required during computation. In a retrofit procedure the initial stiffness and the yield moments and other strength properties of a structure are known or they can be found from design calculations, drawings, and field investigations. What is known is the amount of inelastic deformation;

that is, the damage ratio for each member must be computed given an earthquake motion. In the modified substitute structure method a suitable combination of modal forces must agree with the known yield forces. To achieve this the damage ratios of all the elements must be estimated precisely so that correct substitute stiffness and substitute damping ratios can be used. This, of course, is impossible to do; otherwise there would be no need to perform an analysis. It is, therefore, inevitable that an iterative process must be used. After each iteration damage ratios must be modified to approach nearer to the correct values. This is certainly a disadvantage, because more computations are required and hence more costs. But if the number of iterations are small, it is still an economical alternative to full-scale non-linear dynamic analysis.

Before the procedure for the modified substitute structure method is described in detail, several conditions are listed. They must be satisfied in order to apply the modified substitute structure method properly. These conditions are:

- (1) the system can be analyzed in one vertical plane,
- (2) there is no abrupt change in geometry and preferably in mass along the height of the system,
- (3) reinforcement of all members and joints are known such that their ability to withstand repeated reversals of inelastic deformation without significant strength decay can be estimated, and
- (4) nonstructural components do not interfere with structural response.

The aforementioned conditions are similar to those listed by

Shibata and Sozen⁵ in the substitute structure method. In fact, it should be noted that, after convergence, the final iteration of the modified substitute structure method is identical to the design procedure, and therefore has exactly the same restrictions and validity.

The following is the step-by-step description of the procedure for the modified substitute structure method. It must be remembered that the yield force cannot be exceeded at any time.

- (1) Perform a modal analysis on the assumption of elastic behaviour. Damping ratios must be chosen so that they are appropriate for the given earthquake. Compute the root-sum-square (RSS) forces.
- (2) Find the members in which RSS moments exceed the yield moments. Note that the bigger of the two end moments is used.
- (3) In such members modify the damage ratios according to the formula that will be described later on. The other members will have a damage ratio of one.
- (4) Follow steps (2) to (5) for the substitute structure method which was described on pages 26 and 27 in Chapter 2.2(b). Compute the RSS moments.
- (5) Compare the RSS moments with the yield moments. Modify the damage ratios according to the formula to be discussed later.
- (6) Repeat the steps (4) and (5) until all the computed moments, except in those members for which the damage ratios are one, are equal to the respective yield moments.
- (7) The members in which the damage ratios are greater than one will receive inelastic deformation. Check if each member

can take such deformation. If not, such a member will fail. It is now possible to make an estimate of the locations and extent of damage in the whole structure. Similar checks can be made for other components of internal force.

An ordinary elastic modal analysis is performed in the first iteration, because at this stage it is not clear if a structure will go through inelastic deformations in a given earthquake. A value for damping must be chosen; a ratio of 10% of critical is appropriate for a reinforced concrete structure subjected to a strong earthquake motion. Since it is impossible to exceed the yield moments, those members in which the computed moments are greater than their yield moments will yield. In the third step the first estimate of damage ratios is made. Starting from the second cycle of iteration, the substitute structure method is used to compute the natural periods, mode shapes, and modal forces. Damage ratios calculated at the end of the previous iteration are used to compute the substitute stiffness and substitute damping ratios. The root-sum-square moments are used throughout the iterations. In the substitute structure method they were increased according to equation (2.25) and the column moments were further increased by 20% to obtain the design moments. This approach is acceptable in a design procedure, because it would provide an extra margin of safety. But in order to be on the conservative side it is advisable to use the root-sum-square moments and ignore the factor in equation (2.25). Increasing the column moments by 20% here is, of course, totally absurd. Unless correct damage ratios are obtained in the previous iteration, the computed moments do not agree with the yield moments except for

the members which remain elastic. The damage ratios must be modified and another iteration must be made. At some stage all the damage ratios will converge to the correct values and the iteration process will be stopped. Then an evaluation of the performance of the structure can be carried out as outlined in the last step. It must be noted that the effect of strain hardening is ignored in the discussion above, but it can be included with only a slight modification.

It is now appropriate to explain a way to modify damage ratios at the end of each iteration. Consider the elastoplastic case shown in Fig. 3.1. Suppose at the end of the first iteration, which is an ordinary modal analysis, the computed moment was M_1 which is greater than the yield moment, M_Y . Since the member was assumed to behave elastically, it followed the line OA and reached the point B with the moment, M_1 , and the rotation, ϕ_1 . Since a computed moment cannot exceed M_Y , the stiffness, k , must be reduced in the next iteration. It is assumed that the rotation, ϕ_1 , was correct. A point B' is located on the plastic part of the moment-rotation curve and the slope of the line OB' is used as the stiffness for the next iteration. The damage ratio corresponding to this new stiffness can be calculated from the geometry. The damage ratio at the end of the first iteration is given by,

$$\mu_2 = \frac{M_1}{M_Y} \geq 1 \quad (3.1)$$

where μ_2 = damage ratio to be used in the second iteration

M_1 = computed moment in the first iteration

M_Y = yield moment

Suppose that at the end of the second iteration the computed moment, M_2 , still exceeded the yield moment, M_Y ; that is, it reached the point C on the curve. It means that the assumed stiffness was still too big and that the damage ratio must be increased. This time a point C' is located on the curve and the slope of the line OC' is used to define the new stiffness. A new damage ratio corresponding to the new stiffness can be obtained from the geometry.

$$\mu_3 = \mu_2 \frac{M_2}{M_Y} \quad (3.2)$$

where

μ_3 = damage ratio to be used in the third iteration

μ_2 = damage ratio used in the second iteration

M_2 = computed moment at the end of the second iteration

M_Y = yield moment.

It is possible that the computed moment, M_2 , was less than the yield moment, M_Y . The stiffness must now be increased; that is, the damage ratio must be decreased. The new damage ratio can be computed from the geometry in a similar way and the same relation as in equation (3.2) can be obtained. Attention must be paid this time, since if the new damage ratio is less than one, it must be set at one.

In general, at the end of the n th iteration the new damage ratio can be computed by the following equation.

$$\mu_{n+1} = \mu_n \frac{M_n}{M_y} \geq 1 \quad (3.3)$$

where μ_{n+1} = damage ratio to be used in the $n+1$ th iteration

μ_n = damage ratio used in n th iteration

M_n = computed moment in n th iteration

M_y = yield moment.

If μ_{n+1} equals μ_n for all the members, the iteration process is complete.

When the moment-rotation curve after yield exhibits strain hardening, the situation is a little more complex. If such is the case, the yield moment is not the absolute limit. The computed moment can be and will be greater than the yield moment provided that the damage ratio is greater than one. Derivation of the formula for the new damage ratios is shown in Appendix A. It is,

$$\mu_{n+1} = \frac{M_n \cdot \mu_n}{M_y (1 - s) + s \cdot \mu_n \cdot M_n} \geq 1 \quad (3.4)$$

where μ_{n+1} = modified damage ratio to be used in $n+1$ th iteration

μ_n = damage ratio used in n th iteration

M_n = computed moment in n th iteration

M_y = yield moment

s = ratio of stiffness after yield to initial stiffness.

Inherent limitations of the modified substitute structure method are now discussed. The moment-rotation curve of each member must be such that it can be approximated by a bilinear curve. Furthermore, it must have the same shape as that of the load-deflection curve. If linearly distributed moment with a point of inflection in the mid-span of a member is assumed, this condition is satisfied. The moment capacity of each member is assumed to be the same for both ends and for both positive and negative moments. If the computed moment at one end of the member is greater than at the other end, the bigger moment is chosen to compute the damage ratio.

3.2 Computer Program

The use of a computer is essential for practical applications of the modified substitute structure method. The iterative process that is required in the method can be incorporated in the program quite easily. The program itself can be written with little difficulty. If an elastic modal analysis program is available, relatively few modifications are necessary.

The flow diagram of the modified substitute structure program is shown in Fig. 3.2. Data for structural definition, member properties, and joint locations are read in and stored in the first part of the program. The damage ratios of all the members should be initialized at one. Then the mass matrix should be set up; it remains unchanged throughout the iteration process. The structure stiffness matrix is assembled from member matrices. The flexural part of the member stiffness is modified according to the damage ratio using equation (2.21). Since all the damage ratios are set at one in the first iteration the structure stiffness matrix is the same as in the elastic analysis. This matrix and the mass matrix are used to solve for natural periods, associated mode shapes, and modal participation factors. Since it involves a regular eigenvalue problem, a library subroutine is usually available. Initially a suitable set of damping ratios should be given by the user. Ten per cent damping for all the modes was used by the author. A spectrum subroutine is called and a peak ground acceleration is returned. Then a load vector is set up and the stiffness matrix is inverted to solve for deflections. Modal forces can be computed in the usual

manner. This process is repeated for all the modes and RSS forces and displacements are computed. At the end RSS moments are compared with respective yield moments. If the yield moment of any member is exceeded, iteration is necessary. The damage ratio of such a member is modified according to equation (3.3) or (3.4).

From the second iteration the substitute structure method is used to compute modal forces and displacements. The structure stiffness matrix is reassembled using the new set of damage ratios and the computation of natural periods, mode shapes, and modal participation factors is repeated. Substitute damping ratios of all the members should be calculated at this stage using equation (2.20). Modal forces are calculated twice. Forces for the undamped case are computed first to calculate the flexural strain energy stored in each member. Smeared damping ratios for all the modes are computed using equations (2.23) and (2.24). They are used to get the peak ground accelerations from the spectrum. Modal forces and displacements are recomputed and RSS forces and displacements are obtained at the end. Equation (3.3) or (3.4) is used to modify the damage ratios. Further iterations are necessary until all the damage ratios stop changing. In practice, very many iterations are necessary to achieve this and more practical convergence criteria must be used to keep the number of iterations at a reasonable level. The program used by the author is listed in Appendix B.

The cost of running the program depends directly on the number of iterations. If the convergence can be accelerated, the saving in CPU time and hence cost can be substantial. An attempt was made to achieve accelerated convergence and a method is

described in a subsequent section of this chapter. Obviously the proposed method is more costly than an ordinary modal analysis because of the amount of computation involved, but the storage requirement is roughly the same and the CPU time required for this method is still a fraction of that for the full-scale nonlinear dynamic analysis. Therefore, overall cost of running this analysis is still small compared to the cost of running the nonlinear dynamic analysis. Coupled with ease of data setup, the advantage of the modified substitute structure method over the nonlinear dynamic analysis is substantial.

3.3 Convergence

In order to test whether the modified substitute structure method actually works, test frames are required. The damage ratios of all the members in such frames must be known for a given linear response spectrum. Since the method utilizes the substitute structure method, it is possible to design a frame by the substitute structure method and then subject it to analysis by the modified substitute structure method. When the iteration procedure is complete the computed damage ratios should be equal to the target damage ratios assigned in the design method. Since the RSS forces are used as the computed forces, the design forces in the substitute structure method must also be the RSS forces, not the forces which are increased by the factor in equation (2.25). Two frames were tested this way.

The first test frame is a 2-bay, 3-story frame. The data are shown on Fig. 3.3. The substitute structure method was used to compute the yield moments and natural periods which are also shown on Fig. 3.3. RSS moments were taken as the design moments. The target damage ratios were one for the columns and six for the beams. The same response spectrum as in the previous examples was used (Fig. 2.5). This frame was then subjected to the modified substitute structure analysis to test the convergence of periods and damage ratios. The iteration was carried out 20 times and the natural periods and damage ratios were printed at the end of each iteration. The damping ratios for all three modes were taken as 10% of the critical in the first cycle of iteration. The three natural periods computed in each iteration

are listed on Table 3.1. To illustrate the speed of convergence, each period is normalized to that computed in the substitute structure method and the plot of the normalized periods versus the number of iterations is shown on Fig. 3.4. As can be seen from the plot, the natural period for the first mode converged very rapidly. It took only five iterations for the first mode periods to be within 1% of the correct period. The convergence of the second mod period and the third mode period were slower; they were within 1% of the correct periods after 13 iterations. The second mode periods approached the correct value more rapidly during the first few iterations than the third mode period.

The damage ratios of selected columns and beams are listed in Table 3.2 and the plot is shown in Fig. 3.5. The damage ratios of column 1 and beam 1 converged very rapidly. Only 6 iterations were necessary before they were within 1% of their respective target damage ratios. Convergence of damage ratio in beam 2 was slower and it took 15 iterations to be within 1% of the target damage ratio. Column 2 had the slowest convergence of the four members. Its damage ratio was within 1% of the target damage ratio at the end of 20 iterations.

As can be seen from the two plots, the periods converged faster than the damage ratios. Among the natural periods, the lowest mode period converged at the fastest rate, and the highest mode the slowest. As far as the convergence of the damage ratios is concerned those of the members in the lower story converged faster than in the upper story. This is logical, because the response of the members in the lower story is governed by the lower mode and the convergence of the natural periods and hence

the mode shapes is faster for the lower mode.

The same 2-bay, 3-story frame was used in the second example. The member properties were the same as in the first frame, the target damage ratios were changed. The columns had target damage ratios of two, one, and three. The same damage ratios were assigned to all columns on the same axis. The target damage ratios for beams were six in one bay and two in the other bay. The substitute structure method was used to compute the yield moments, which were RSS moments. Those forces and the natural periods are shown in Fig. 3.6. The frame was then analyzed by the modified substitute structure method.

The natural periods computed in the first 20 iterations are tabulated in Table 3.3. The plot of normalized periods are shown in Fig. 3.7. The convergence of the first two periods was again very rapid. The period for the third mode, however, was relatively slow. It was within 4.3% of the correct value after 20 iterations. The damage ratios converged very slowly. Fig. 3.8 shows the damage ratios at the end of selected numbers of iterations. At the end of 20 iterations the damage ratios of the third-story columns and beams were still quite different from the target ones. The iteration was carried out 200 times and by then they did converge to the correct values. The plot of damage ratios against the number of iterations is shown in Fig. 3.9. The rate of convergence of damage ratios were much slower in the second example than in the first example. Fig. 3.9 shows that about 100 iterations were necessary to achieve reasonable estimate of damage ratios. The same conclusion in the previous example applies in the second example.

The results of these two examples showed the following.

- (1) The natural periods converge at a faster rate than the damage ratios.
- (2) The natural periods for the lower modes converge faster than those in the higher modes.
- (3) In general, the damage ratios of the upper story columns and beams converge at a slower rate than those of the lower stories.
- (4) Both the damage ratios and the natural periods do not converge monotonically. This point is particularly true in the first few cycles of iterations.
- (5) The rate of convergence slows down as the number of iterations increases. The most rapid changes occur during the first few cycles of iteration.

These observations were confirmed in the other examples that will be shown later on.

It is, in practice, impossible to carry out the iteration process until all the damage ratios cease to fluctuate. As soon as a good estimate of damage ratios is obtained, the iteration procedure should be stopped. Some criterion must be established for this purpose. It is possible, but not practical, to keep track of every damage ratio at the end of each iteration. It is also impractical to set the limit on the number of iterations at a certain number. The two examples in this section illustrated this point very clearly. If the number of iterations is set at 30, say, then the last 10 to 15 iterations is totally unnecessary in the first example. On the other hand, inaccurate estimate of damage ratios results in the second example. Two approaches

seem possible as suitable convergence criteria. One approach is to compare the values of the damage ratio of each member at the end of the iteration with that of the previous iteration. The following formula may be used.

$$\left| \frac{(\mu_i)_n - (\mu_i)_{n-1}}{(\mu_i)_{n-1}} \right| < \delta \quad (3.5)$$

where $(\mu_i)_n$ = damage ratio of i th element at the end of n th iteration
 $(\mu_i)_{n-1}$ = damage ratio of the same element at the end of $n-1$ th iteration
 δ = constant

If this is true for all the elements in the structure, the iteration is complete and the forces, displacements, and damage ratios can be printed. An alternative approach is to compare the computed moments with the yield moments. The following formula is suitable for this purpose.

$$\left| \frac{(M_i)_n - (M_{yi})}{(M_{yi})} \right| < \epsilon \quad (3.6)$$

where $(M_i)_n$ = computed RSS moment in i th element during n th iteration
 (M_{yi}) = yield moment for i th element
 ϵ = constant.

If this inequality is satisfied for all the elements with damage ratios greater than one, no more iteration is necessary.

A definite advantage of the first method is that it is a direct comparison of the damage ratios computed in the latest two

iterations. The second method is an indirect comparison of the damage ratios. It is not clear how much change is made on damage ratios. The first approach has a definite disadvantage, because the denominator changes at every iteration. Because of this reason the second approach was adopted by the author. It is hoped that this criterion produces a more uniform result for different types of structures. With a little experience a suitable value for ϵ can be specified. In running a computer program it is desirable to set the limit on the number of iterations, because no output would be obtained if a value for ϵ was too small and CPU time exceeded the limit set by the user.

In spite of the foregoing discussion, it should be noted that, in practice, because of the inaccuracies in modeling the structure, in predicting the earthquake, and in correlating damage ratio with actual damage, the results are not significant to a high degree of precision.

3.4 Accelerated Convergence

The cost of running the modified substitute structure method is roughly proportional to the number of iterations that is necessary to meet the convergence criterion. If there is a way to accelerate the convergence, the method becomes a more powerful tool. An effort was made to achieve this goal and the following procedure was developed.

It was observed in the two examples in the last section that the most rapid changes in the damage ratio occurred during the first several cycles of the iteration process and then the damage ratios gradually approached the final values. The damage ratios are modified at the end of each iteration by the use of equation (3.3) or (3.4). It appeared possible to make overcorrections on the damage ratios in order to speed up the convergence. It is easy to keep track of the difference between the new damage ratio of an element, and the damage ratio of the same element in the previous iteration. The following formula was proposed for overcorrection of damage ratios.

$$(\mu_i)'_n = (\mu_i)_n + \alpha (\mu_i)_n - (\mu_i)_{n-1} \quad (3.7)$$

where

$(\mu_i)'_n$ = overcorrected damage ratio of i th element
used for n th iteration

$(\mu_i)_n$ = damage ratio of i th element computed at the
end of $n-1$ th iteration using equation (3.3)
or (3.4)

$(\mu_i)_{n-1}$ = damage ratio of i th element used in $n-1$

th iteration

α = positive constant.

What is proposed in equation (3.7) is that some fraction of the difference between the modified damage ratio and the previous damage ratio be added to the modified damage ratio. Since α is a positive constant, the overcorrected damage ratio is smaller than the modified one when the damage ratio is altered to have a lower value than the previous one, but overcorrected damage ratios cannot be less than one. It was found that applying this overcorrection from the beginning could lead to an unexpected result, because the damage ratios change quite rapidly during the first stage of the iteration procedure. The damage ratios may fluctuate up and down violently from one iteration to another. It is strongly advisable that the constant, α , be set to zero during the first five to ten iterations, so that the overcorrection procedure is applied when the damage ratios change at a small rate. If such a precaution is taken, the value of α may be set at as high as one to achieve faster but still smooth convergence.

The following example illustrates the usefulness of the procedure. It also shows how closely the damage ratios approach the exact values when different limits are used as convergence criteria. The second example in the previous section was used. All the relevant information is shown in Fig. 3.6. Recall the convergence criterion proposed in the previous section. It was

$$\left| \frac{(M_i)_n - (M_{yi})}{(M_{yi})} \right| < \epsilon \quad (3.6)$$

where ϵ is a constant. ϵ was set at 10^{-2} , 10^{-3} , and 10^{-4} . When the relation in (3.6) was satisfied for all the members, the iteration procedure was stopped. Six runs were made in total. In the first three runs no overcorrection was made and the numbers of iterations required to achieve the three convergence criteria were recorded. In the next three runs the same three convergence criteria were used; that is, ϵ was set at 10^{-2} , 10^{-3} , and 10^{-4} , but the overcorrection of damage ratios was applied. α was set at 1.0 at the end of the fifth iteration and the number of iterations required was recorded for each run. The results are given in Table 3.4.

When ϵ was set at 10^{-2} , it took 29 iterations to satisfy this criterion without overcorrection of damage ratios. When the damage ratios were overcorrected, the number of iterations was reduced to 18 for a saving of 11 iterations. At $\epsilon = 10^{-3}$ 158 iterations were required without overcorrection technique. With it, the number was reduced to only 81 for a saving of 77 iterations. At $\epsilon = 10^{-4}$ the convergence criterion was not met after 200 iterations when overcorrections were not made, but it was met after 124 iterations when they were made. Clearly this technique accelerated the convergence of the damage ratios. The number of iterations was reduced by one third to almost one half. The saving in computation is substantial when the convergence is slow in a case such as the example used here. The gain is not so significant when the convergence is fast, as it is in the first example in the previous section. Since it is impossible to predict the rate of convergence beforehand, this technique should be used all the time. On rare occasions the method produced bad

results in which the damage ratios oscillated. In order to avoid this possibility, α may be set at a constant less than one or the application of the technique may be delayed until more than 10 iterations are completed.

Table 3.5 shows how closely the damage ratios of all the members approached the exact value when different ϵ values were specified. Overcorrections were made in all cases. The same applies to the natural periods. When an ϵ of 10^{-2} was reached, some of the damage ratios were still quite far from the exact ones; the third-story columns and beams fall in this category. The natural period for the third mode differs the most from the exact one but the difference is less than three percent. At $\epsilon = 10^{-3}$ almost all the damage ratios are very close to the exact values. The natural periods are even closer to the exact values than the damage ratios. At $\epsilon = 10^{-4}$ both the damage ratios and the natural periods are practically exact. ϵ set at 10^{-2} is probably too coarse. ϵ should be set at somewhere between 10^{-3} and 10^{-2} . It was found from other runs that ϵ set at 10^{-3} produced satisfactory results. However, if the modified substitute structure method is used to obtain a rough estimate ϵ may be set at a value a little smaller than 10^{-2} ; and this generally is all that is warranted in practice.

It may be possible to incorporate the overcorrection of damage ratios into the formula for modifying the damage ratios at the end of the iteration. When equations (3.3) and (3.4) were derived, it was assumed that the same rotation would be obtained in the next iteration. The substitute stiffness and hence the damage ratio was increased or decreased accordingly to satisfy

this assumption. But this assumption is not absolutely necessary. Another assumption is possible and with such an assumption a new formula may be derived to achieve faster convergence. Further study is possible in this area.

As a final remark in this chapter it is worth noting that the two examples in the previous section, even though they were identical frames, except for the yield moments, lay on the two extreme sides as far as the rate of convergence was concerned. It was very rare that the damage ratios of a structure converged at a faster rate than they did in the first example, or at a slower rate than in the second example. Even when the size of a structure in the first example was considerably greater than the structure in the second example, fewer iterations were required to satisfy the same convergence criterion. In general, less than 20 iterations are necessary to obtain a good estimate on damage ratios for most of the structures in practice.

CHAPTER 4 EXAMPLES

4.1 Assumptions and Comments

The goal of the modified substitute structure analysis is to predict the behaviour of an existing reinforced concrete structure under a given earthquake motion. Tests must be performed to find out whether the method fulfills this intent. It is almost impossible to do an actual experiment. The test must be done analytically. Among many analytical methods, a nonlinear dynamic analysis produces the most accurate prediction of the behaviour of a structure which is subjected to an earthquake motion. It is, therefore, essential that the modified substitute structure method produce a result which is comparable to that obtained from the nonlinear dynamic analysis.

A series of test frames were analyzed by the modified substitute structure method. The same frames were also subjected to analyses using the nonlinear dynamic analysis program. The results from the two analyses were compared. The extent of damage represented by damage ratios, locations of damage and the displacements are the quantities of interest. Before the results are described in detail, all the relevant information and assumptions will be discussed in this section.

A total of four frames were tested. They were not modeled

from actual existing buildings, but they were intended to represent small- to medium-sized reinforced concrete structures. A test on a larger structure was not possible mainly due to the limitations of the nonlinear dynamic analysis program. The high cost involved in the analysis was another reason to limit the size of a test frame. In order to satisfy the second condition listed in section 3.2, they were all regular frames with no abrupt change in geometry. The dimensions of a frame were determined so that they would represent an actual building of comparable size. Member sizes and properties were chosen somewhat arbitrarily and are not necessarily completely realistic. Since the method would be used in practice for analysis of buildings that may not have been designed to resist earthquakes, the member properties were deliberately chosen in an arbitrary fashion. It was felt that if the modified substitute structure method worked for these test frames, it would work for more realistic structures. Since the test was analytical, there was no restriction on the choice of these parameters.

The following assumptions were made in the modeling of frames for use with the modified substitute structure program. Beams and columns were modeled as line members. Their axial deformations were ignored. The bottom columns were assumed to be fixed at ground level. A joint was modeled as a point. Moment capacities at the two ends of a member were taken to be equal. $P-\Delta$ effect in the columns were not included.

Upon running a program overcorrection of damage ratios was applied after the first ten cycles of iteration was over. α in the equation (3.7) was set at 0.95. Equation (3.6) was used as

a convergence criterion and ϵ was set at 10^{-3} . Iteration was stopped as soon as this convergence criterion was satisfied.

A nonlinear dynamic analysis program for frames, SAKE,¹² was used to compute the response history of each frame. The stiffness after yield was taken as 2% of the initial stiffness. The analysis was made with viscous damping proportional to stiffness, corresponding to a damping ratio of 2% for the first mode. Joints were modeled as infinitely rigid beams, with sizes proportioned according to the member sizes. A time step corresponding to 1/30 to 1/50 of the smallest period was used for numerical iteration. Response calculations were done at every five to ten time steps.

Choosing a proper response spectrum is beyond the scope of this thesis. The design spectrum A in Shibata and Sozen's paper⁵ was used for the modified substitute structure analysis. As mentioned in section 2.3, it was derived from response spectra of six earthquake motions (Fig. 2.5). Equation (2.26) was used to compute the response acceleration when the damping ratio was different from 2%. The maximum ground acceleration was 0.5 g. Four of the six earthquake records, from which the design spectrum was made, were used to compute the response histories. They were El Centro EW, El Centro NS, Taft S69E, and Taft N21E. Each record was normalized to give a peak ground acceleration of 0.5 g. The duration of each earthquake record was chosen such that each frame received the maximum damage during that duration. Unless otherwise noted, the first 15 seconds of each earthquake record were used for computation. CPU time for running the two programs is given to illustrate the difference in cost, but it should be

noted that the cost for storage was much higher for the nonlinear dynamic analysis program, because it required more memory.

The damage ratios and displacements were used for comparison of the two analyses. Since the design spectrum was the average spectrum of the six earthquakes, the results of the modified substitute structure analysis should be viewed as "average" of the four nonlinear dynamic analyses.

4.2 Examples

(a) 2-Bay, 2-Story Frame

The two-bay, two-story frame of Fig. 4.1 was used as a test frame. The widths of both bays were 30 feet. The ground story was 12 feet in height and the second story was 10 feet high. The floor weights for the first and second story were 120 kips and 100 kips respectively. The exterior columns were bigger than the interior columns. Their cracked transformed moments of inertia were taken as approximately one-half of the gross section. The moments of inertia for beams were about one-third of the gross section. An elastic analysis was run to compute the natural periods. As shown in Table 4.1, the periods for the two modes were 0.50 sec. and 0.13 sec. respectively, representing a short period structure. The yield moments were assigned randomly such that each member was expected to receive a different amount of inelastic deformation.

In the modified substitute structure analysis it took 24 iterations to satisfy the convergence criterion. The CPU time on the Amdahl V/6-II computer was 0.91 sec. The natural periods of the substitute frame computed in the last iteration were 0.76 sec. for the first mode and 0.18 sec. for the second mode (See Table 4.1). The floor displacements were computed as the root-sum-square of the modal displacements and are shown in Table 4.2. The displacement of the first floor was 1.8 in. and that of the second floor was 3.8 in. The distribution of damage ratios was quite random as expected (See Fig. 4.2). All the first-story columns yielded. The damage ratios for those columns were 4.2,

2.6, and 1.4 respectively. The second-story columns did not yield very much. One of the exterior columns remained elastic. All the four beams yielded. The first-floor beam in the left bay had the biggest damage ratio at 4.8.

Response histories of the test frame to four earthquake motions were computed by the computer program, SAKE.¹² The first 15 seconds of earthquake records were used for response computation. 0.003 sec. was chosen as the time step for numerical integration. CPU time was 12.9 sec. for El Centro EW motion, 12.2 sec. for El Centro NS, 11.8 sec. for Taft S69E, and 11.4 sec. for Taft N21E. Results of the nonlinear analyses are shown in Fig. 4.3 and Table 4.2. The two components of the El Centro earthquake resulted in more damage to the test frame than the two components of Taft earthquake. The displacements and damage ratios in Fig. 4.3. and Table 4.2 were the maximum values recorded in the response histories. The displacement of the first floor ranged from 1.3 in. to 2.8 in. for different motions. The mean maximum displacement was 2.1 in. The second floor displacement ranged from 2.7 in. to 5.3 in. with a mean of 4.2 in. The damage ratios in Fig. 4.3 correspond to the bigger of the two damage ratios for each member.

In the El Centro EW motion all of the first-story columns suffered extensive damage with damage ratios ranging from 3.3 to 9.6. On the other hand, none of the columns on the second story yielded. A recorded damage ratio less than one in Fig. 4.3 implies that the maximum computed moment was that fraction of the yield moment. The left exterior column had the least damage. All four beams yielded with their damage ratios ranging from 2.8 to

6.4. In the El Centro NS motion the first-story columns suffered approximately the same amount of damage as in the previous case. The damage ratios for the beams were also approximately the same as those in the El Centro EW motion. Two of the second-story columns, however, yielded with damage ratios of 1.3.

The Taft S69E motion produced the least damage. As in the two previous cases the first story columns yielded, but the damage ratios were roughly a half of those with El Centro. The same applies to the beam damage ratios. The three columns on the second story remained elastic, but the maximum moments were comparable to those found in the El Centro EW motion. The Taft N21E motion was more severe, but it was not strong enough for the second-story columns to yield. The damage ratios for the other columns ranged from 2.0 to 6.5 and those for the beams from 2.0 to 4.6. The members which remained elastic reached roughly the same maximum moments in all four motions, but those which yielded suffered different amounts of damage in each motion.

When the average floor displacements from the nonlinear dynamic analyses are compared with those from the modified substitute structure analysis as in Table 4.2, it is found that the latter predicted smaller displacements in both stories. The difference was greater for the first-floor displacement which was about 20% off than for the second-floor displacement which was about 10% off. Nevertheless the estimate was reasonable.

Fig. 4.2 shows the comparison of the average damage ratios of the four motions with the predicted values. In a qualitative sense the modified substitute structure analysis correctly predicted that the columns on the first story would yield and

that the extent of damage would be greatest for the left exterior column and least for the right exterior column. But the predicted damage ratios were about 60% of the average damage ratios of the four motions. The prediction for the second-story columns was good except for the right exterior column. The modified substitute structure method predicted that this column would yield slightly, but it did not happen. It only reached 60% of its moment capacity. The prediction of damage ratios for the beams was quite good. Although they were slightly underestimated, they were all within 20% of the average values. The cost of running one nonlinear analysis was about 13 times that of the modified substitute structure analysis in this example.

(b) 3-bay, 3-story Frame

The three-bay, three-story frame was tested in the second example. Data is shown in Fig. 4.4. The width of bays was 30 feet for the exterior bays and 20 feet for the interior bay. The first story was 15 feet high and the second and third stories were 12 feet high. The floor weights were 240 kips for the first floor, 200 kips for the second, and 180 kips for the third. As in the last example, exterior columns were bigger than interior columns. In each group of columns the first-story columns and the second-story columns were given the same dimension. The third-story columns were made smaller than the others. The beam sizes were reduced at higher floors. One half of the moment of inertial of the gross section was used for the cracked transformed section. The right exterior column on the second story had much smaller moment of inertia than its counterpart. The moment

of inertia of each beam was taken as one third of that of the gross section. The yield moments of the columns were set at high values, especially in the first story, so that the columns would not yield too much. The beam yield moments were smaller in the left bay than in the other bays.

An elastic analysis was performed prior to the test to compute the natural periods of the elastic frame. As shown in Table 4.3, they were 0.94 sec., 0.30 sec., and 0.14 sec. These periods were much longer than those in the previous example.

The results of the modified substitute structure analysis are shown in Fig. 4.5, Table 4.3, and Table 4.4. Only 14 iterations were necessary to satisfy the convergence criterion. It took 0.92 sec. of CPU time to do all the necessary computation. The three natural periods of the substitute frame were 1.22 sec., 0.36 sec., and 0.16 sec. The increase in natural periods over those from the elastic analysis was less for this frame than the previous frame. The horizontal displacements of the three floors were 2.2 in. for the first, 5.0 in. for the second, and 8.0 in. for the third, indicating a fairly uniform pattern of displacements (See Table 4.4). Predicted damage ratios are shown in Fig. 4.5. A damage ratio less than one is equivalent to the ratio of the computed moment to the yield moment. If the two end moments were different in a member, the bigger of the two was used.

All the columns on the first story had damage ratios of 1.1, indicating that their yield moment capacities were slightly exceeded. One of the columns on the second story yielded to a damage ratio of 1.5, but the other three remained in the elastic

range. The moment capacities of the third-story columns were fully utilized, as their damage ratios were almost 1.0 exactly. Two beams in the right exterior bay remained essentially elastic; others had damage ratios ranging from 2.0 to 5.2.

Nonlinear dynamic analyses were run to compute the response histories of the frame in the four earthquake motions. The first 15 seconds of the records were used. Since this was a bigger frame than the previous one, a considerably longer time on the Amdahl V/6-II computer was required for computation. The average CPU time of one run was about 28 seconds, double the time required in the previous example. A time increment of 0.003 sec. was selected for numerical integration.

The results of four runs are shown in Fig. 4.6. Displacements are shown in Table 4.4. They exhibited a large variation from one earthquake to another. El Centro EW component produced the biggest displacements, twice as big as those in Taft N21E component. El Centro NS produced the second biggest displacement and Taft S69E motion followed. The average displacements were 2.2 in. for the first floor, 4.7 in. for the second, and 7.5 in. for the third. The third-floor displacement, for example, ranged from 5.2 in. in Taft N31E to 10.6 in. in El Centro EW. The same trend was found in damage ratios.

The damage ratios were the highest in the El Centro EW motion. All the columns on the first story had damage ratios around 1.8. The right interior columns on the second and third stories yielded as well, but the rest of the columns remained elastic. The two exterior columns on the third story had the lowest computed moments. All the beams yielded with damage

ratios ranging from 1.5 to 6.4. The beams in the right bay experienced the least damage. Inelastic deformations occurred in the same beams and columns in the El Centro NS motion. The damage ratios of these members, however, were lower in this motion than in EW motion. The moment capacities were reached in the two columns on the second story, but they did not yield.

In the Taft S69E motion only one column underwent inelastic deformation, the right interior column on the second story, with, damage ratio of 1.2. All the columns on the first story and two on the third story had computed moments equal to or a little less than their respective yield moments. Two of the beams did not yield, although their damage ratios were almost one. Damage ratios of the other beams ranged from 1.8 to 4.6 which were much lower than the values found in the El Centro EW motion. The damage ratios were the lowest in the Taft N21E motion. All of the columns and two beams remained elastic and those which yielded had damage ratios ranging from 1.5 to 4.0.

Average damage ratios are shown in Fig. 4.5. When these values are compared with those predicted by the modified substitute structure analysis, there is a remarkable agreement. The prediction of beam damage ratios is excellent without exception. Even the worst one was off by only 15%. The prediction of column damage ratios was a little worse than for the beams. Only the damage ratios of the exterior columns on the third story were slightly off, but others were in good agreement. The average displacements also agreed very well with those predicted by the modified substitute structure analysis, as shown in Table 4.4. At least for this example it is safe to say that the modified

substitute structure analysis correctly predicted the results of the nonlinear dynamic analysis. This is a remarkable achievement when the difference in CPU time is concerned.

(c) 1-Bay, 6-Story Frame

Fig. 4.7 shows the data for the one-bay, six-story frame that was used as the third test frame. The width of the frame was 35 feet, and the story height was constant at 13 feet for an overall height of 78 feet. The floor weight was constant up to the fifth story at 100 kips, but at the top story it was reduced to 90 kips. The column sizes were decreased at every second story. Beam size was constant up to the fifth floor, with a smaller beam being used at the top floor. The moment of inertia of all the members were taken as approximately one-half of the values based on gross section. The yield moments of the columns were reduced progressively up the height of the frame. The yield moments of the beams were large, except at the top, compared to those of the columns. It was hoped that columns would receive a fair amount of damage.

Elastic periods were computed for all six modes and the values are shown in Table 4.5. The natural periods for the first two modes were 1.1 sec. and 0.37 sec. respectively. The smallest period was 0.08 sec.

The modified substitute structure analysis was carried out in the usual manner. It was necessary to perform 96 iterations to achieve the convergence. CPU time was 2.3 sec. The natural periods of the substitute frame, as shown in Table 4.5, were considerably longer than the periods of the actual frame. The

period for the first mode was 1.85 sec. and the second mode period was 0.84 sec. Usually the natural period for the highest mode of the substitute structure is not much different from that of the actual frame, but they were quite different in this example. The former was 0.13 sec. and the latter was 0.08 sec. The displacement pattern was also quite unique (See Table 4.6). The displacement of the second floor was much greater than the first floor. There was a big difference between the fourth-floor displacement and the fifth-floor displacement.

The damage ratios are shown in Fig. 4.8. The analysis predicted that the damage ratios would vary widely among the members. The column in the first three stories were 2.5, 6.6, and 2.9 respectively. The large damage ratio for the second-story column is the reason for the big jump in displacement between the second and third floor. Two columns, the one in the fourth story and the one in the sixth story, did not yield. A large inelastic deformation was predicted in the fifth-story column with a damage ratio of 16.6. The first-floor beam had a damage ratio of 1.5, indicating a small amount of inelastic deformation. The beams on the next three floors did not yield. The beams on the fifth and sixth floors were given large damage ratios of 9.5 and 6.8 respectively.

Response histories of the frame were computed by the non-linear dynamic analysis program, using the first 20 sec. of the four earthquake records. The time increment for numerical integration was set at 0.004 sec. The average CPU time was 42.6 sec. The damage ratios for individual earthquake motions are shown in Fig. 4.9. El Centro EW motion produced by far the worst result.

The damage due to other motions were similar to each other in magnitude.

In El Centro EW motion all the members except the top-story column suffered severe damage and the floor displacements were large, as shown in Table 4.6. Damage ratios of the columns in the first five stories ranged from 6.3 to 14.4 in the first story. The third-story column was also damaged badly with a damage ratio of over 10. All the beams experienced a large amount of inelastic deformation, with damage ratios ranging from 6.3 to 10.8, with the highest value in the fifth-floor beam. In El Centro NS motion all six columns yielded. The smallest damage ratio was 1.3 and the highest was 5.2. The columns on the third, fourth and fifth stories were damaged more than the other three. All the beams also yielded. The damage ratios increased up the height of the building except at the fifth floor where the damage ratio of the beam was the highest at 8.1. The displacements were small compared to those found in El Centro EW motion. The displacement of the first floor was particularly small (See Table 4.6).

In Taft S69E motion every member of the frame yielded. Among the columns those in the first four stories received the most damage, with damage ratios about six. The damage ratios of the beams on the first three floors were approximately the same at about 3.5. The other three were damaged to a greater extent. The damage ratio of the fifth-floor beam was the highest at 9.5, while the other two beams had damage ratios of about seven. The increase in displacements was quite uniform in the first four floors. Taft N21E motion resulted in quite a different pattern

of damage ratios. Most of the damage in the columns was concentrated in the second-story column and the third-story column with damage ratios of 7.9 and 6.6 respectively. The damage ratios of the other four columns were small. The damage in the beams was concentrated in the first two floor beams, where the damage ratios were 5.5 and 3.2. The other four beams escaped with minor damage. The displacements above the third floor did not increase significantly.

The average displacements are shown in Table 4.6 and average damage ratios in Fig. 4.8. They were very different from the figures computed by the modified substitute structure analysis. The displacement patterns were quite different. The prediction by the modified substitute structure analysis resulted in an underestimate of the displacements of the first four floors. The prediction of damage ratios was also poor. The damage was not concentrated in a particular column or a beam, but was spread over the whole structure. The modified substitute structure method failed in this test frame.

(d) 3-Bay, 6-Story Frame

The 3-bay, 6-story frame shown in Fig. 4.10 was used as the fourth test frame. Each bay was 24 ft. wide and story height was constant at 11 ft. A weight of 200 kips was concentrated at each story. Members sizes were uniform along the height. They were 24 in. by 24 in. for columns and 18 in. by 30 in. for beams. One half of the moment of inertia of the gross section was used to compute the initial stiffness of columns, and one third for beams. In this example all the columns were intended to remain elastic.

For this purpose the substitute structure method was used to compute design moments. These moments were used as a guide to establish the yield moments.

The periods are summarized in Table 4.7. The computed periods for the first two modes were 1.1 sec. and 0.34 sec. respectively, while the period for the highest mode was 0.075 sec. These elastic periods were comparable to those of the last test frame.

The modified substitute structure analysis was carried out in the usual manner; 16 iterations were required to satisfy the convergence criterion. The CPU time was 2.30 sec. on the Amdahl V/6-II computer. As shown in Table 4.7, the natural periods for the first two modes were 1.66 sec. and 0.48 sec. respectively, while the shortest period was 0.076 sec. The first two periods of the substitute frame were much longer than the corresponding periods of the elastic frame, but the other periods were relatively unchanged. As far as the displacements, shown in Table 4.8, were concerned, the second-floor displacement was quite large compared to the first-floor displacement. The increase in displacement from the fifth floor to the sixth floor was small. The relative displacement was quite uniform for the other floors, the top deflection being 8.8 in.

Damage ratios are shown in Fig. 4.11. Those of the columns were roughly constant at around 0.8; that is, the computed moments of all the columns were about 80% of the yield moments. All the yielding took place in the beams. The beams in the exterior bays had higher damage ratios than those in the interior bay. In both bays the bottom beams had the highest damage ratios.

They decreased at an increasing rate with height in the frame. For the beams in the exterior bays the damage ratios ranged from 3.5 to 4.5. For those in the interior bay they ranged from 2.0 to 2.7.

Response histories of the frame to the four earthquake motions were computed. The first 15 sec. of records were used in each run. Numerical integration was performed every 0.002 sec. and the response calculation was done after every five time steps. Each nonlinear dynamic analysis was expensive, as it required, on the average, 120 sec. of CPU time. A summary of results is shown in Fig. 4.12.

In El Centro EW motion three of the exterior columns yielded. They were the third-, fourth- and fifth-story columns and their damage ratios were about 1.5. None of the interior columns yielded, but the maximum moments of the three columns were equal to or just below the yield moments. All the beams yielded to some extent. The second-floor beams received the highest damage ratios. The first-floor beams and the third-floor beams were damaged to the same extent as the second-floor beams. Damage ratios decreased rapidly with height above the third story. The top beam in the interior bay almost remained elastic. The top deflection was 9.8 in.

Response of the frame to El Centro NS motion was moderate. None of the columns yielded with their damage ratios ranging from 0.58 to 0.96. In both the interior bay and the exterior bays the highest damage ratio was found in the first-floor beams. It was 3.2 for the interior bay and 5.0 for the exterior bay. The damage ratios decreased steadily with height. The top beam in

the interior bay did not yield. The top deflection was 6.3 in. The floor displacement did not increase much above the third-story.

Taft S69E motion was more severe than El Centro NS motion. The columns on the fifth story yielded. The damage ratio of the exterior column was 1.5 and the interior column 1.1. The maximum moments of several columns were very close to the yield moments. In the exterior bay the maximum damage ratio was 5.5 at the bottom beam. The damage ratios of the beams on the next three floors were about the same at 4.8. The top beam had the lowest damage ratio at 2.8. The same trend was found in the beams in the interior bay, but the damage ratios were smaller. The highest damage ratio was 3.5 and the lowest was 1.6. The displacement at the top was 7.3 in.

Taft N21E motion produced similar results to those in El Centro NS motion. All the columns remained in the elastic range. The damage ratios ranged from 0.58 to 0.89. The fifth-story columns were quite far from yielding. Damage ratios of the beams decreased with height in each bay. In the exterior bay they were 4.4 at the bottom and 1.0 at the top. In the interior bay they were 2.8 and 0.61 respectively. The displacement of the top floor was 5.4 in. which was the smallest for the four records.

The average damage ratios and displacements are shown in Fig. 4.11 and Table 4.8. The prediction by the modified substitute structure method was compared with the average values of the four nonlinear analysis results. Column damage ratios were predicted reasonably well. Those of the three exterior columns

were slightly underestimated, but they were not bad. The damage ratios of the beams on the first two floors were overestimated. Those on the top three floors were underestimated. In more general terms, the modified substitute structure analysis predicted fairly uniform damage ratios in the beams up the height of the frame with a small decrease towards the top floor, but the average damage ratios were higher at the bottom and decreased quite rapidly with height. The prediction was still reasonable, especially when the two top beams were excluded. As far as displacements were concerned, the two methods agreed very well up to the third floor. The modified substitute structure analysis overestimated the displacements above the third floor, but the difference was not substantial. In this example the modified substitute structure method worked reasonably well.

(e) Observations

Four test frames were analyzed by the modified substitute structure method. The results were compared with those by the nonlinear dynamic analysis. The method worked very well in the three-bay, three-story frame. Average damage ratios and displacements of the four earthquake motions agreed with those predicted in the modified substitute structure analysis. The method was less successful in the two examples, the two-bay, two-story frame and the three-bay, six-story frame. But it was still possible to obtain good estimates of damage ratios and displacements. For these three frames damage ratios converged very rapidly. The difference in the CPU time was enormous, especially in the three-bay, six-story frame. When this point is taken into

consideration, it is reasonable to classify the results of these three examples as success.

The method did not work well for the single-bay, six-story frame. The damage ratios predicted by the method were quite different from those computed in the nonlinear dynamic analysis. It should be pointed out that the frame was badly designed and that excessive yielding took place in every member in the frame. The modified substitute structure method does not seem to work in such badly designed structures. But at least the method was able to predict that the frame would behave very poorly. In practice it will be rare that such a structure exists in an area where a strong earthquake is likely to occur. Most importantly, however, it must be observed that the actual behaviour of this structure, as determined by the full dynamic analysis, was truly unpredictable. That is to say, it behaved differently in different earthquakes, so it is not surprising that the modified substitute structure method was unable to predict the behaviour satisfactorily. It is suspected that a structure in which there is widespread and extensive yielding may exhibit this type of behaviour and should, therefore, be considered unsafe, even if damage ratios would be otherwise acceptable.

The results found in the two-bay, two-story frame and the three-bay, six-story frame may be considered as typical of the modified substitute structure method. Considering that these frame were highly hypothetical and that no particular effort was made to control the behaviour of the structure, the method would be likely to work at least as well in a real structure, the behaviour of which is likely to be more controlled.

Since the modified substitute structure analysis is so much cheaper to run than the nonlinear dynamic analysis, it can be used repeatedly to see the effect of modifications. From the results of such analyses a recommendation can be made on what steps can be taken to upgrade the performance of a building to a satisfactory level.

CHAPTER 5 FACTORS AFFECTING MODIFIED SUBSTITUTE STRUCTURE METHOD

5.1 Effect of Higher Modes

Design Spectrum A in Ref. 5 was used as a smoothed response spectrum in the previous chapter. Spectrum B from the same references was derived from the 8244 Orion, San Fernando 1971 record and is shown in Fig. 5.1. Among the four test frames, the 3-bay, 6-story frame shown in Fig. 4.10 was selected and the frame was analyzed by the modified substitute structure method in the same manner as before, except that Design Spectrum B was used as a smoothed response spectrum. The modified substitute method had worked reasonably well for this frame when Design Spectrum A in Fig. 2.5 was used. The purpose of this analysis was to see if the method could work equally well for a different type of earthquake motion, represented by a different response spectrum.

The properties of the test frame were unchanged and the analysis was carried out with the same assumptions as in Chap. 4. The maximum ground accelerations was taken as 0.5 g. With the new response spectrum it took 27 iterations to satisfy the convergence criterion set in Chap. 4. Natural periods for the actual frame and the substitute frame are shown in Table 5.1 and

displacements in Table 5.2. Damage ratios are shown in Fig. 5.2. Most of the inelastic deformations occurred in the beams, all of which yielded. Damage ratios in the beams in a given bay increased with height up the frame. Only the second-story columns yielded.

A nonlinear dynamic analysis was done, using the first 20 seconds of the 8244 Orion 1971 record to compute the response history of the frame. The maximum ground acceleration was normalized at 0.5 g as before. Maximum displacements are shown in Table 5.2 and damage ratios in Fig. 5.2. The results of the nonlinear analysis were quite different from those of the modified substitute structure analysis. A plot of damage ratios for beams in the exterior bay is shown in Fig. 5.3. It is clear that the modified substitute structure method grossly overestimated the damage ratios of upper-story beams. A similar trend was seen in the previous example, though it was much less noticeable.

Although this finding was very disappointing, an effort was made to find out the reason why the method failed to work for the test frame with this response spectrum. The floor weights of the test frame were changed to see if the natural periods of the frame had any effect. They were reduced from 200 kips per floor to 130 kips per floor to decrease the natural periods. The rest of the properties were the same as shown in Fig. 4.10. The modified substitute structure analysis and the nonlinear dynamic analysis were carried out in an identical manner. Natural periods of the actual frame and the substitute frame are listed in Table 5.3. Displacements in the two analyses are shown in Table 5.4 and damage ratios in Fig. 5.4. The results of the two analyses

agreed very well this time. The displacements computed in the modified substitute structure analysis were almost identical at all levels to those in the nonlinear dynamic analysis. Beam damage ratios agreed very well as shown in Fig. 5.5 in which the damage ratios for beams in the exterior bay are plotted. Columns yielded slightly at three locations in the nonlinear dynamic analysis, though the modified substitute structure method predicted that all the columns would remain in the elastic range. Nevertheless, column damage ratios agreed very well in general. Thus natural periods did affect the accuracy of the modified substitute structure analysis.

There are two ways to explain why the analysis of two frames, identical except for the floor weights, resulted in failure in one case and success in another. One possible explanation is that an actual response spectrum is very rugged with many peaks and troughs. When a smoothed spectrum is used, the response acceleration at a certain period may be overestimated, while that at another period may be underestimated. The natural periods of the substitute frame in the first case were such that correct response accelerations were not obtained from a smoothed response spectrum. The other explanation is based on the effect of higher modes. The shape of a response spectrum is such that responses due to higher modes play a more prominent role for a structure with longer periods. For a typical structure the longest period, and possibly the second longest period, may correspond to the downward sloping part of the response spectrum. As the natural periods of a substitute frame increase, response accelerations for the lower modes become smaller and less

significant compared to those for the higher modes. Since the modal damping ratios of substitute structures decrease for higher modes, higher modes affect response calculations even more. Therefore, it is possible that the substitute structure method overestimates the effect of higher modes and that this point shows up more clearly in a structure with longer periods.

In order to see which explanation was more likely to be true, a test frame with shorter periods was analyzed using the original smoothed response spectrum; that is, Design Spectrum A in Fig. 2.5 was used. The analysis procedure in Section 4.2(d) was repeated. The floor weight of the 3-bay, 6-story frame was reduced to 130 kips at all levels, but the rest of the properties were as shown in Fig. 4.10. The response histories of the frame to four earthquake motions were also computed by the nonlinear dynamic analysis program. Natural periods of the actual frame and the substitute frame are in Table 5.5 and displacements are listed in Table 5.6. Damage ratios are shown in Fig. 5.6 and Fig. 5.7. Average damage ratios from the four nonlinear analyses agreed well with those in the modified substitute structure analysis. Better agreement was observed in the response of upper stories for this frame than the test frame used in the last chapter. Thus, although the difference was less apparent in the case of Design Spectrum A, the frame with shorter periods again worked better.

This seems to support the second explanation. Although the difference between a smoothed response spectrum and an actual response spectrum may affect response computations in the modified substitute structure method, the results described in this

section favours the argument that the modified substitute structure method works better for a structure with shorter periods. Or conversely, the method overestimates the contribution from higher modes. The substitute damping ratio is calculated in accordance with equation (2.20) in Chapter 2, and modal damping ratios are computed on the assumption that each element contributes to the modal damping in proportion to the strain energy associated with it in each mode shape. This has the effect of making modal damping ratios higher in the lower modes. In terms of energy it implies that lower modes dissipate more energy. This is probably true, but when response calculations are made, this works against the original intention. Since response accelerations in higher modes with smaller damping ratios are much greater, responses in higher modes are probably given more weight than they should have. When the response acceleration is calculated from the design spectra in Ref. 5, lower damping ratios do in fact have a proportionally greater effect; this should have the effect of slightly de-emphasizing higher modes, which tend to have lower damping, but the evidence here indicates that this effect should be increased to de-emphasize them still further.

5.2 Spectrum

A smoothed response spectrum deviates from a real response spectrum at many places. Although the curve is drawn in such a way that the difference in the two spectra is minimized, a sizable difference may occur at certain periods. This point arises often when a smoothed response spectrum is derived from more than one response spectrum. Recall that in the examples in Chapter 4 the damage due to El Centro EW motion was consistently higher than that anticipated in the modified substitute structure analysis. On the other hand, the response histories of test frames to Taft S69E motion agreed reasonably well with the modified substitute structure analysis. These results may partly be caused by the discrepancy between a smoothed response spectrum and an actual response spectrum.

A computer program was used to generate the response spectra for El Centro EW motion and Taft S69E motion.¹⁴ The difference between a smoothed spectrum and El Centro EW spectrum is illustrated in Fig. 5.8. The two spectra are reasonably similar in shape and magnitude at 2% damping ratio except at a few places where peaks in the actual spectrum are considerably above the smoothed spectrum. At 10% damping ratio, however, El Centro EW spectrum is consistently above the smoothed spectrum for a period greater than 0.4 sec. The response acceleration from the actual spectrum is 50% to 100% greater than the smoothed spectrum. It appears that the big difference in the two spectra at high damping ratios explains in a qualitative manner the discrepancy in the results of the modified substitute structure analysis and

the nonlinear dynamic analysis. The smoothed response spectrum and Taft S69E spectrum are plotted in Fig. 5.9. For both damping ratios the smoothed spectrum is reasonably close to the actual spectrum. This seems to explain qualitatively why the results of the two analysis were not very far apart.

From these observations it seemed possible that a better estimate of damage ratios and displacement could be obtained if an actual response spectrum was used instead of the smoothed spectrum. Response accelerations were computed at a short increment of periods for several damping ratios ranging from $\beta = 0.0$ to $\beta = 0.20$ from El Centro EW record and Taft S69E record. In total 50 periods for both cases were chosen to complete a table of response spectra. The maximum ground acceleration was normalized at 0.5 g. The modified substitute structure analysis was performed in the same way as before except for the following change. The spectral acceleration was read directly or interpolated from the table. The period was interpolated first and then the damping. Suppose that the period, T , and the damping ratio, β , were known and that the spectral acceleration corresponding to this period and damping was to be computed. Two periods, T_1 and T_2 , were located in the table such that T lay between T_1 and T_2 . Then two damping ratios, β_1 and β_2 , were found from the table such that β was between β_1 and β_2 . Using a linear interpolation, spectral accelerations corresponding to T at β_1 and T at β_2 were calculated. A linear interpolation was again performed to compute the acceleration at β .

Several frames were analyzed by the modified substitute structure method, using El Centro EW spectrum and Taft S69E

spectrum. Although the response spectra were no longer smooth, the damage ratio converged. In other words, it was possible to find a substitute structure such that the computed moments were equal to the yield moments for all the members which yielded. The number of iterations increased in many cases. It was found that the overcorrections of damage ratios resulted, in some cases, in unstable behaviour; the damage ratios oscillated from one iteration to another.

The 3-bay, 6-story frame in Fig. 4.10, with floor weights taken as 130 kips at all levels, was analyzed by the modified substitute structure method, using El Centro EW spectrum. Twenty iterations were necessary to achieve convergence. With a smoothed response spectrum it took 13 iterations to satisfy the identical convergence criterion. The results from this analysis were compared with those from the previous analyses. The natural periods are summarized in Table 5.7, the displacements in Table 5.8, and the damage ratios in Fig. 5.10. The natural periods of the substitute frame were longer with El Centro EW spectrum than with the smoothed spectrum. The displacements agreed a little better with those from the nonlinear dynamic analysis. The damage ratios were higher with the real response spectrum than with the smoothed response spectrum. They were closer to the damage ratios found in the nonlinear dynamic analysis, but the modified substitute structure method still underestimated the damage ratios at lower levels and overestimated those at upper levels. The results confirmed the observation that the smoothed spectrum was unconservative for El Centro EW motion.

The analysis was repeated, using Taft S69E spectrum. It

took 14 iterations for the damage ratios to converge, while 13 iterations were required with the smooth response spectrum. The comparison of natural periods is shown in Table 5.7, the displacements in Table 5.9, and damage ratios in Fig. 5.11. The same trend observed in the analysis with El Centro EW spectrum was present, but the two modified substitute structure analyses did not differ significantly. It indicates that the smoothed response spectrum represented Taft S69E motion well. Compared with the nonlinear dynamic analysis, the real response spectrum produced slightly better results than the smoothed spectrum, but the improvement was marginal.

The same frame, except that the floor weight was set at 200 kips, was next tested. This is the identical frame used in Section 4.2(d). The analysis with El Centro EW spectrum was done in the same manner. The periods, displacements, and damage ratios are shown in Table 5.10, Table 5.11, and Fig. 5.12 respectively. Thirty-three iterations were required, while it took 16 iterations with the smoothed spectrum. The results were very disappointing. The modified substitute structure method with El Centro EW spectrum badly overestimated the displacements and the damage ratios, especially for the beams. The displacements were too large at all levels, but the deviation from the nonlinear dynamic analysis results became progressively larger at upper levels. Some yielding in the columns was observed, but those columns did not yield in the nonlinear analysis while others did. The beam damage ratios increased with height when El Centro EW spectrum was used. But in the nonlinear analysis the opposite trend was observed.

The analysis was repeated with Taft S69E spectrum. The number of iterations was 23, an increase of 7 iterations over the analysis with the smoothed spectrum. The results are summarized in Table 5.10, Table 5.12, and Fig. 5.13. They compared more favorably this time with those from the nonlinear analysis. The modified substitute structure method with Taft S69E spectrum, again, overestimated the displacements and damage ratios, but not as badly as in the last example.

The results for the two test frames indicate that using a real response spectrum does not guarantee a better estimate of damage ratios and displacements. This observation was confirmed in the analyses of other frames. A marginal improvement was achieved with the use of a real response spectrum while a bad estimate of damage ratios resulted in some cases. The improvement, if any, was so small and the increase in computation so big that it would not be practical to employ this approach. It is more useful to make a smoothed response spectrum closer to the real response spectrum and perform the modified substitute structure analysis with the smoothed spectrum. The difference in result between this analysis and the nonlinear dynamic analysis should be regarded as an inherent error due to the approximate nature of this analysis.

It must, of course, also be borne in mind that the future earthquake will not have a record identical to those of the past, either. Thus the smoothed spectrum represents the future earthquake just as well as does the "real" spectrum from a past earthquake. However, the foregoing discussion does indicate that one source of "error" in the modified substitute structure method lay in the smoothing and averaging of the spectrum.

5.3 Guidelines for Use of Method

As was illustrated in the example in Chapter 4, the modified substitute structure works very well for some structures, while it works poorly for others. An effort was made to establish the conditions which must be satisfied in order to apply the method successfully for analysis of existing buildings. The author, however, has so far been unable to set firm guidelines. More research is necessary to achieve this goal; therefore, the following comments should be interpreted with caution.

The modified substitute structure method is an extension of the substitute structure method. Therefore, the success of the former depends greatly on the success of the latter. As described in Chapter 2, certain conditions must be satisfied in order for the method to work. They are also applicable to the modified substitute structure method with the exception of one condition. The preliminary results indicate that the damage ratios of beams in a given bay or the damage ratios of columns on a given axis need not be the same.

The modified substitute structure method works well for small structures. The 2-bay, 2-story frame and the 3-bay, 3-story frame in the last chapter can be used to support this argument. Although their member properties and strengths were not very uniform, the results agreed very well with those from the nonlinear dynamic analysis. It appears that any structure up to four-story high can be analyzed by the modified substitute structure method quite successfully.

Some caution is necessary to interpret the results for

medium-rise structures. Although the method works reasonably well for most of the structure, there are instances when it produces erroneous results. When a structure is badly underdesigned for a given ground motion and yielding takes place in almost all the members, the modified substitute structure method may work very poorly. The 6-story frame in Chapter 4 is a good example. Though the method can show qualitatively that a structure is behaving poorly, the damage ratios and displacements may be quite different from the nonlinear dynamic analysis. Intuition should be used to judge whether the results are reasonable. In this particular 6-story frame, however, it was noted that the "actual" behaviour was erratic: the dynamic analysis led to a very different answer from the different earthquake records. Thus one reason why the modified substitute structure method was unable to give a good answer was that there was no "real" answer. One may conclude that when there are few load paths and extensive yielding the behaviour of the structure in future earthquakes is essentially unpredictable, and the modified substitute structure method will, of course, fail.

As long as the damage ratios are not very high, say, less than five in any member, the results can be received with confidence. The method seems to work better when yielding is concentrated in beams. The method may overestimate the damage ratios for upper-story beams, but they are usually not very far from those in the nonlinear analysis. All of the 3-bay, 6-story frames can be used as evidence for this argument. A multi-bay structure seems to work better with the method.

High-rise structures, greater than 10 stories, say, have

not been tested. They can be analyzed by the modified substitute structure method at a relatively small cost. The damage ratios converge quite rapidly, but their accuracy has not been compared with the nonlinear dynamic analysis, mainly because of high cost involved in such an analysis. It is hoped that the method works as well for high-rise structures as it does for medium-rise structures.

5.4 Further Studies

The modified substitute structure method was proposed for analysis of existing reinforced concrete structures. The emphasis of the research by the author was placed on the development of the procedure for the proposed method. Although a series of test frames were analyzed and the results were compared with the nonlinear dynamic analysis, the findings are still preliminary. More researches are needed to establish the true effectiveness and the limitations of the modified substitute structure method. Some of the areas for further studies are discussed in this section.

A multi-bay, high-rise structure has not been tested, and the performance of the method for such a frame is not known precisely. The results from the modified substitute structure analysis should be compared with the nonlinear dynamic analysis. Though the cost for the nonlinear analysis will be undoubtedly high, the careful choice of an earthquake record may help keep it at a reasonable level. More realistic structures should also be tested. Actual reinforced concrete structures may be used as test frames for this purpose. The results of such analysis will help set up better guidelines for applicability of the method as it stands at the present time.

An attempt should also be made to improve the present procedure. The method becomes more flexible and, hence, more practical if some of the restrictions are removed. For example, at present a single value for the yield moment is assigned to each member. If the moment capacities of the two end of a member

different, the method cannot be applied correctly without a suitable simplification in the modeling of such a member. The current procedure should be modified to handle this case. It is also desirable to include the effect of axial forces in the analysis. Behaviour of columns can be estimated more precisely if such modifications are made.

As was discussed briefly in the first section of this chapter, the present method for computation of "smeared" or average modal damping ratios may not be the best way: it appears that the effect of higher modes are overemphasized. Perhaps a new way to combine the damping ratio for each member can be developed to give more realistic modal damping ratios.

So far only reinforced concrete frame structures were tested. In practice, it is very rare to find reinforced concrete structures without shear walls. The applicability of the modified substitute structure method to shear walls should be investigated. If the present method did not work well with shear walls, a different way of modifying stiffness and damping ratios would have to be developed.

It is possible that the modified substitute structure method can be altered to handle structures made of other materials, such as steel. If suitable rules to modify stiffness and damping ratios are developed for steel structures, the method can be used in a similar manner for analysis of existing steel buildings. It probably is not very difficult to study the hysteresis loop of a steel structure after several cycles of inelastic deformation. The stiffness and damping properties may be determined in a similar manner to that used by Gulkan and Sozen.⁸

CHAPTER 6 CONCLUSION

The modified substitute structure method has been presented for determining damage ratios in an existing reinforced concrete building. These values are required for establishing the location and extent of damage which would occur in an earthquake. It is obvious that they cannot be predicted precisely for uncertain future seismic events; thus, in spite of its imprecision, the method may constitute a useful part of the rational retrofit procedure.

At present it is not always possible to predict the accuracy of the modified substitute structure analysis, but the method appears to work well for structures in which yielding is not extensive and widespread. In addition the preliminary findings indicate that it works better if yielding occurs mainly in beams. There is an indication that the effect of higher modes is over-emphasized. It is hoped that further research would clarify requirements for successful application of the method.

Although not perfected, the modified substitute structure method offers a cheap and effective way of estimating damage ratios or ductility demands under one or more level of seismic activity. Though less precise, it is much cheaper than a full-scale nonlinear dynamic analysis and, as an additional advantage, an analysis can be done on a smaller sized computer. Its

advantage over a linear elastic analysis is that it takes account of the redistribution of forces as members begin to yield. A slightly higher cost of computation is amply rewarded with this additional information on inelastic behaviour of a structure, which cannot be obtained by a conventional modal analysis.

	Mode	Natural Periods in sec		Smeared Damping Ratios	
		Computed	S & S*	Computed	S & S*
10-Story Frame	1	3.1807	3.18	0.1061	0.106
	2	0.8763	0.87	0.0805	0.081
	3	0.3945	0.39	0.0525	0.053
	4	0.2172	0.22	0.0383	0.038
	5	0.1358	0.14	0.0312	0.032
	6	0.0930	0.093	0.0272	0.027
	7	0.0681	0.068	0.0244	0.024
	8	0.0531	0.053	0.0224	0.022
	9	0.0442	0.044	0.0211	0.021
	10	0.0397	0.040	0.0204	0.020
5-Story Frame	1	1.5868	1.58	0.0991	0.099
	2	0.4101	0.41	0.0680	0.068
	3	0.1751	0.18	0.0409	0.041
	4	0.0967	0.097	0.0283	0.028
	5	0.0670	0.067	0.0218	0.022
3-Story Frame	1	0.8525	0.85	0.0852	0.086
	2	0.1883	0.19	0.0454	0.045
	3	0.0784	0.078	0.0245	0.025

* Shibata and Sozen⁵

Table 2.1 Natural Periods and Smeared Damping Ratios for 3-, 5-, and 10-Story Frames

		Damage Ratios				
		El Centro EW	El Centro NS	Taft S69E	Taft N21E	Average
10-Story Frame	Columns	1 2.0	0.85	0.98	0.95	1.2
		2 4.4	0.90	1.1	1.4	2.0
		3 4.8	0.97	0.90	1.1	1.9
		4 2.5	0.91	0.88	0.92	1.3
		5 6.9	0.94	0.97	1.0	2.5
		6 1.0	0.81	0.95	1.1	0.98
		7 1.1	0.72	0.98	1.2	0.99
		8 1.8	0.90	0.95	1.7	1.35
		9 0.96	0.89	0.90	0.96	0.93
		10 4.0	0.92	0.90	0.92	1.7
	Beams	1 6.5	4.1	5.0	4.9	5.1
		2 7.6	4.3	5.0	5.0	5.5
		3 8.3	4.6	4.9	5.1	5.7
		4 8.1	4.7	4.5	5.1	5.6
		5 8.6	4.7	4.1	5.0	5.6
		6 9.3	4.8	4.2	4.8	5.8
		7 9.8	4.7	4.1	4.6	5.8
		8 9.9	4.4	3.9	4.2	5.6
		9 9.9	4.1	3.6	4.0	5.4
		10 9.9	3.9	3.4	4.0	5.3
5-Story Frame	Columns	1 1.1	0.98	0.87	0.84	0.95
		2 3.9	0.86	0.84	0.70	1.6
		3 0.97	0.97	0.89	0.78	0.90
		4 1.1	1.1	0.93	0.88	1.0
		5 1.0	0.89	0.87	0.85	0.90
	Beams	1 5.4	4.8	4.4	3.7	4.6
		2 7.1	4.6	4.4	3.3	4.8
		3 7.1	4.7	4.1	3.2	4.8
		4 6.7	4.4	4.1	2.8	4.5
		5 6.7	4.2	3.9	2.4	4.3
3-Story Fr.	Col.	1 0.95	0.90	0.64	0.77	0.82
		2 0.89	0.94	0.61	0.65	0.73
		3 0.91	0.89	0.84	0.86	0.88
	Bm.	1 6.3	5.8	4.0	4.9	5.3
		2 6.1	6.0	3.3	4.5	5.0
		3 6.0	6.3	2.7	4.1	4.8

Table 2.2 Computed Damage Ratios for 3-, 5-, and 10-Story Frames

		Damage Ratios			
		El Centro EW		Taft S69E	
		Computed	S & S*	Computed	S & S*
10-Story Frame	Column 1	2.0	0.95	0.98	0.58
	2	4.4	1.2	1.1	0.80
	3	4.8	1.0	0.90	0.70
	4	2.5	0.98	0.88	0.80
	5	6.9	2.8	0.97	0.90
	6	1.0	1.2	0.95	0.80
	7	1.1	0.96	0.98	0.80
	8	1.8	0.98	0.95	0.85
	9	0.96	0.85	0.90	0.80
	10	4.0	1.7	0.90	0.80
	Beam 1	6.5	6.9	5.0	5.5
	2	7.6	7.2	5.0	5.5
	3	8.3	7.5	4.9	5.0
	4	8.1	7.8	4.5	4.9
	5	8.6	7.5	4.1	4.8
	6	9.3	8.8	4.2	4.6
	7	9.8	9.6	4.1	4.8
	8	9.9	9.9	3.9	3.8
	9	9.9	9.8	3.6	3.0
	10	9.9	10.0	3.4	2.2
5-Story Frame	Column 1	1.1	0.90	0.87	0.70
	2	3.9	2.2	0.84	0.70
	3	0.97	0.94	0.89	0.80
	4	1.1	2.3	0.93	0.80
	5	1.0	0.96	0.87	0.90
	Beam 1	5.4	7.0	4.4	4.4
	2	7.1	8.3	4.4	4.3
	3	7.1	8.4	4.1	3.6
	4	6.7	7.3	4.1	2.5
	5	6.7	6.9	3.9	1.5
3-Story Frame	Column 1	0.95	0.97	0.64	0.65
	2	0.89	0.90	0.61	0.61
	3	0.91	0.90	0.84	0.90
	Beam 1	6.3	6.8	4.0	4.5
	2	6.1	6.3	3.3	3.7
	3	6.0	6.0	2.7	3.0

* Shibata and Sozen⁵

Table 2.3 Comparison of Damage Ratios for 3-, 5-, 10-Story Frames

	Natural Periods for the First Modes in sec			
	Initial Elastic	Substitute Structure	Nonlinear Analysis Average	Equal-Area Stiffness
3-Story Frame	0.50	0.85	0.65	0.72
5-Story Frame	0.85	1.58	1.20	1.29
10-Story Frame	1.58	3.18	2.50	2.55

Table 2.4 Computed Natural Periods for 3-, 5-, and 10-Story Frames

No. of Iterations	Natural Periods in sec		
	Mode 1	Mode 2	Mode 3
1	1.0679	0.3233	0.1804
2	1.3701	0.3632	0.1917
3	1.7655	0.4484	0.2231
4	1.7810	0.4486	0.2129
5	1.7945	0.4513	0.2074
6	1.8004	0.4505	0.2033
7	1.8066	0.4496	0.2009
8	1.8076	0.4476	0.1990
9	1.8073	0.4455	0.1975
10	1.8069	0.4439	0.1964
11	1.8067	0.4431	0.1960
12	1.8060	0.4423	0.1956
13	1.8052	0.4414	0.1952
14	1.8046	0.4405	0.1948
15	1.8046	0.4397	0.1944
16	1.8041	0.4390	0.1940
17	1.8036	0.4386	0.1937
18	1.8035	0.4383	0.1936
19	1.8036	0.4381	0.1934
20	1.8036	0.4380	0.1933
Subst. (a)	1.8036	0.4377	0.1932

(a) Natural periods computed in the substitute structure analysis

Table 3.1 Natural Periods for 2-Bay, 3-Story Frame A

No. of Iterations	Damage Ratios			
	Column 1	Column 2	Beam 1	Beam 2
1	1.000	1.155	2.853	1.344
2	1.205	1.848	6.084	2.538
3	1.079	1.964	6.382	3.281
4	1.000	2.030	6.281	4.119
5	1.000	1.986	6.116	4.758
6	1.000	1.881	6.021	5.195
7	1.000	1.749	5.982	5.453
8	1.000	1.621	5.975	5.612
9	1.000	1.508	5.981	5.716
10	1.000	1.409	5.988	5.785
11	1.000	1.324	5.992	5.827
12	1.000	1.250	5.996	5.857
13	1.000	1.188	5.999	5.882
14	1.000	1.134	6.002	5.905
15	1.000	1.087	6.004	5.926
16	1.000	1.057	6.006	5.945
17	1.000	1.038	6.006	5.961
18	1.000	1.025	6.006	5.973
19	1.000	1.017	6.006	5.988
20	1.000	1.011	6.006	5.992
Subst. (a)	1.000	1.000	6.000	6.000

(a) Target damage ratios in the substitute structure analysis

Table 3.2 Damage Ratios for 2-Bay, 3-Story Frame A

No. of Iterations	Natural Periods in sec		
	Mode 1	Mode 2	Mode 3
1	1.0674	0.3233	0.1804
2	1.2606	0.3694	0.2062
3	1.6682	0.4758	0.2666
4	1.6338	0.4609	0.2579
5	1.6371	0.4601	0.2568
6	1.6379	0.4605	0.2563
7	1.6382	0.4620	0.2560
8	1.6375	0.4636	0.2556
9	1.6366	0.4650	0.2552
10	1.6360	0.4663	0.2546
12	1.6350	0.4682	0.2534
14	1.6339	0.4692	0.2518
16	1.6331	0.4697	0.2503
18	1.6325	0.4699	0.2489
20	1.6320	0.4700	0.2476
Subst. (a)	1.6307	0.4633	0.2375

(a) Natural periods computed in the substitute structure analysis

Table 3.3 Natural Periods for 2-Bay, 3-Story Frame B

α	Number of Iterations		
	$\xi = 10^{-2}$	$\xi = 10^{-3}$	$\xi = 10^{-4}$
0.0	29	158	200
1.0	18	81	124
Diff	11	77	76

Table 3.4 Number of Iterations - 2-Bay, 3-Story Frame B

Member	Damage Ratios				
	$\epsilon = 10^{-2}$	$\epsilon = 10^{-3}$	$\epsilon = 10^{-4}$	After 100 Iterations	Exact
Col. 1	1.969	1.998	2.001	2.000	2.
2	1.489	2.002	2.003	2.003	2.
3	3.476	2.017	1.996	2.002	2.
Col. 4	1.000	1.000	1.000	1.000	1.
5	1.000	1.000	1.000	1.000	1.
6	1.496	1.036	1.005	1.013	1.
Col. 7	2.973	2.999	3.002	3.001	3.
8	3.143	3.013	3.003	3.005	3.
9	3.582	3.049	3.003	3.019	3.
Beam 1	6.016	5.993	5.995	5.995	6.
2	6.160	6.000	5.999	5.999	6.
3	4.675	5.956	5.991	5.981	6.
Beam 4	1.992	2.001	2.002	2.001	2.
5	1.968	1.999	2.001	2.000	2.
6	1.496	1.964	1.995	1.987	2.
No. of Iterations	18	81	124	100	

Table 3.5 Damage Ratios for 2-Bay, 3-Story Frame B

Mode	Natural Periods in sec	
	Initial Elastic	Substitute
1	0.50	0.76
2	0.13	0.18

Table 4.1 Natural Periods for 2-Bay, 2-Story Frame

Displacements in inches						
Level	Centro EW	Centro NS	Taft S69E	Taft N21E	Average	Subst.
1	2.8	2.6	1.3	1.9	2.1	1.8
2	5.3	5.1	2.7	3.6	4.2	3.8

Table 4.2 Displacements for 2-Bay, 2-Story Frame

Natural Periods in sec			
Mode	Initial Elastic	Substitute	Nonlinear Average
1	0.94	1.22	1.04
2	0.30	0.36	
3	0.14	0.16	

Table 4.3 Natural Periods for 3-Bay, 3-Story Frame

Displacements in inches						
Level	Centro EW	Centro NS	Taft S69E	Taft N21E	Average	Subst
1	3.0	2.4	1.8	1.6	2.2	2.2
2	6.7	5.2	3.8	3.0	4.7	5.0
3	10.6	7.9	6.2	5.2	7.5	8.0

Table 4.4 Displacements for 3-Bay, 3-Story Frame

Mode	Natural Periods in sec		
	Initial Elastic	Substitute	Nonlinear Average
1	1.08	1.85	1.65
2	0.37	0.84	
3	0.21	0.38	
4	0.15	0.28	
5	0.10	0.17	
6	0.077	0.13	

Table 4.5 Natural Periods for 1-Bay, 6-Story Frame

Level	Displacements in inches					
	Centro EW	Centro NS	Taft S69E	Taft N21E	Average	Subst
1	3.7	0.74	1.4	2.4	2.1	0.71
2	8.2	1.7	3.3	4.8	4.5	2.1
3	12.0	3.0	4.8	6.1	6.5	2.9
4	14.5	4.5	6.7	6.6	8.1	3.3
5	17.0	6.5	9.4	6.9	10.0	6.8
6	19.3	8.4	11.6	7.2	11.6	8.6

Table 4.6 Displacements for 1-Bay, 6-Story Frame

Mode	Natural Periods in sec		
	Initial Elastic	Substitute	Nonlinear Average
1	1.07	1.66	1.25
2	0.34	0.48	
3	0.19	0.24	
4	0.12	0.14	
5	0.090	0.096	
6	0.075	0.076	

Table 4.7 Natural Periods for 3-Bay, 6-Story Frame

Level	Displacements in inches					
	Centro EW	Centro NS	Taft S69E	Taft N21E	Average	Subst
1	1.3	1.1	1.3	0.98	1.2	1.1
2	3.5	2.9	3.1	2.5	3.0	3.0
3	5.9	4.5	4.5	3.7	4.7	5.0
4	7.9	5.5	5.8	4.6	6.0	6.7
5	9.2	6.1	6.6	5.1	6.8	7.9
6	9.8	6.3	7.3	5.4	7.2	8.8

Table 4.8 Displacements for 3-Bay, 6-Story Frame

Mode	Natural Periods in sec	
	Initial Elastic	Substitute
1	1.07	2.24
2	0.34	0.63
3	0.19	0.29
4	0.12	0.16
5	0.090	0.11
6	0.075	0.078

Table 5.1 Natural Periods for 3-Bay, 6-Story Frame A - Spectrum B

Level	Displacements in inches	
	Substitute	Nonlinear
1	1.4	1.6
2	5.2	4.5
3	9.4	8.0
4	13.3	10.9
5	16.8	13.1
6	19.7	14.0

Table 5.2 Displacements for 3-Bay, 6-Story Frame A - Spectrum B

Mode	Natural Periods in sec	
	Initial Elastic	Substitute
1	0.86	1.20
2	0.27	0.34
3	0.15	0.17
4	0.099	0.11
5	0.073	0.076
6	0.060	0.061

Table 5.3 Natural Periods for 3-Bay, 6-Story Frame B - Spectrum B

Level	Displacements in inches	
	Substitute	Nonlinear
1	1.1	1.2
2	3.3	3.3
3	5.5	5.5
4	7.4	7.4
5	8.7	8.5
6	9.4	9.1

Table 5.4 Displacements for 3-Bay, 6-Story Frame B - Spectrum B

Mode	Natural Periods in sec	
	Initial Elastic	Substitute
1	0.86	1.20
2	0.27	0.34
3	0.15	0.17
4	0.099	0.11
5	0.073	0.076
6	0.060	0.061

Table 5.5 Natural Periods for 3-Bay, 6-Story Frame B - Spectrum A

Level	Displacements in inches					
	Centro EW	Centro NS	Taft S69E	Taft N21E	Average	Subst
1	1.3	1.1	1.1	0.95	1.1	0.94
2	3.4	2.8	2.9	2.6	2.9	2.6
3	5.4	4.3	4.5	4.1	4.6	4.3
4	6.9	5.4	5.6	5.2	5.8	5.5
5	7.7	6.0	6.2	5.9	6.4	6.4
6	8.0	6.3	6.4	6.1	6.7	6.8

Table 5.6 Displacements for 3-Bay, 6-Story Frame B -
Spectrum A

Mode	Natural Periods in sec			
	Initial Elastic	Modified Subst. Str. Analysis		
		Smooth Spectrum	Centro EW Spectrum	Taft S69E Spectrum
1	0.86	1.20	1.32	1.23
2	0.27	0.34	0.36	0.34
3	0.15	0.17	0.18	0.18
4	0.099	0.11	0.11	0.11
5	0.073	0.076	0.076	0.076
6	0.060	0.061	0.061	0.061

Table 5.7 Natural Periods for 3-Bay, 6-Story Frame B --
El Centro EW Spectrum and Taft S69E Spectrum

Displacements in inches			
Level	Substitute Structure		Nonlinear El Centro EW
	Smooth Spectrum	El Centro EW Spectrum	
1	0.94	1.1	1.3
2	2.6	3.2	3.4
3	4.3	5.4	5.4
4	5.5	7.2	6.9
5	6.4	8.4	7.7
6	6.8	9.0	8.0

Table 5.8 Displacements for 3-Bay, 6-Story Frame B -
El Centro EW Spectrum

Displacements in inches			
Level	Substitute Structure		Nonlinear Taft S69E
	Smooth Spectrum	Taft S69E Spectrum	
1	0.94	0.98	1.1
2	2.6	2.8	2.8
3	4.3	4.5	4.3
4	5.5	5.8	5.4
5	6.4	6.8	6.0
6	6.8	7.3	6.3

Table 5.9 Displacements for 3-Bay, 6-Story Frame B -
Taft S69E Spectrum

Natural Periods in sec				
Mode	Initial Elastic	Modified Subst. Str. Analysis		
		Smooth Spectrum	Centro EW Spectrum	Taft S69E Spectrum
1	1.07	1.66	2.04	1.82
2	0.34	0.48	0.58	0.52
3	0.19	0.24	0.28	0.25
4	0.12	0.14	0.16	0.15
5	0.090	0.096	0.11	0.098
6	0.075	0.076	0.082	0.076

Table 5.10 Natural Periods for 3-Bay, 6-Story Frame A -
El Centro EW Spectrum and Taft S69E Spectrum

Displacements in inches			
Level	Substitute Structure		Nonlinear El Centro EW
	Smooth Spectrum	El Centro EW Spectrum	
1	1.1	1.5	1.3
2	3.0	4.8	3.5
3	5.0	8.4	5.9
4	6.7	11.6	7.9
5	7.9	14.3	9.2
6	8.8	16.4	9.8

Table 5.11 Displacements for 3-Bay, 6-Story Frame A -
El Centro EW Spectrum

Level	Displacements in inches		
	Substitute Structure		Nonlinear Taft S69E
	Smooth Spectrum	Taft S69E Spectrum	
1	1.1	1.3	1.3
2	3.0	3.9	3.1
3	5.0	6.7	4.5
4	6.7	9.2	5.8
5	7.9	11.2	6.6
6	8.8	12.4	7.3

Table 5.12 Displacements for 3-Bay, 6-Story Frame A -
Taft S69E Spectrum

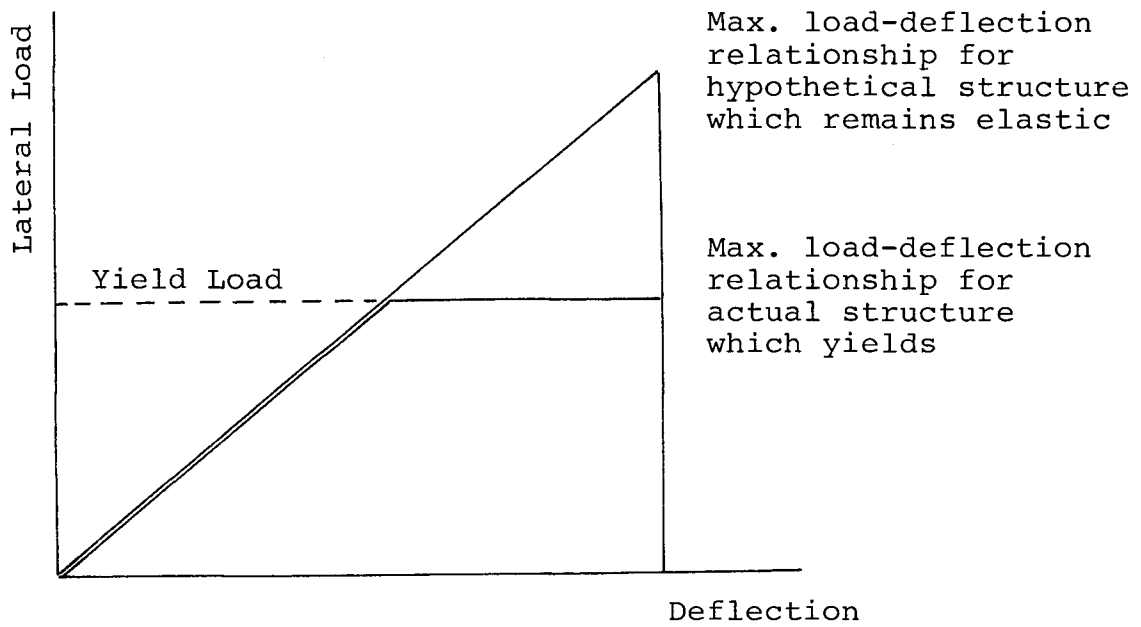


Fig. 1.1 Load-Deflection Curve for Elastic and Elasto-Plastic Structure

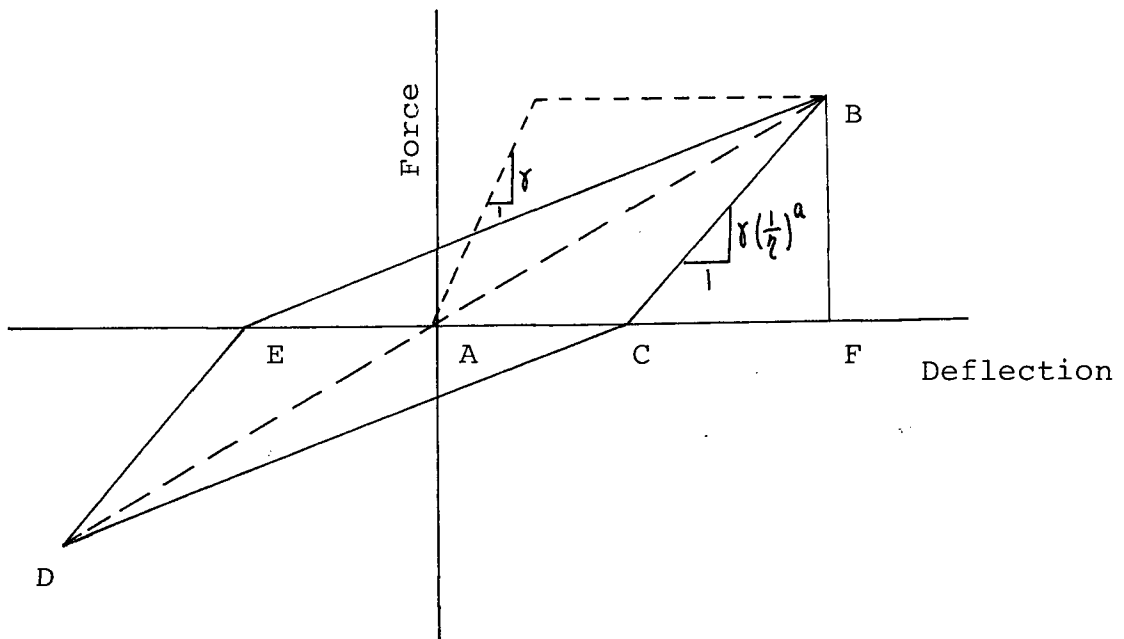


Fig. 2.1 Idealized Hysteresis Loop for Reinforced Concrete System

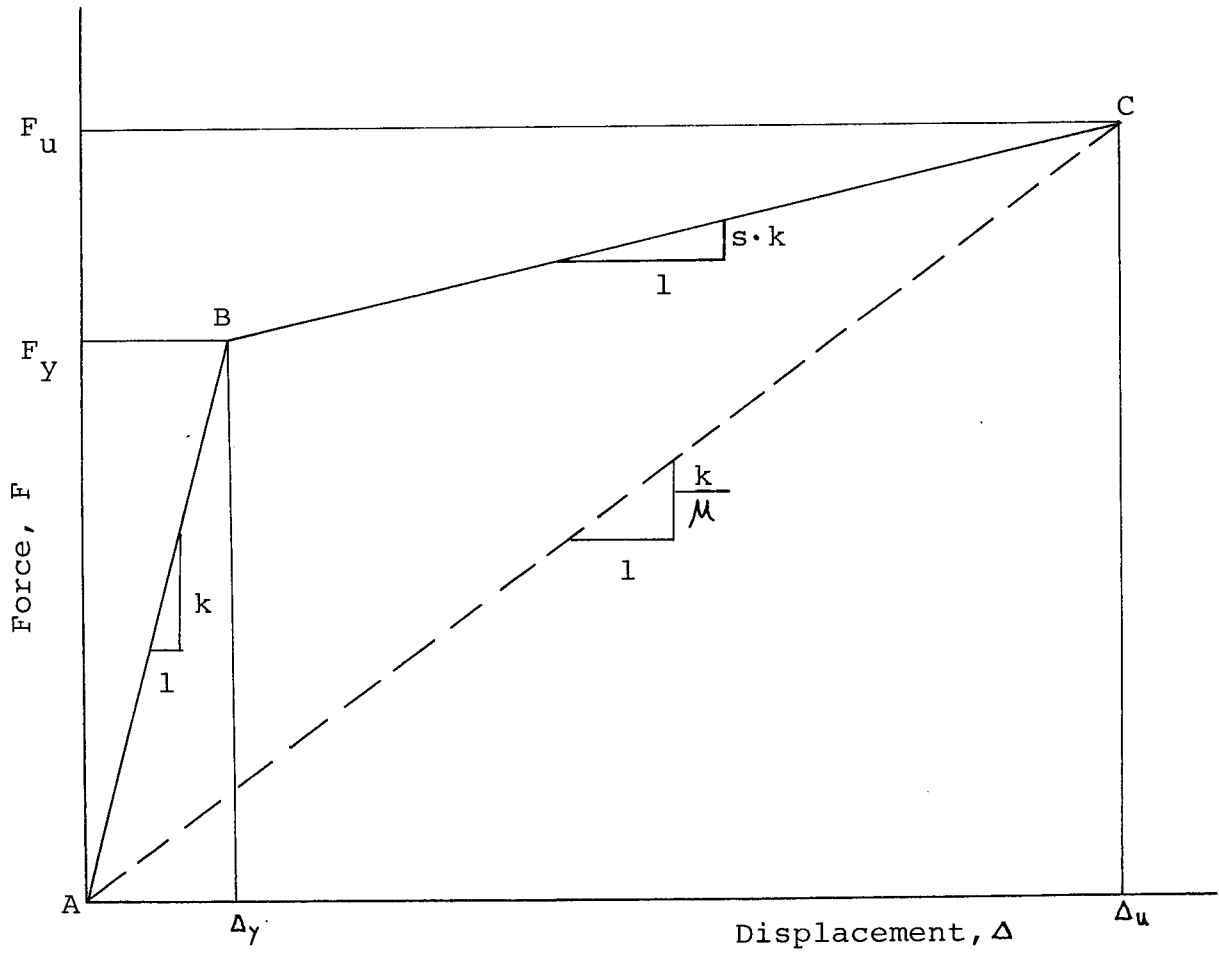


Fig. 2.2 Force-Displacement Curve - Definition of Damage Ratio

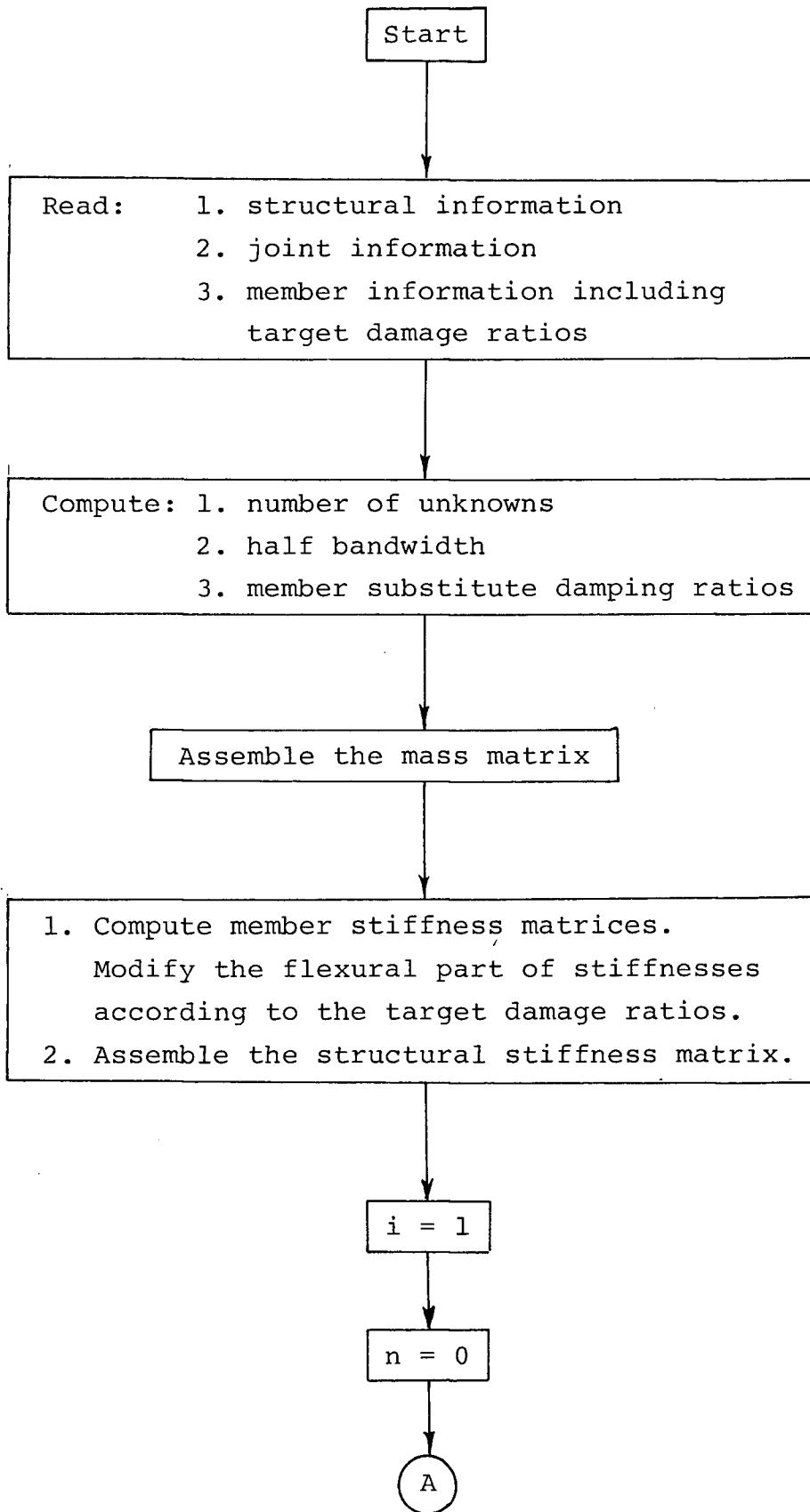


Fig. 2.3 Flow Diagram for Substitute Structure Method

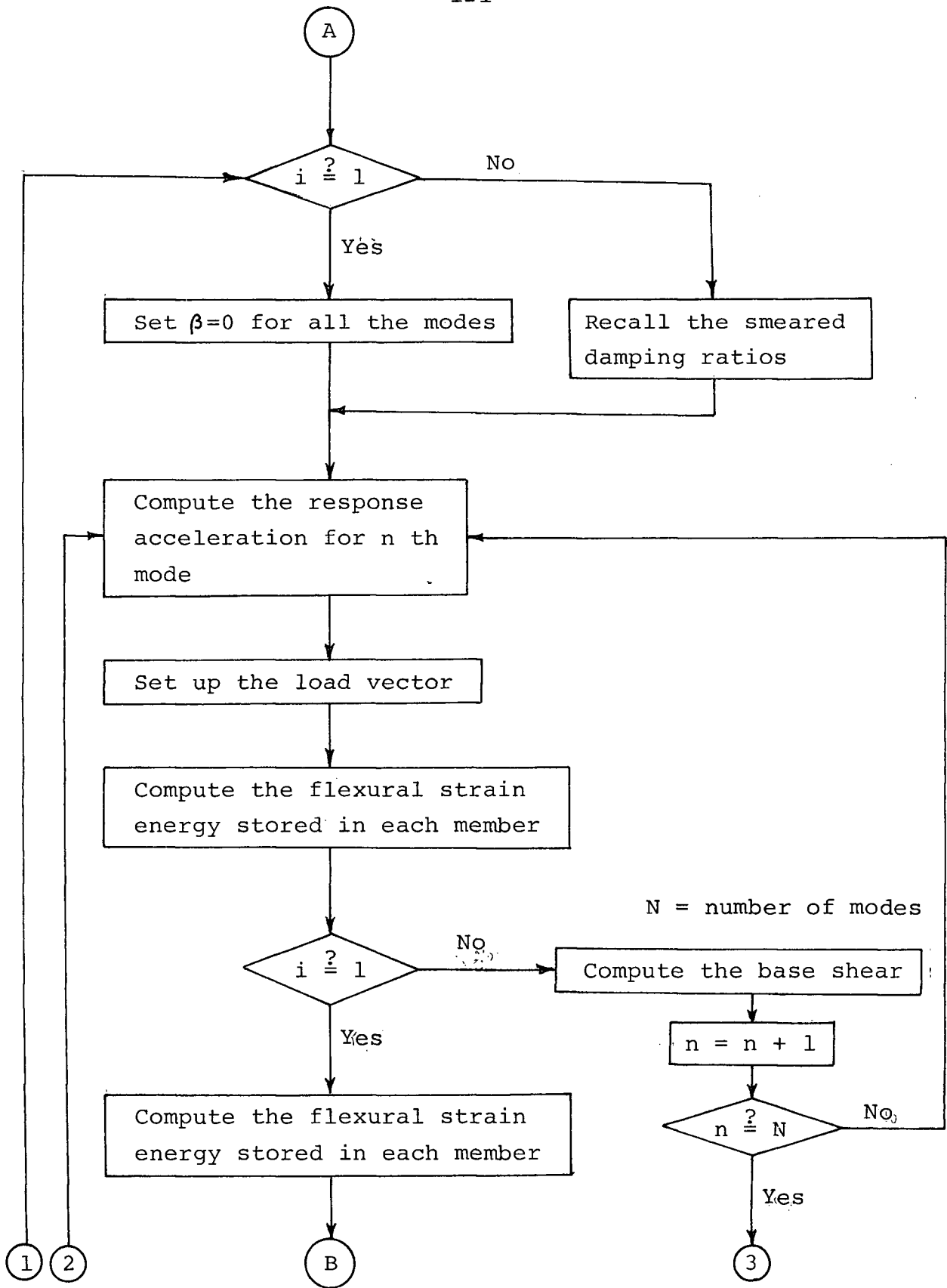


Fig. 2.3 Flow Diagram for Substitute Structure Method

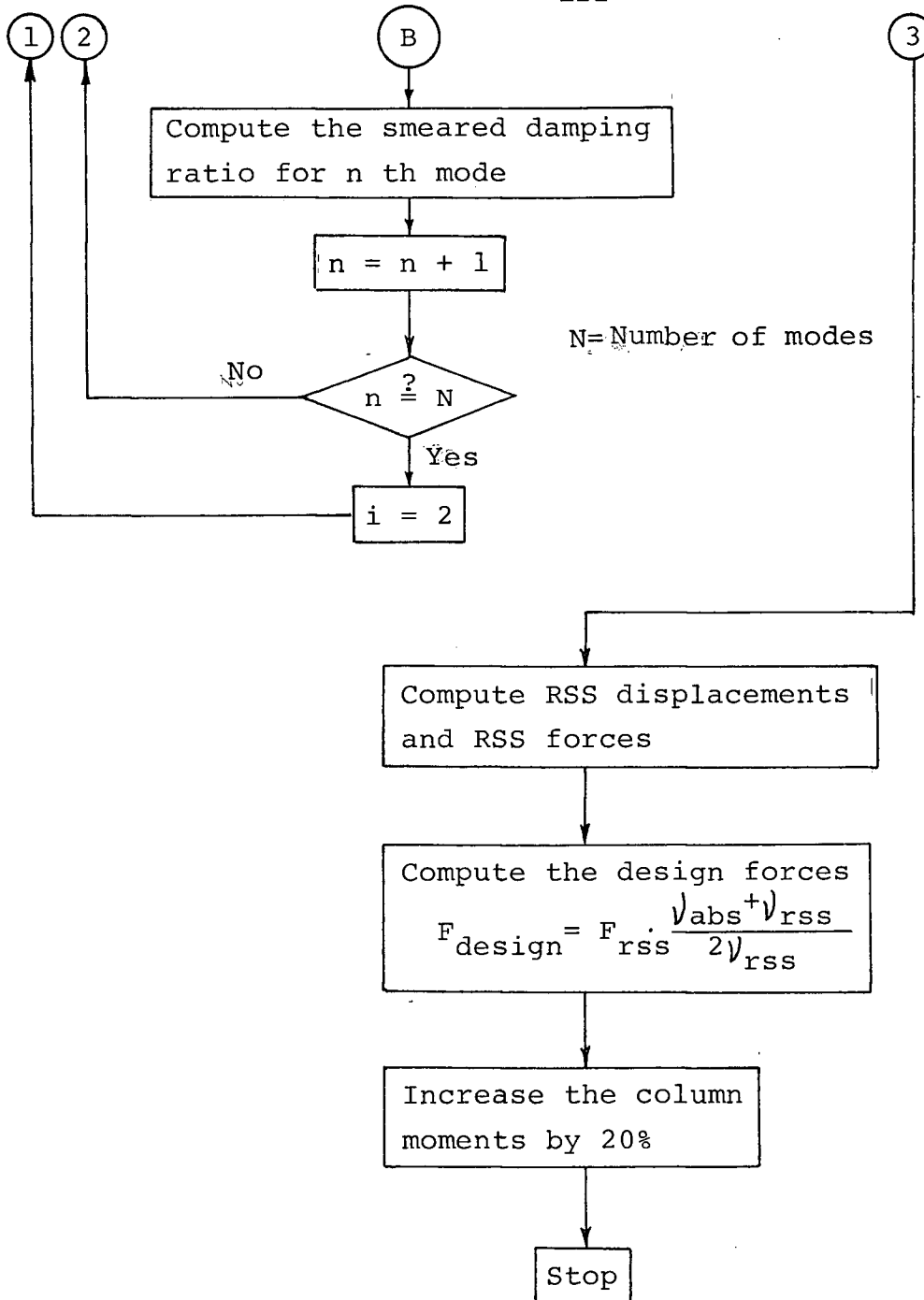


Fig. 2.3 Flow Diagram for Substitute Structure Method

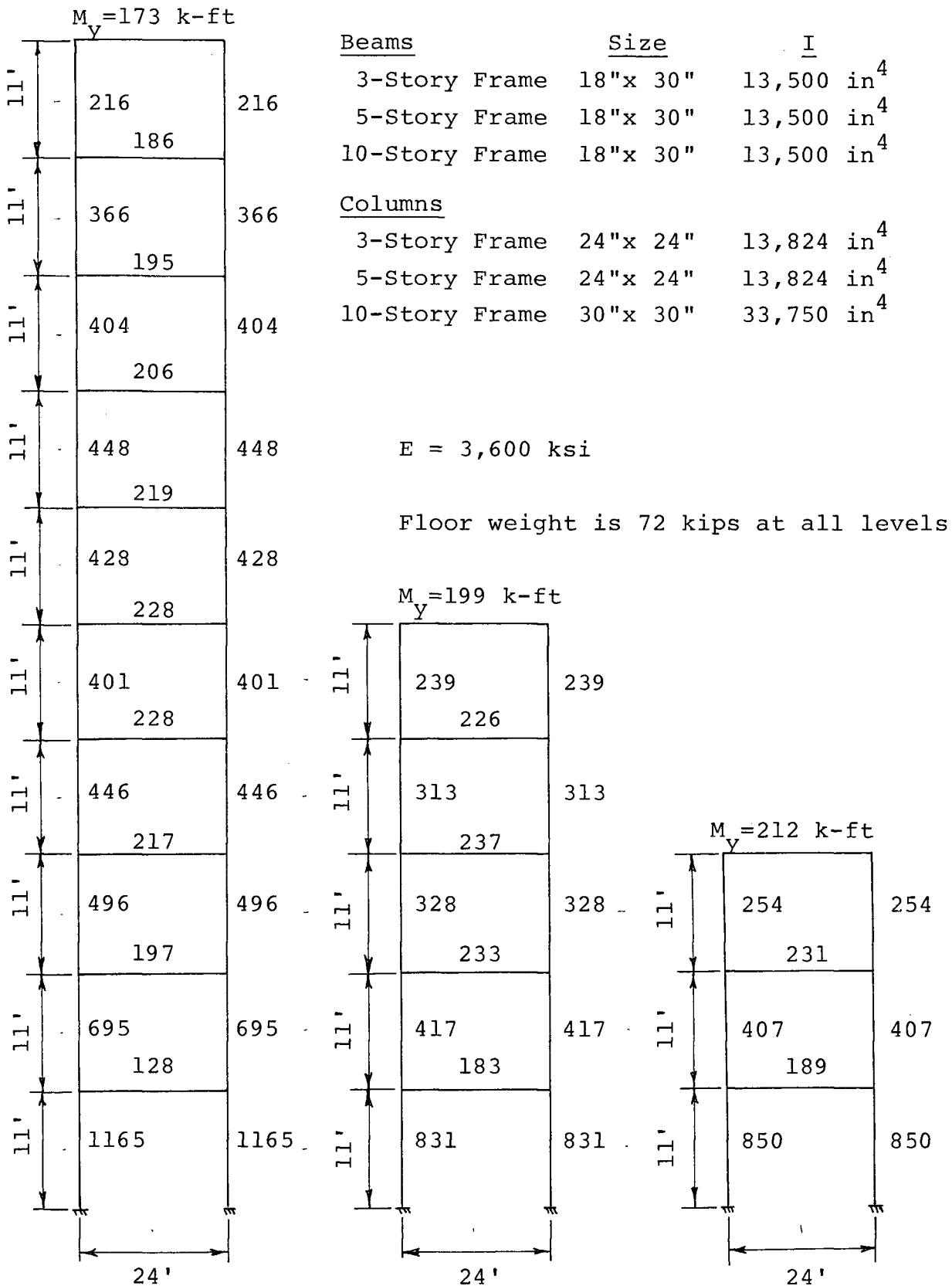
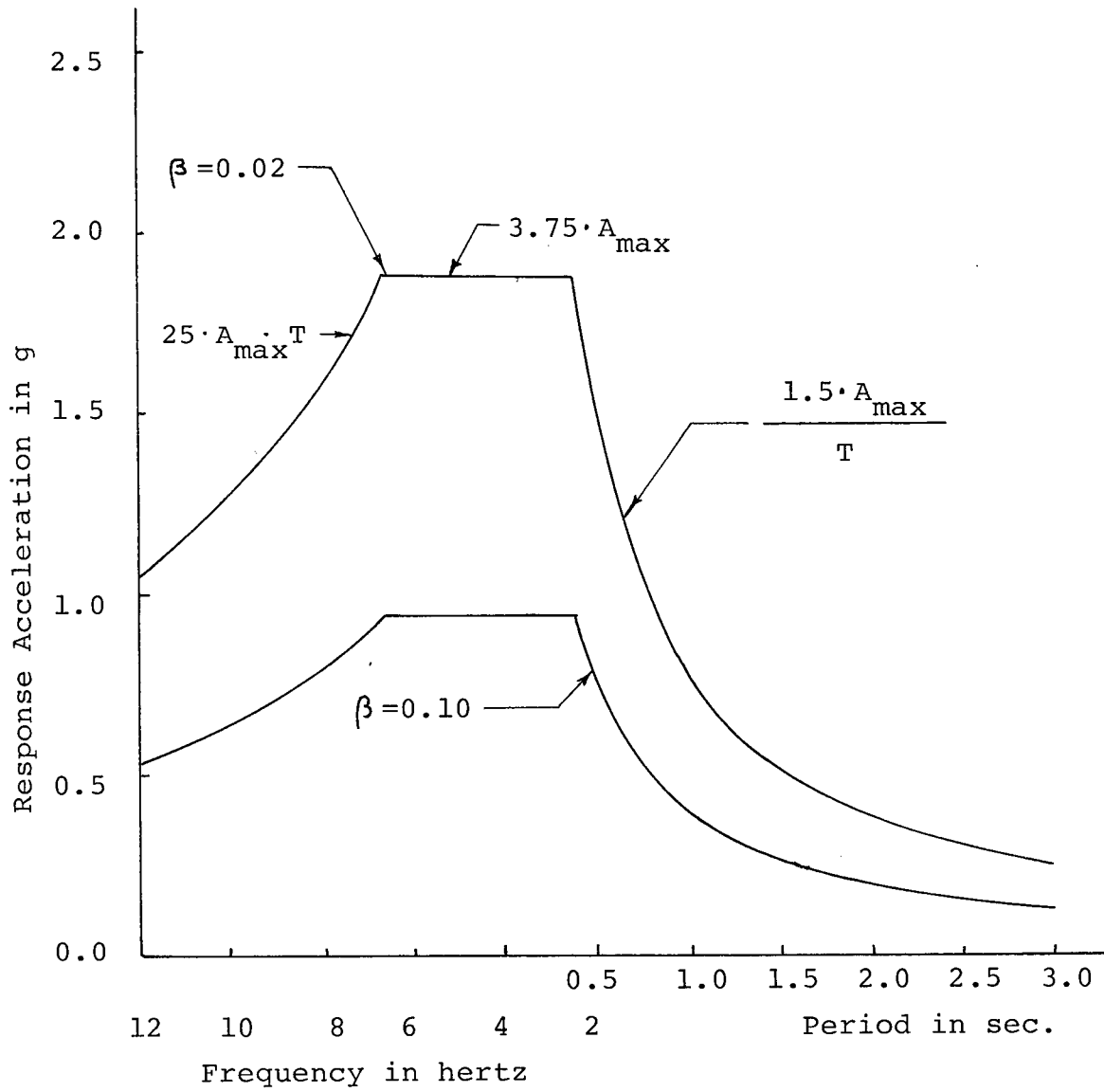
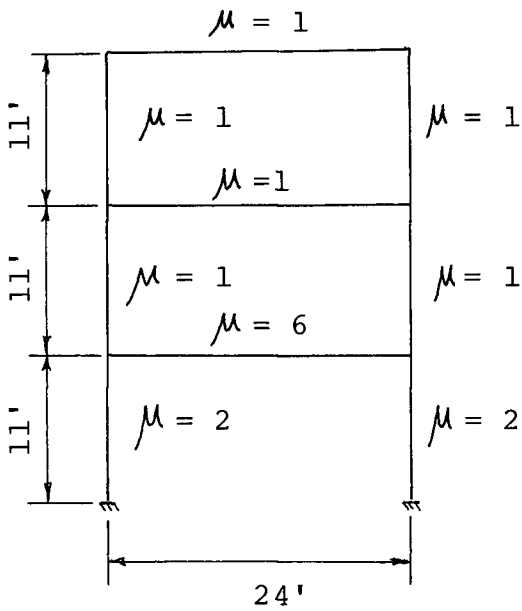


Fig. 2.4 Member Properties and Design Moments for 3-, 5-, 10-Story Frames



$$\frac{\text{Response Acceleration for}}{\text{Response Acceleration for } \beta=0.02} = \frac{8}{6 + 100\beta}$$

Fig. 2.5 Smoothed Response Spectrum - Design Spectrum A



$W = 72$ kips

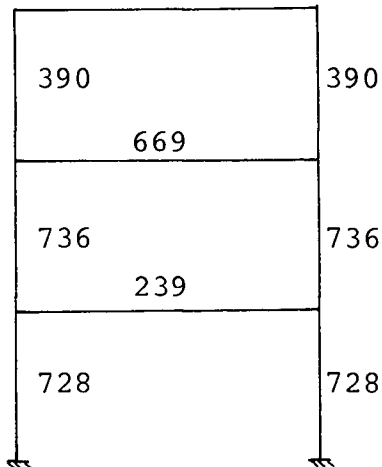
$W = 72$ kips

$W = 72$ kips

μ = Target damage ratio

$M_Y = 325$ k-ft

$E = 3600$ ksi



Yield Moments

		Size	I
<u>Columns</u>	1st Story	24" x 24"	10,368 in ⁴
	2nd Story	24" x 24"	13,824 in ⁴
	3rd Story	24" x 24"	13,824 in ⁴
<u>Beams</u>		18" x 30"	13,500 in ⁴

Fig. 2.6 Soft Story Frame A - Member Properties and Yield Moments

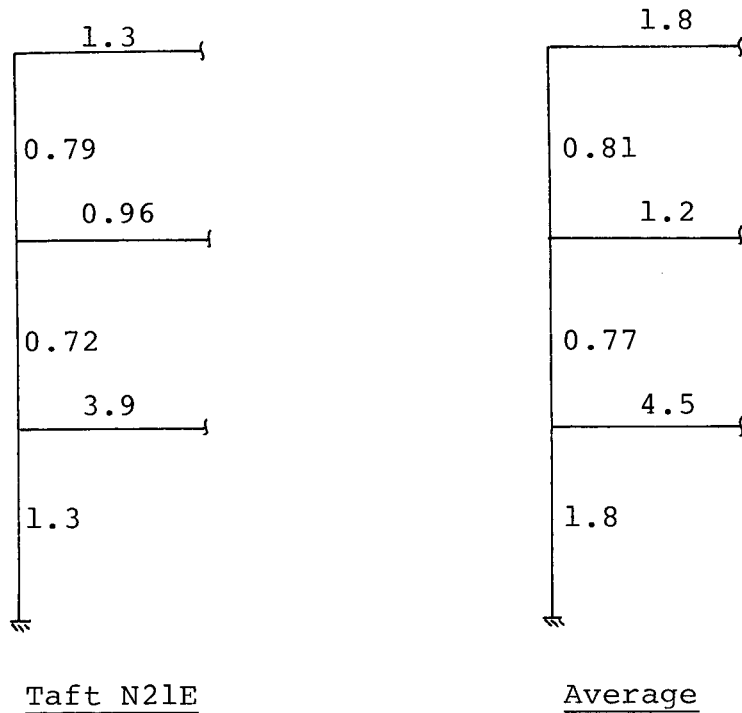
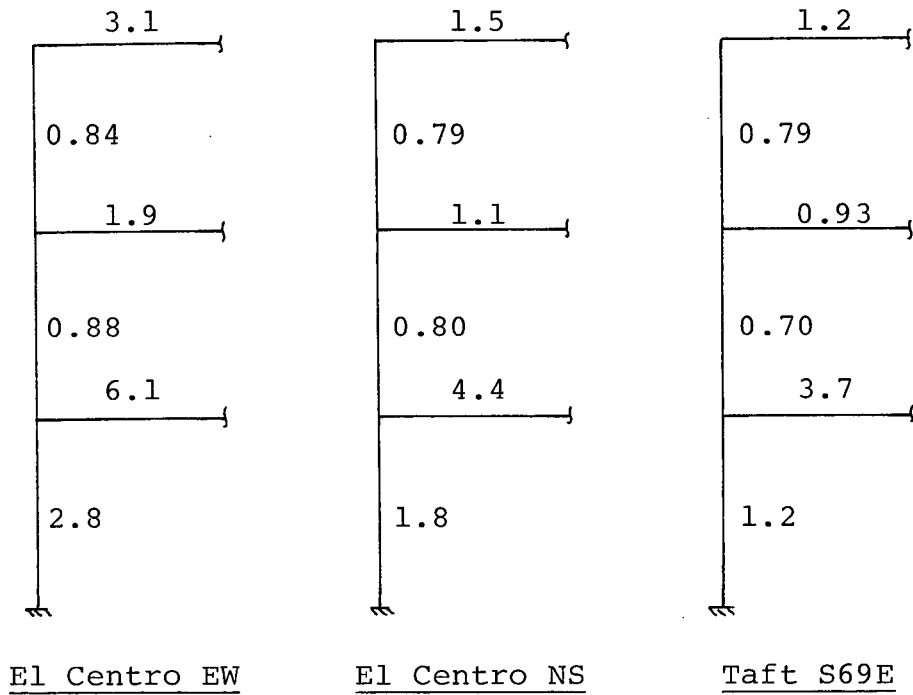


Fig. 2.7 Soft Story Frame A - Damage Ratios for Individual Earthquakes

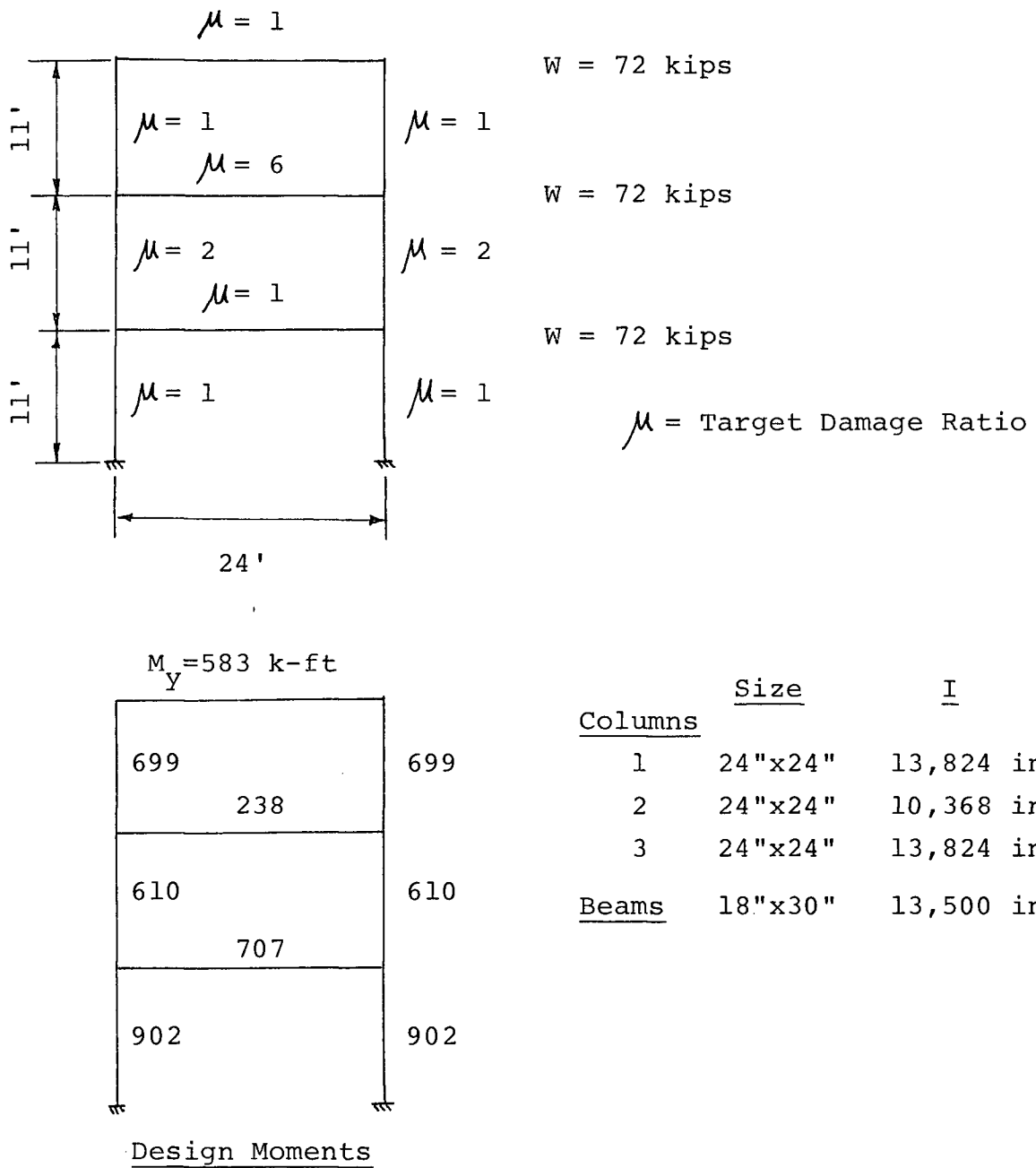


Fig. 2.8 Soft Story Frame B - Member Properties and Yield Moments

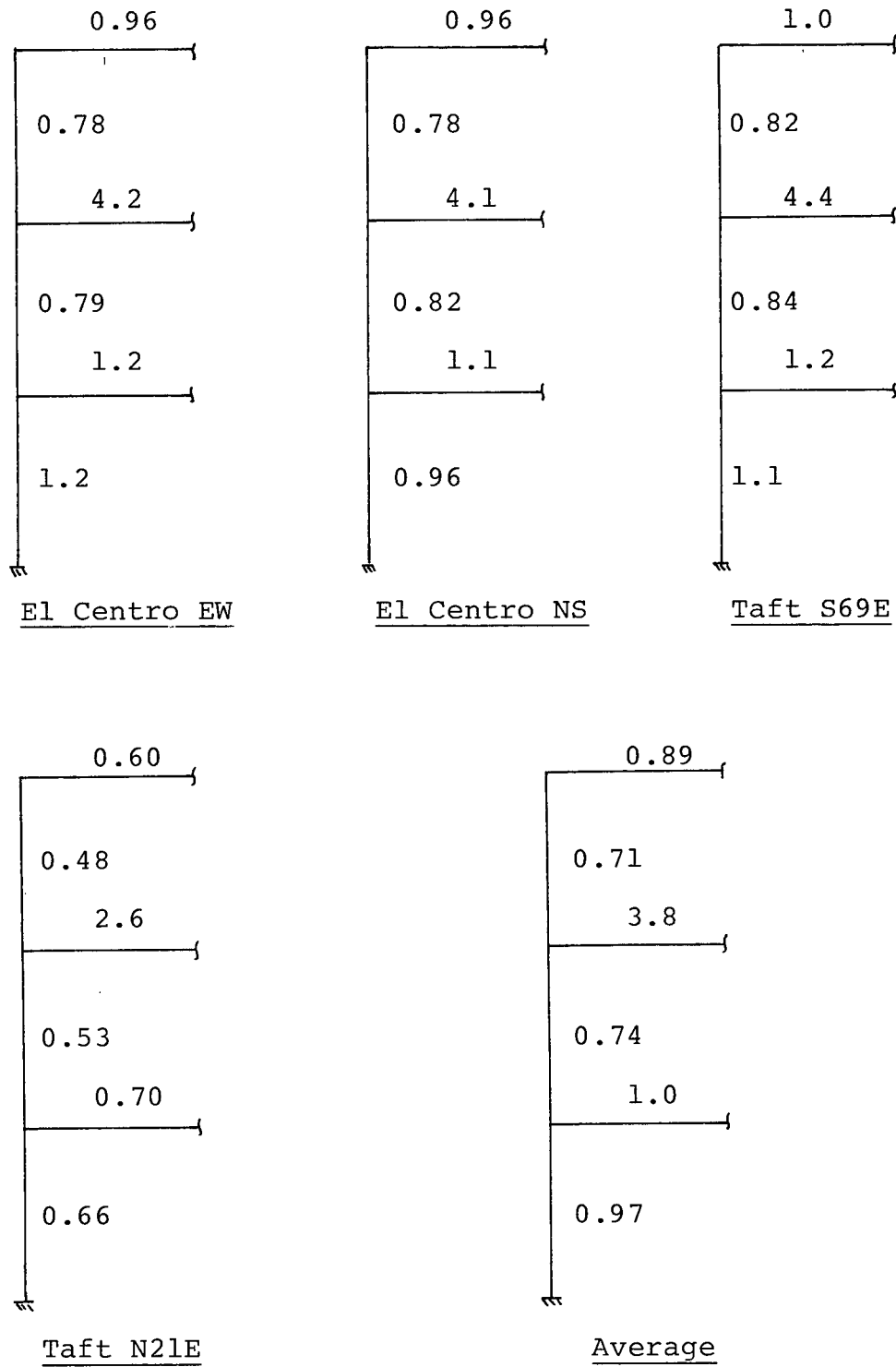
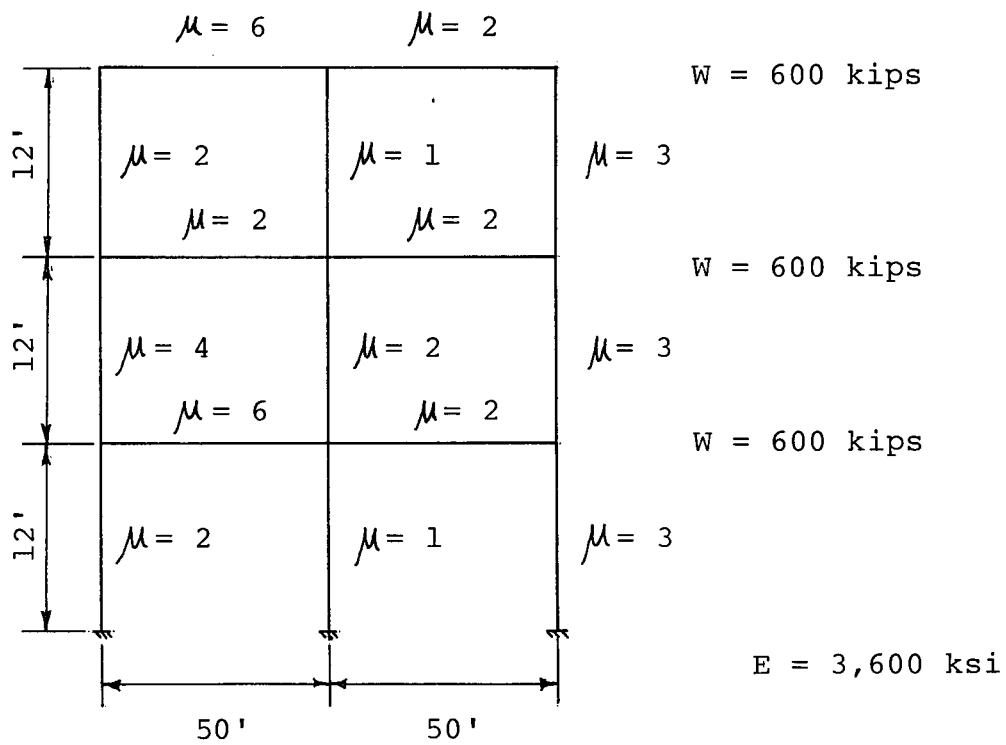


Fig. 2.9 Soft Story Frame B - Damage Ratios for Individual Earthquakes


 $M_y = 339$ k-ft

745

478	1061	614
962	1069	
610	1288	823
524	1323	
1127	2513	938

Yield Moments

	<u>Size</u>	<u>I</u>
Columns	21" x 21"	16,000 in ⁴
Beams	20" x 36"	40,000 in ⁴

Fig. 2.10 2-Bay, 3-Story Frame - Member Properties and Yield Moments

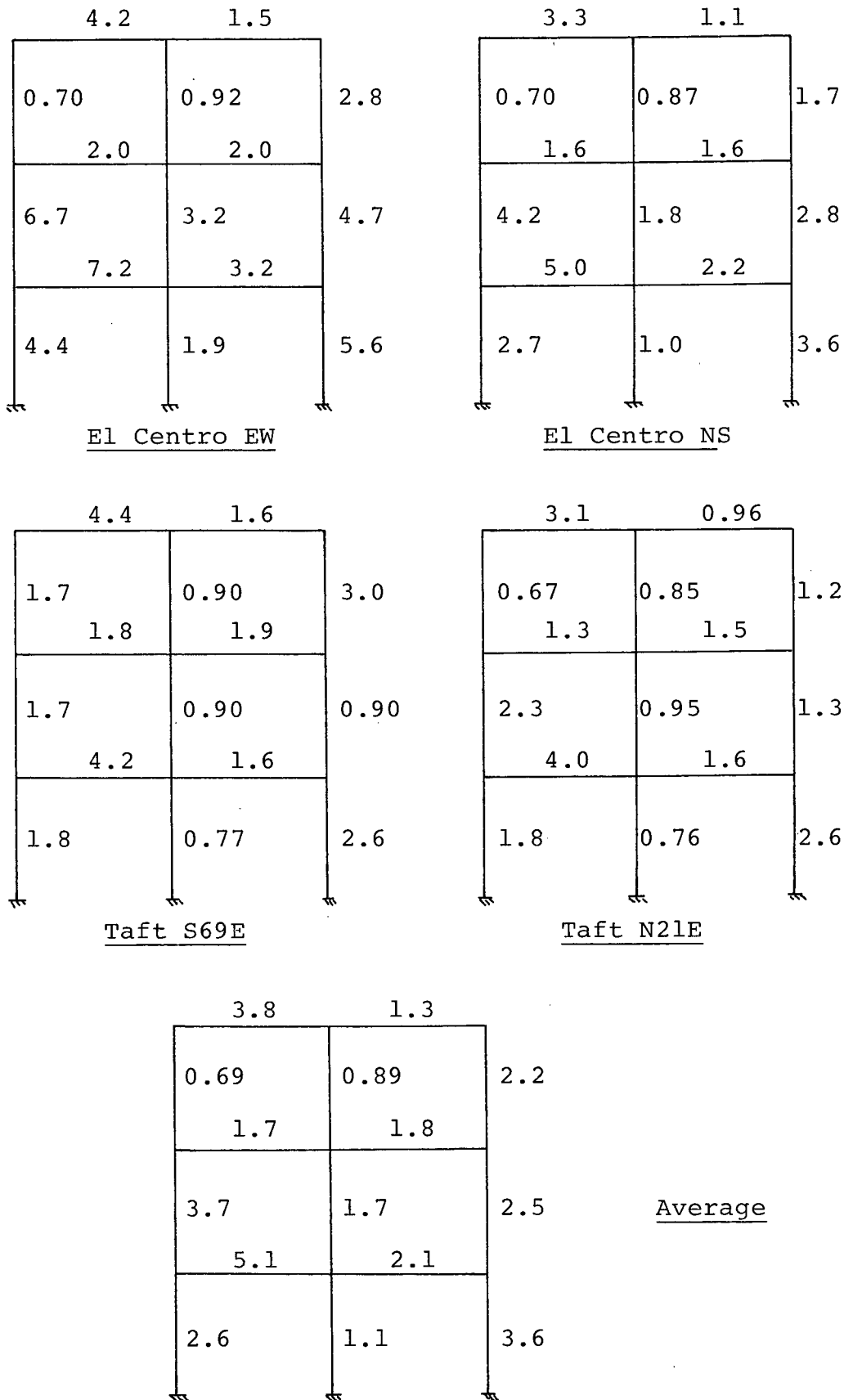


Fig. 2.11 2-Bay, 3-Story Frame - Damage Ratios for Individual Earthquakes

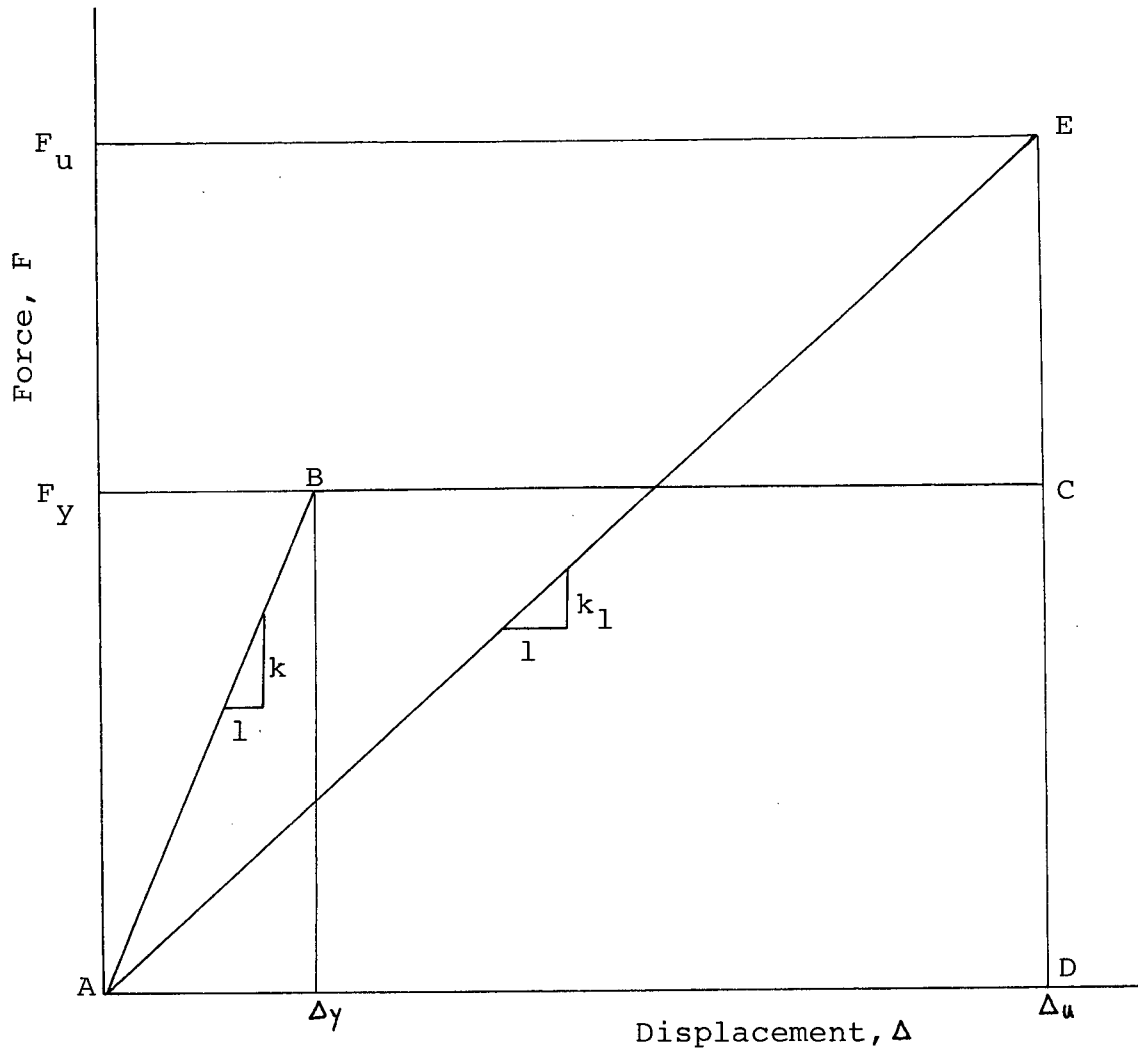


Fig. 2.12 Force-Displacement Curve - Definition of Equal-Area Stiffness

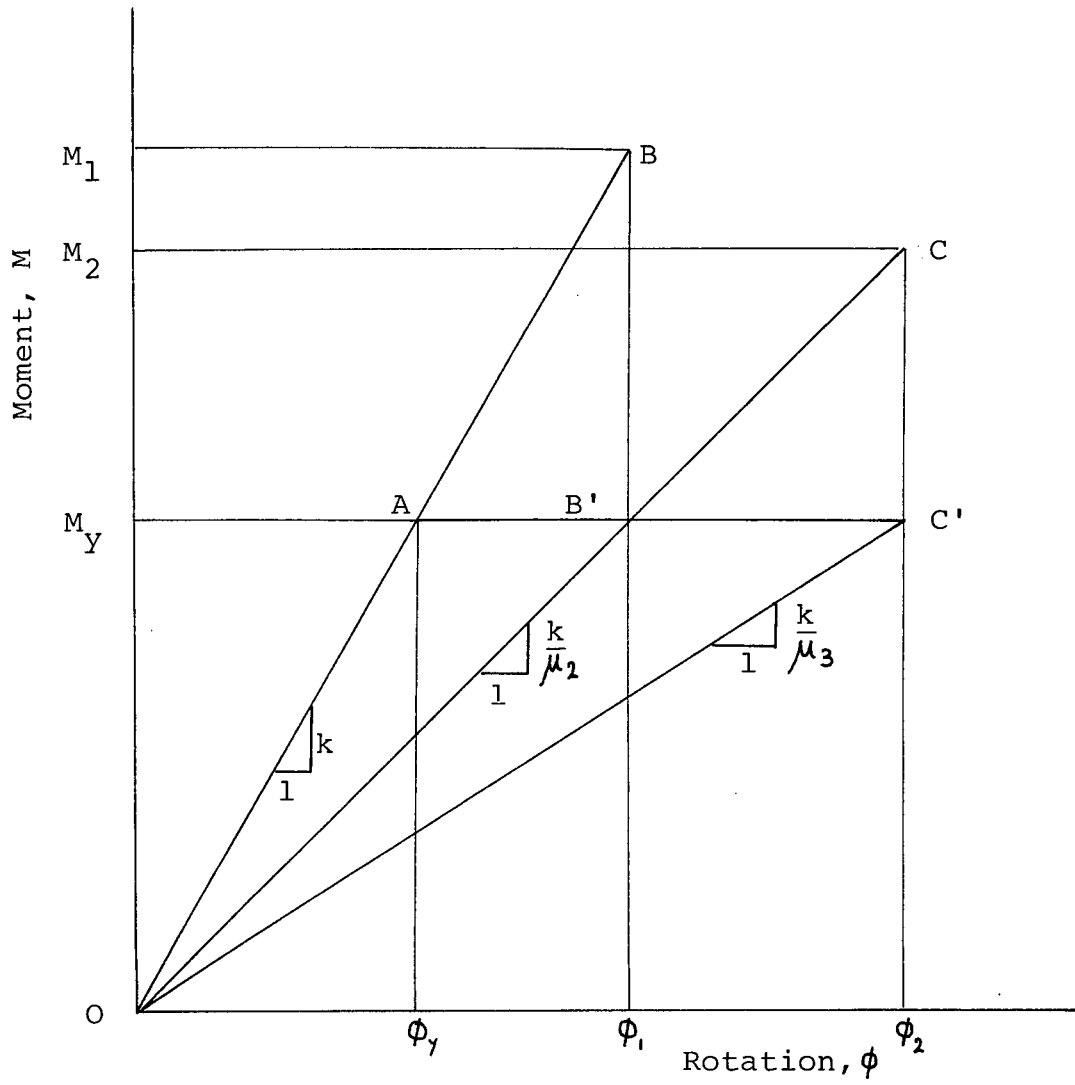


Fig. 3.1 Moment-Rotation Curve - Modification of Damage Ratio

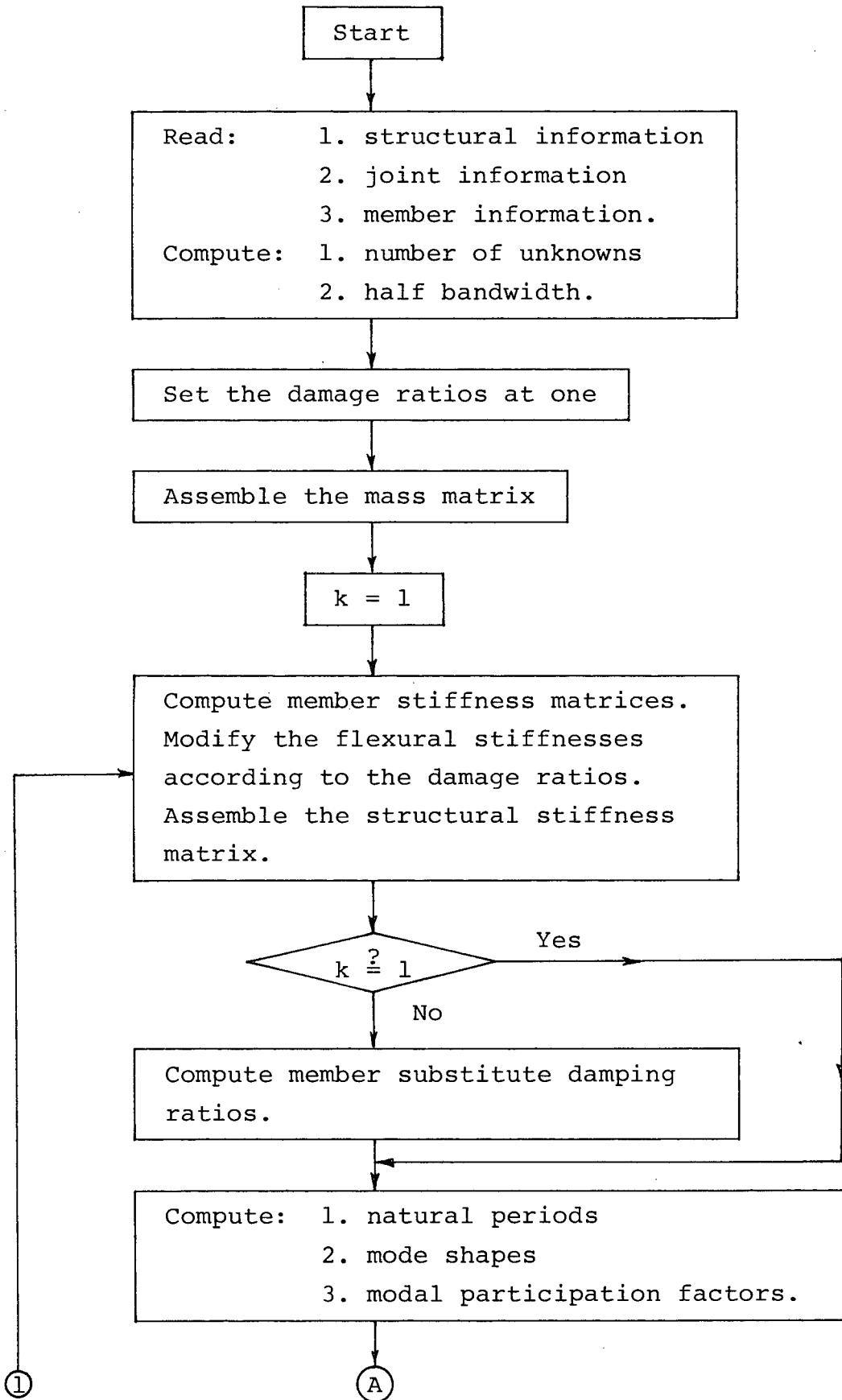


Fig. 3.2 Flow Diagram for Modified Substitute Structure Method

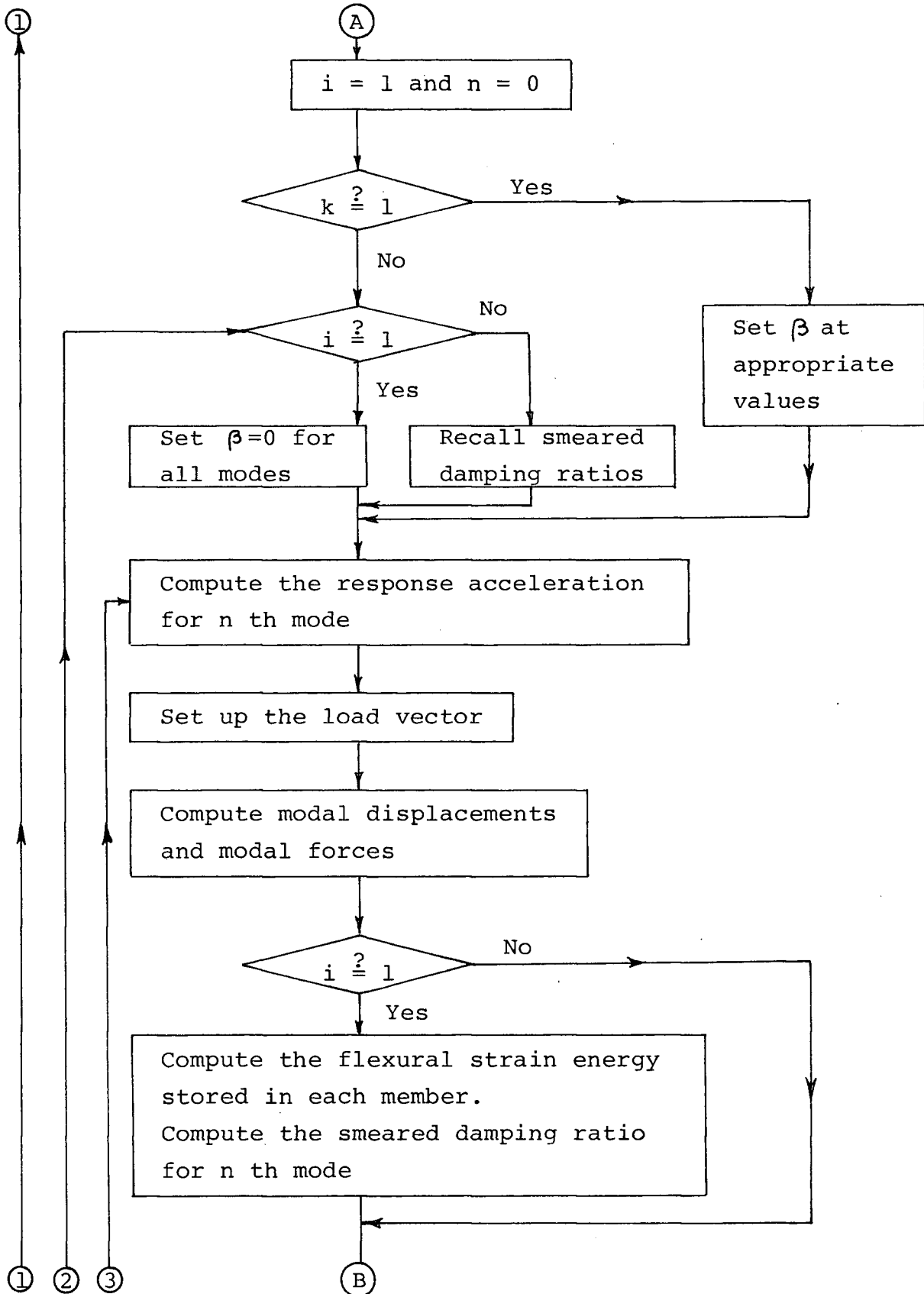


Fig. 3.2 Flow Diagram for Modified Substitute Structure Method

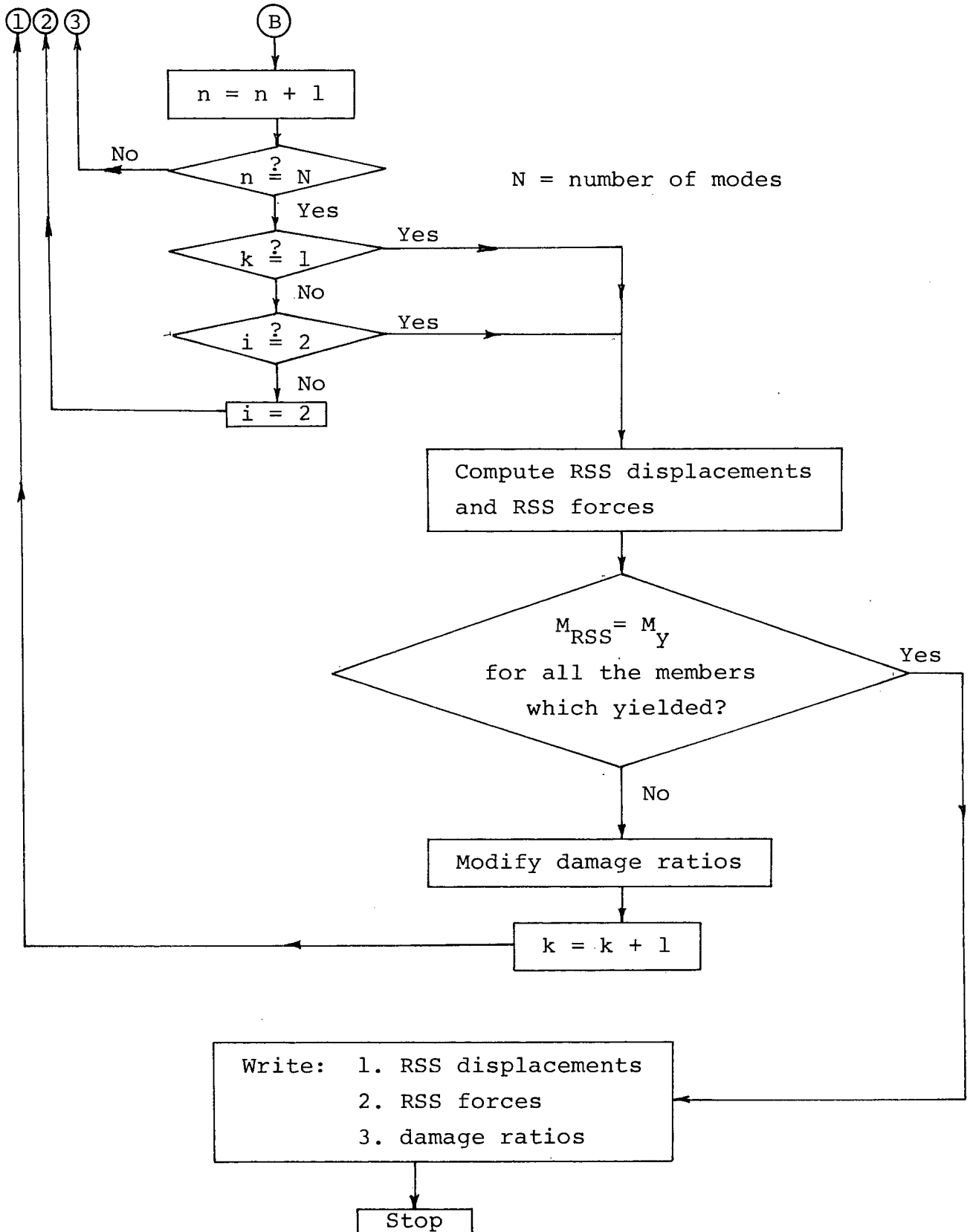
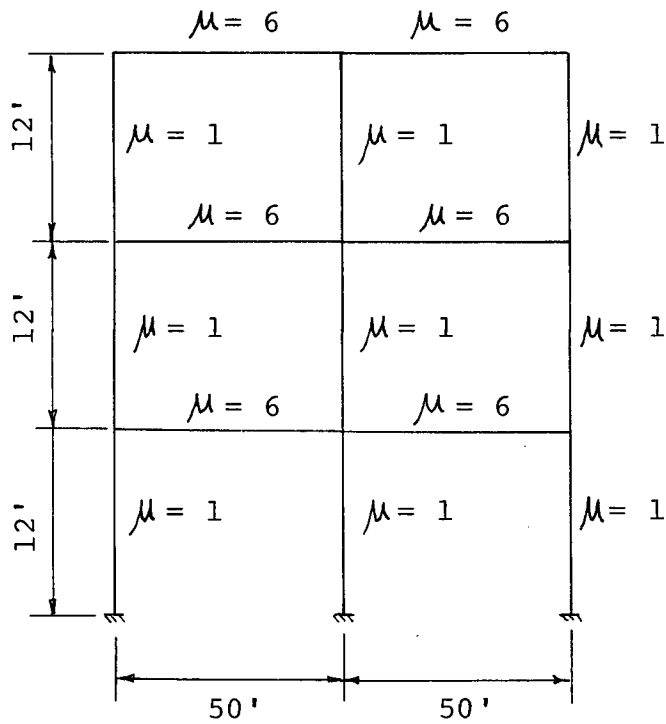


Fig 3.2 Flow Diagram for Modified Substitute Structure Method



$W = 600$ kips

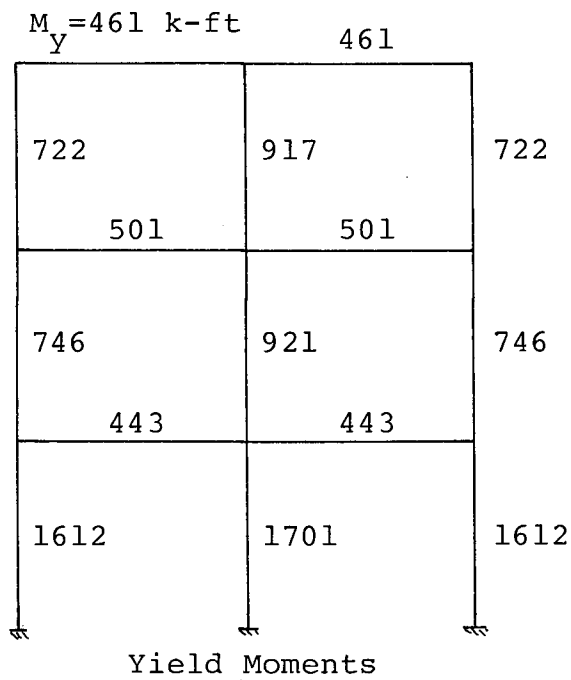
$W = 600$ kips

$\mu = \text{Target Damage Ratio}$

$W = 600$ kips

$E = 3,600$ ksi

	<u>Columns</u>	<u>Beams</u>
Size	21" x 21"	20" x 36"
I	16,000 in ⁴	40,000 in ⁴



Natural Periods

Mode 1 1.804 sec.

Mode 2 0.438 sec.

Mode 3 0.193 sec.

Fig. 3.3 2-Bay, 3-Story Frame A - Member Properties and Yield Moments

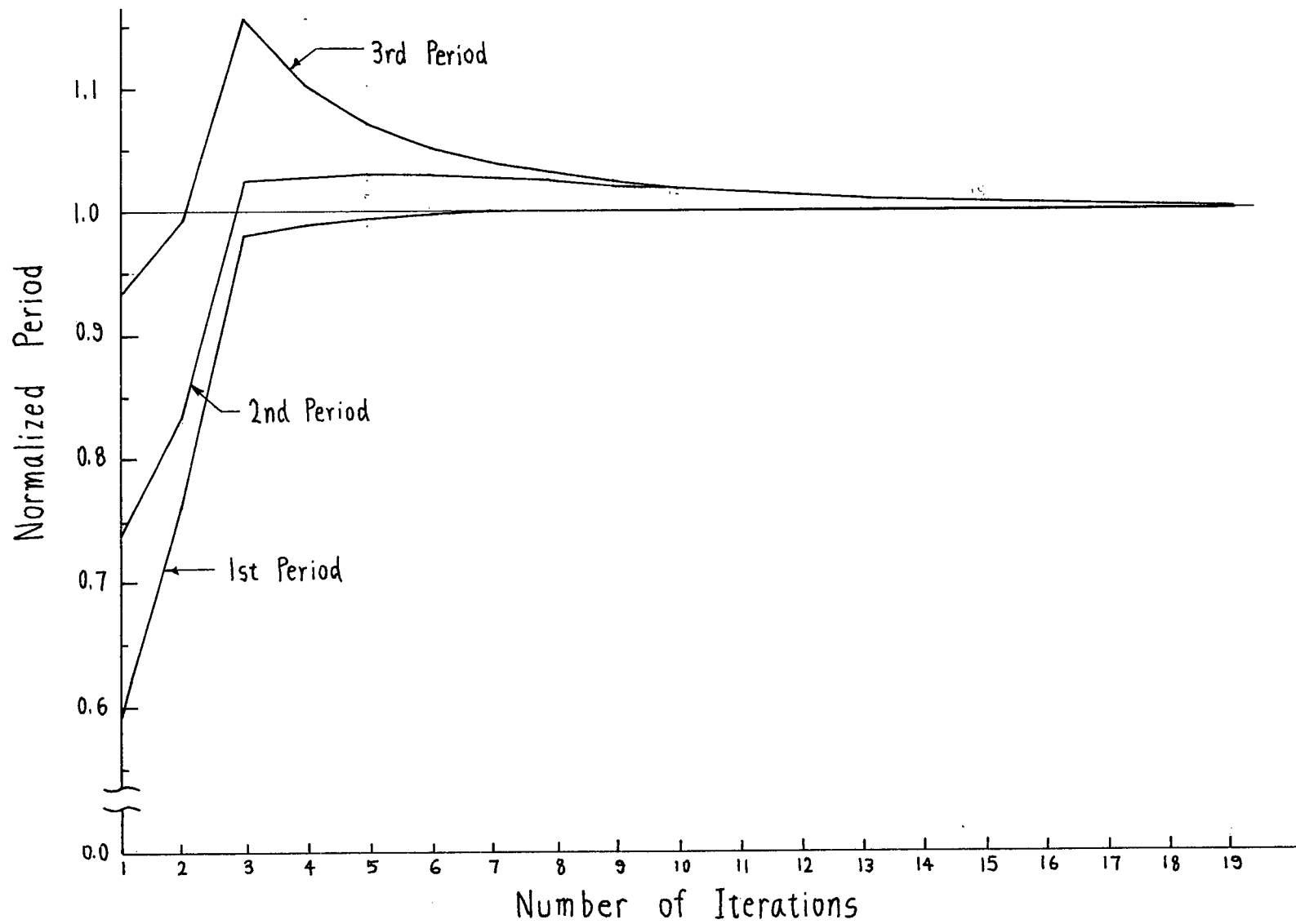


Fig. 3.4 2-Bay, 3-Story Frame A - Plot of Periods vs. Number of Iterations

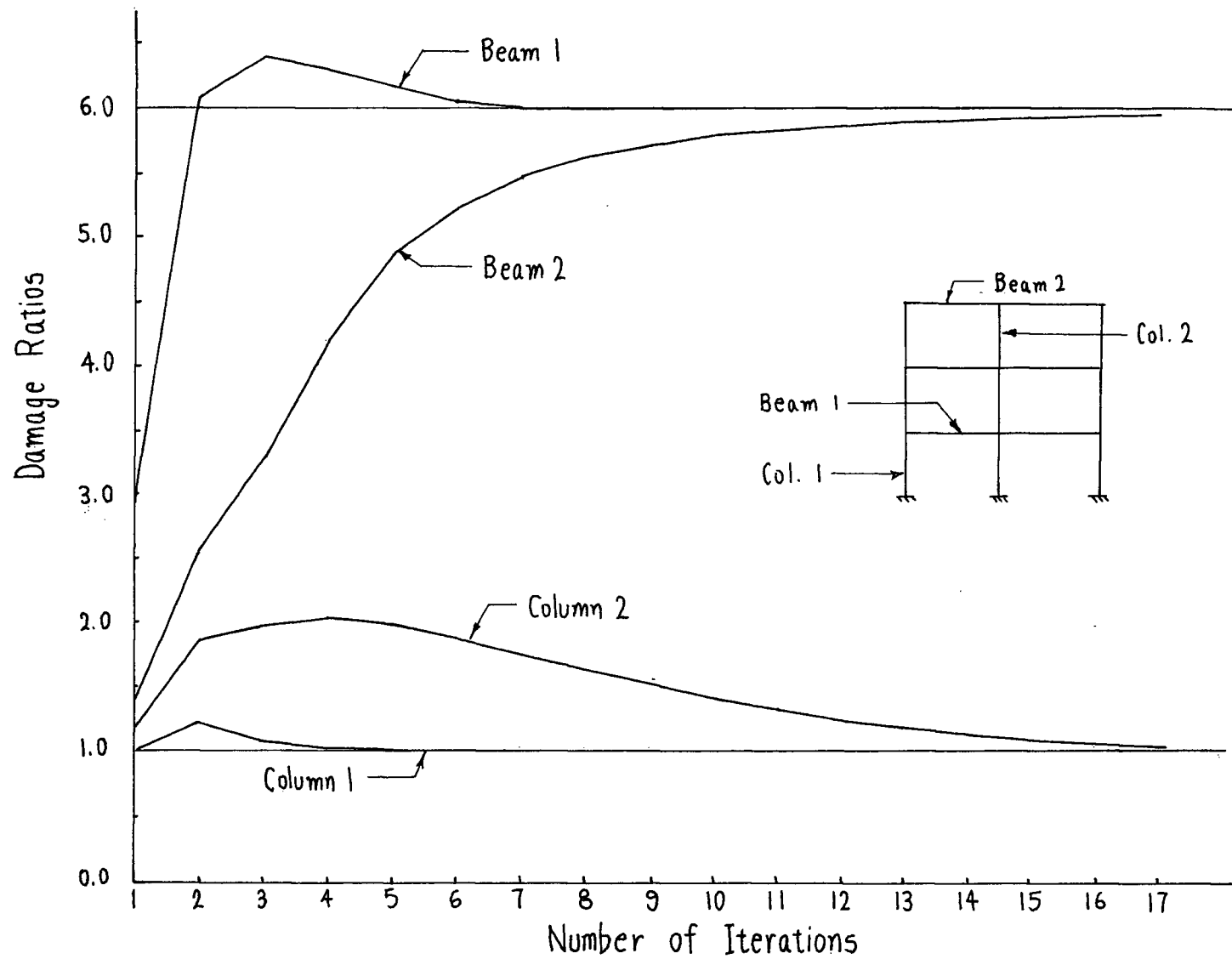


Fig. 3.5 2-Bay, 3-Story Frame - Plot of Damage Ratios vs. Number of Iterations

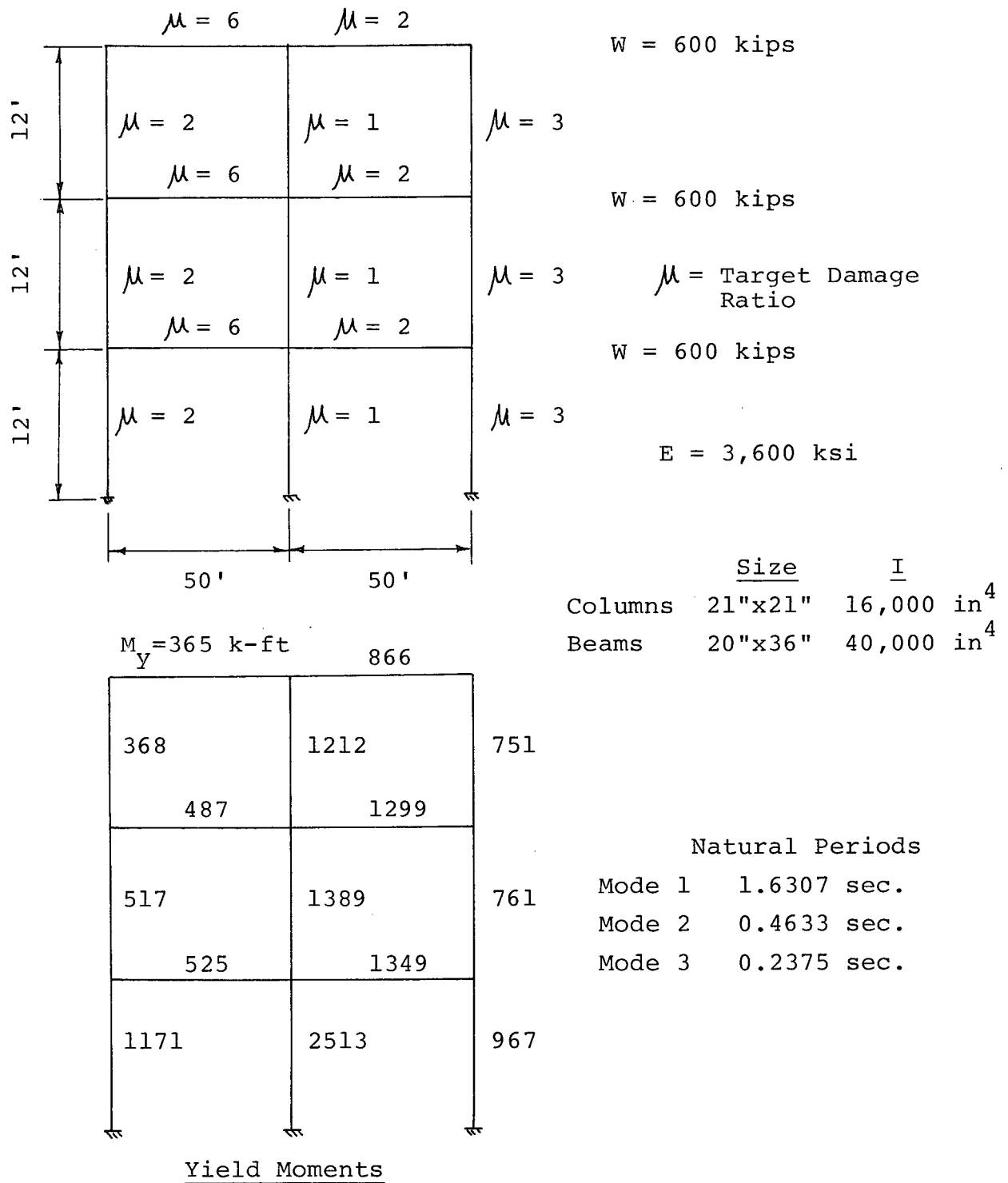


Fig. 3.6 2-Bay, 3-Story Frame B - Member Properties and Yield Moments

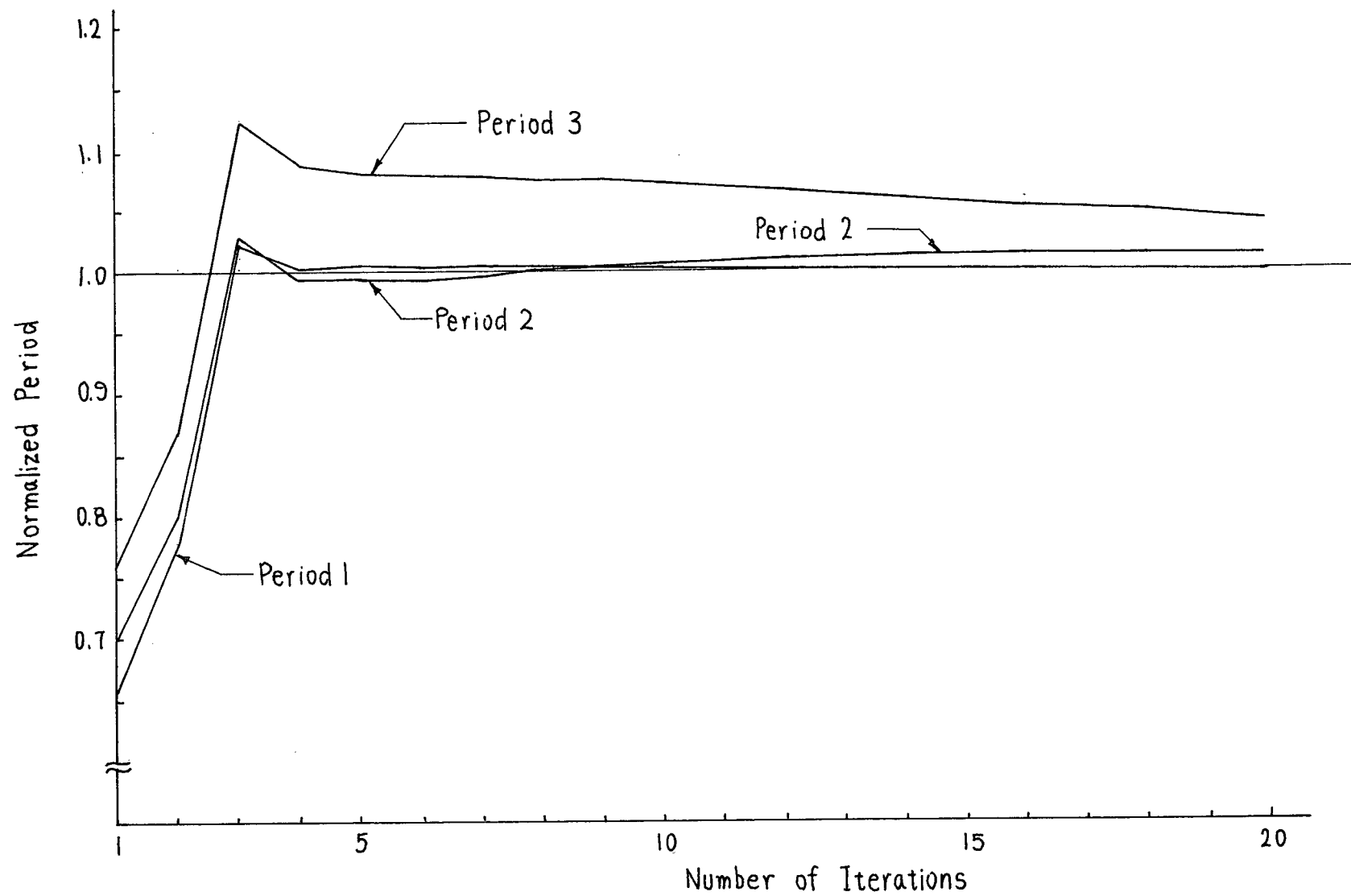
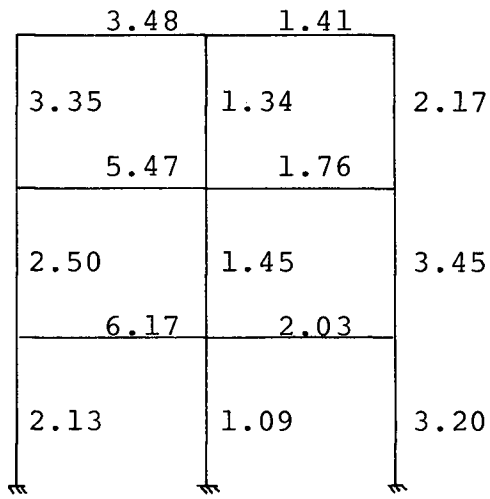
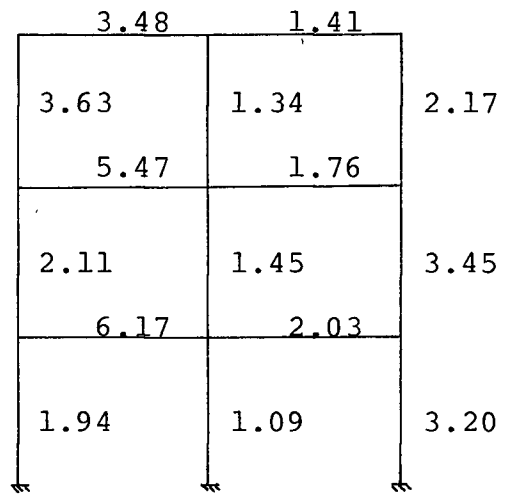


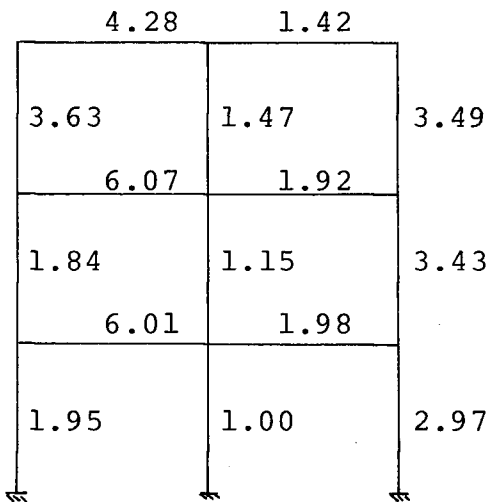
Fig. 3.7 2-Bay, 3-Story Frame B - Plot of Periods vs. Number of Iterations



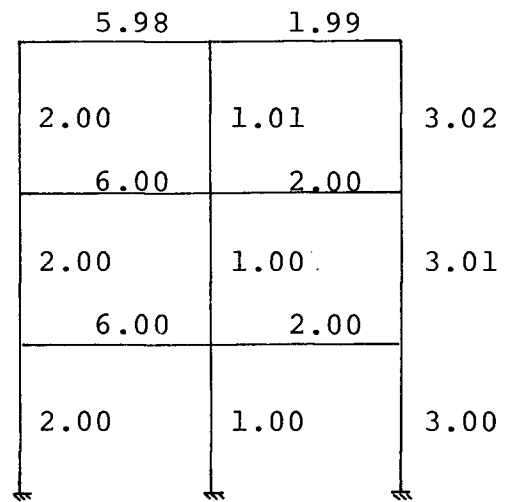
After 4 iterations



After 12 iterations



After 20 iterations



After 200 iterations

Fig. 3.8 2-Bay, 3-Story Frame B - Damage Ratios
Computed at the End of 4, 12, 20, and
200 Iterations

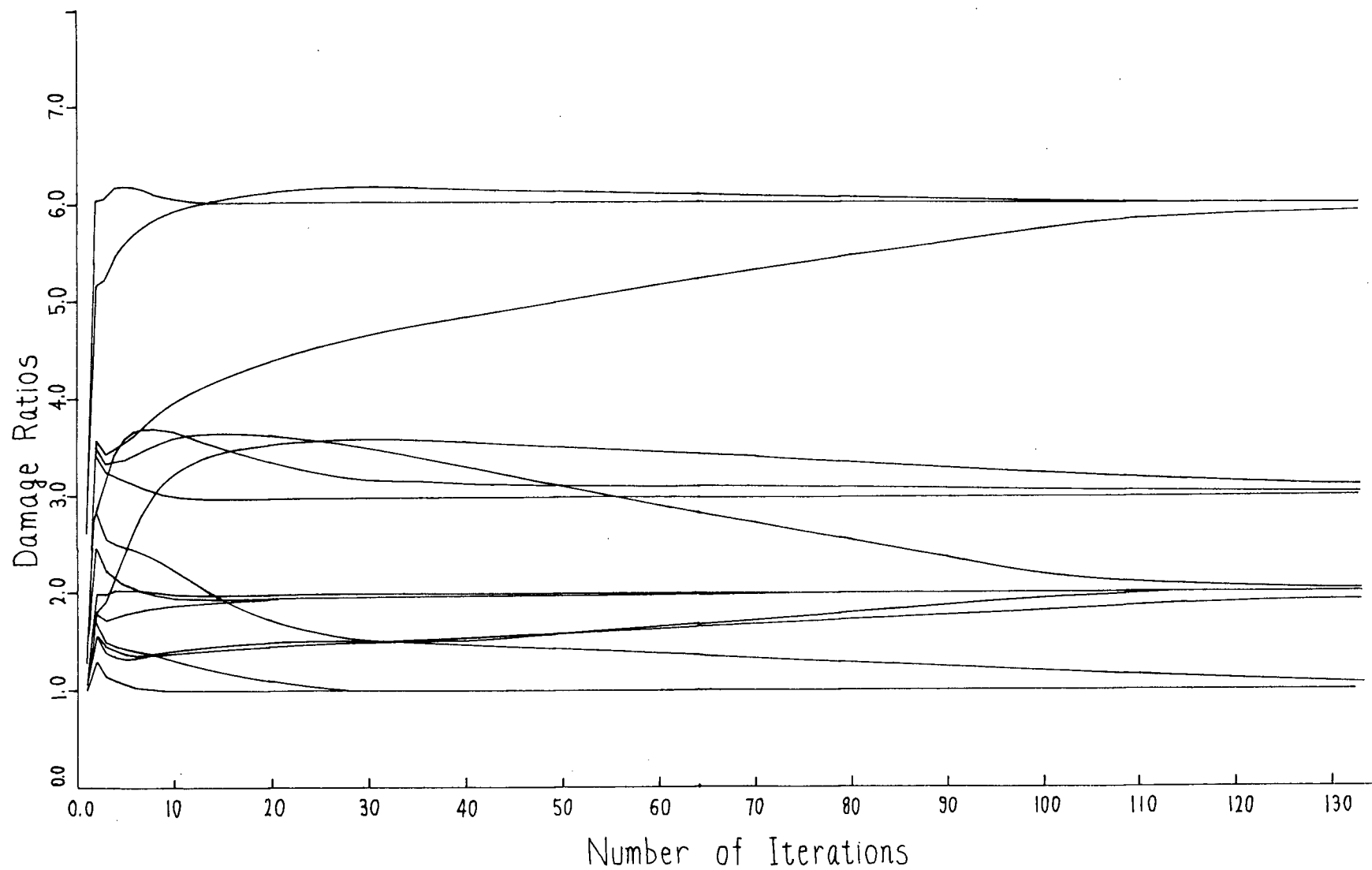
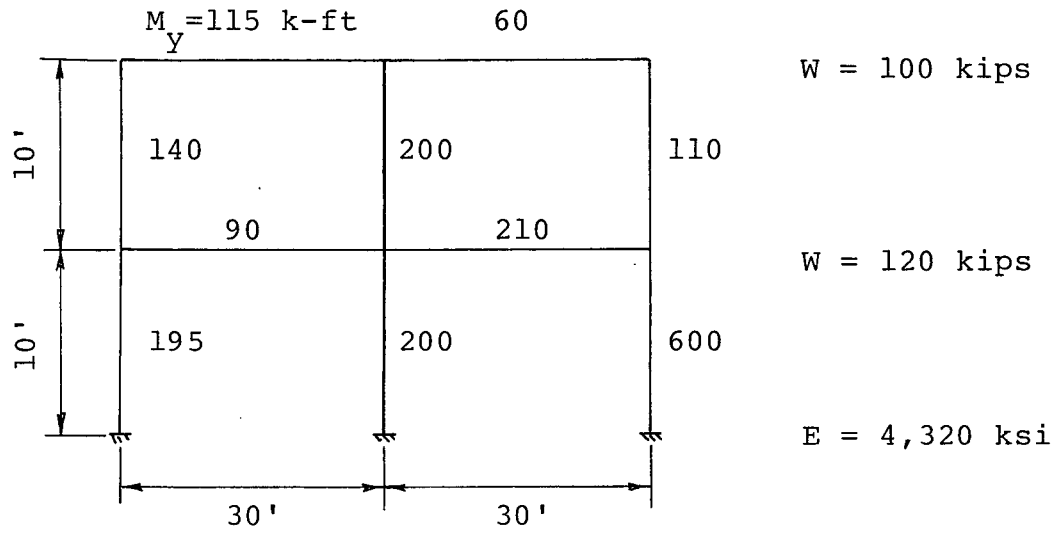


Fig. 3.9 2-Bay, 3-Story Frame B - Plot of Damage Ratios vs. Number of Iterations



	<u>Size</u>	<u>I</u>
Exterior Columns	21" x 21"	8,100 in ⁴
Interior Columns	18" x 18"	4,375 in ⁴
Beams 1st Story	18" x 21"	4,630 in ⁴
2nd Story	15" x 18"	2,430 in ⁴

Fig. 4.1 2-Bay, 2-Story Frame - Member Properties and Yield Moments

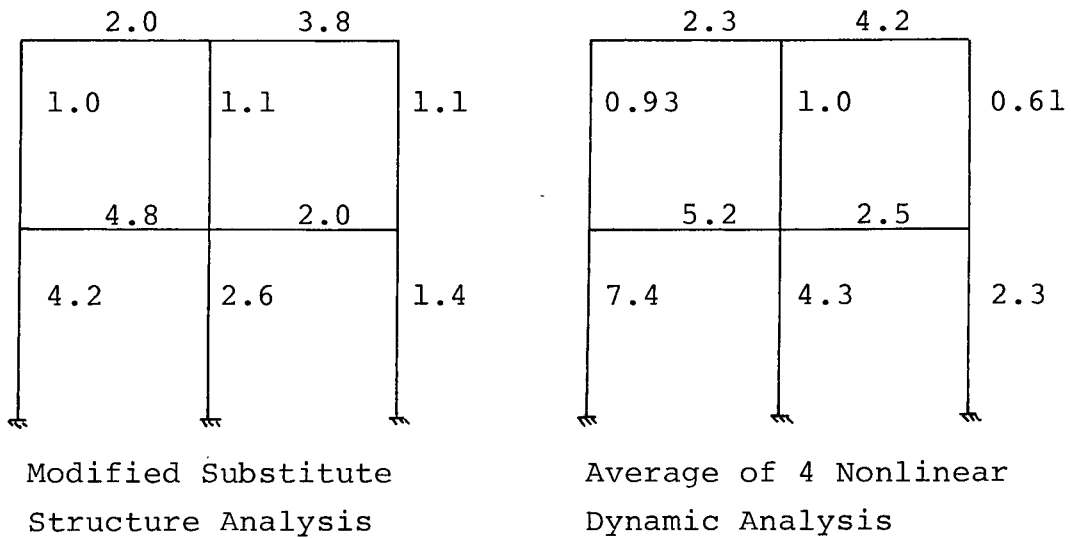


Fig. 4.2 2-Bay, 2-Story Frame - Damage Ratios

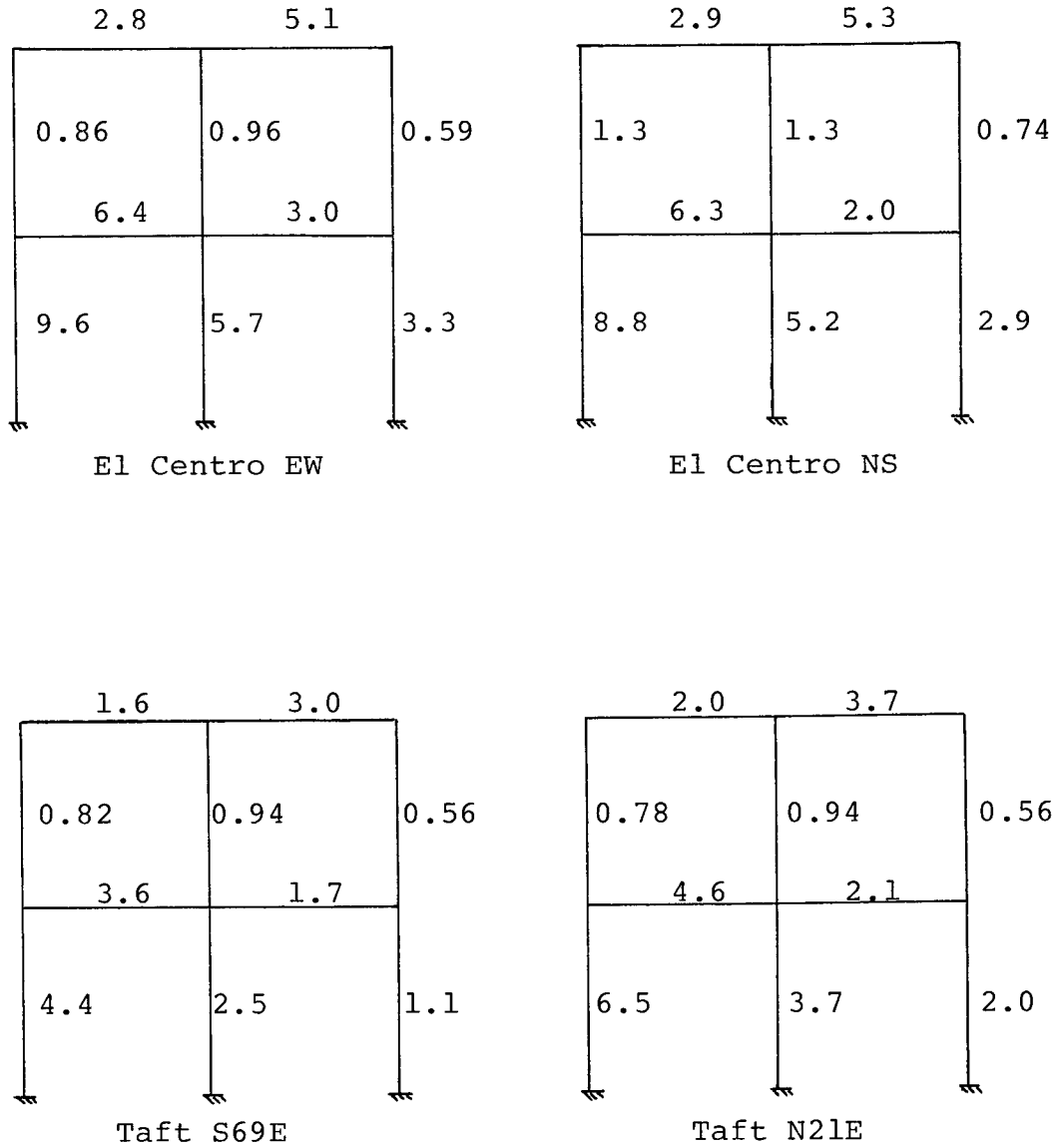
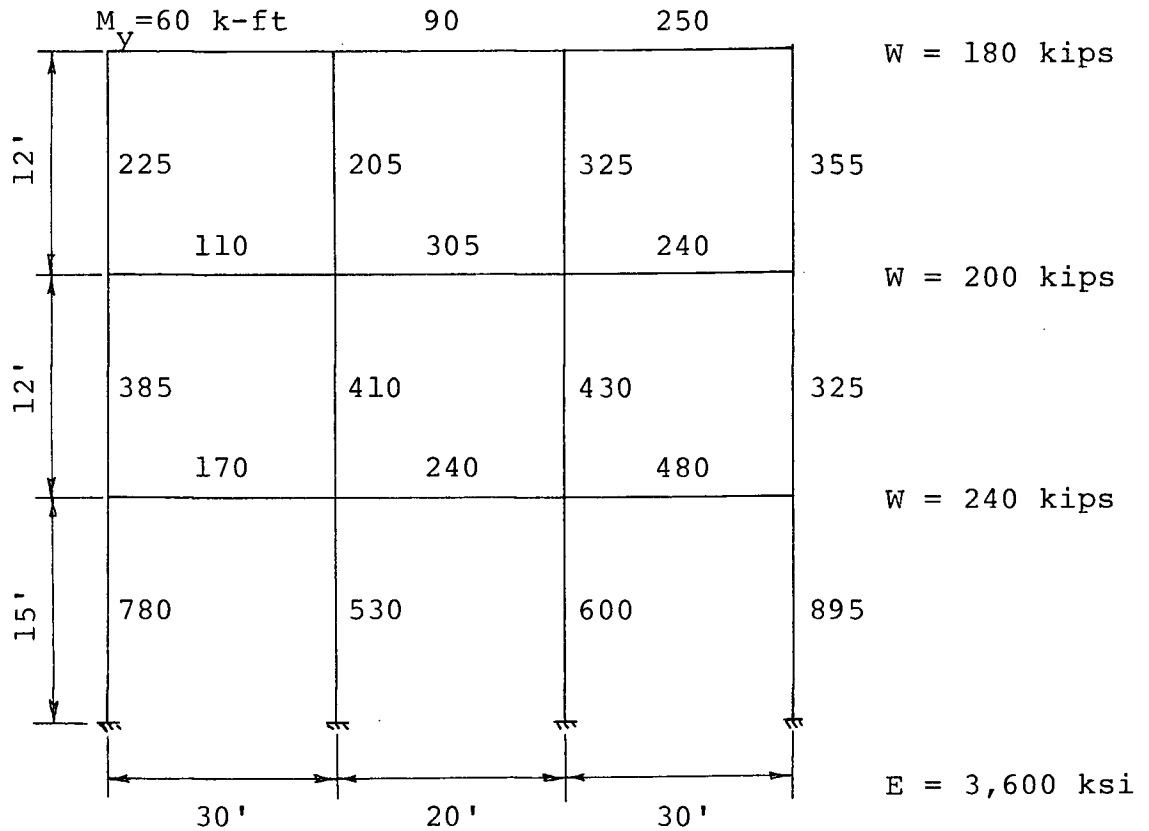


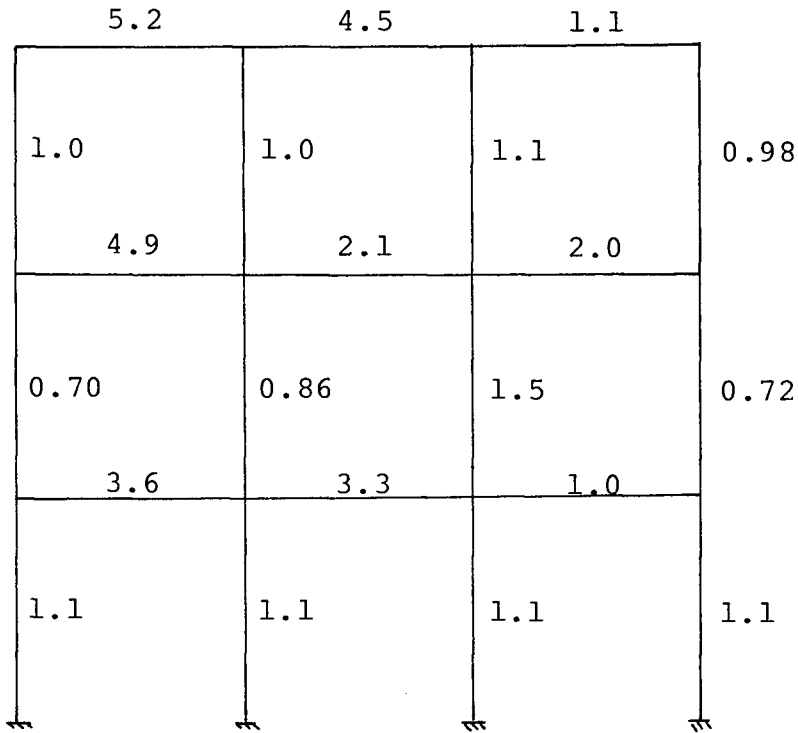
Fig. 4.3 2-Bay, 2-Story Frame - Damage Ratios for Individual Earthquakes



		Size	I
Exterior Columns	1	24" x 24"	13,800 in ⁴
	2	24" x 24"	13,800 in ⁴ (a)
	3	21" x 21"	8,100 in ⁴
Interior Columns	1	21" x 21"	8,100 in ⁴
	2	21" x 21"	8,100 in ⁴
	3	18" x 18"	4,375 in ⁴
Beams	1	18" x 24"	6,910 in ⁴
	2	18" x 21"	4,630 in ⁴
	3	18" x 18"	2,920 in ⁴

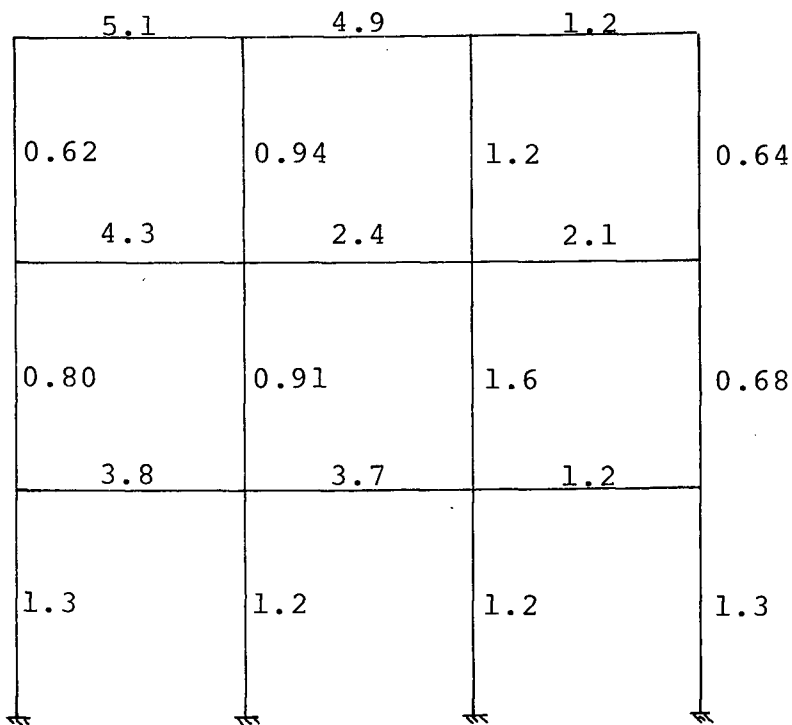
(a) I for the right-hand-side column is 4,375 in⁴

Fig. 4.4 3-Bay, 3-Story Frame - Member Properties and Yield Moments



Modified Substitute Structure

Analysis



Average of 4 Nonlinear Dynamic Analysis

Fig. 4.5 3-Bay, 3-Story Frame - Damage Ratios

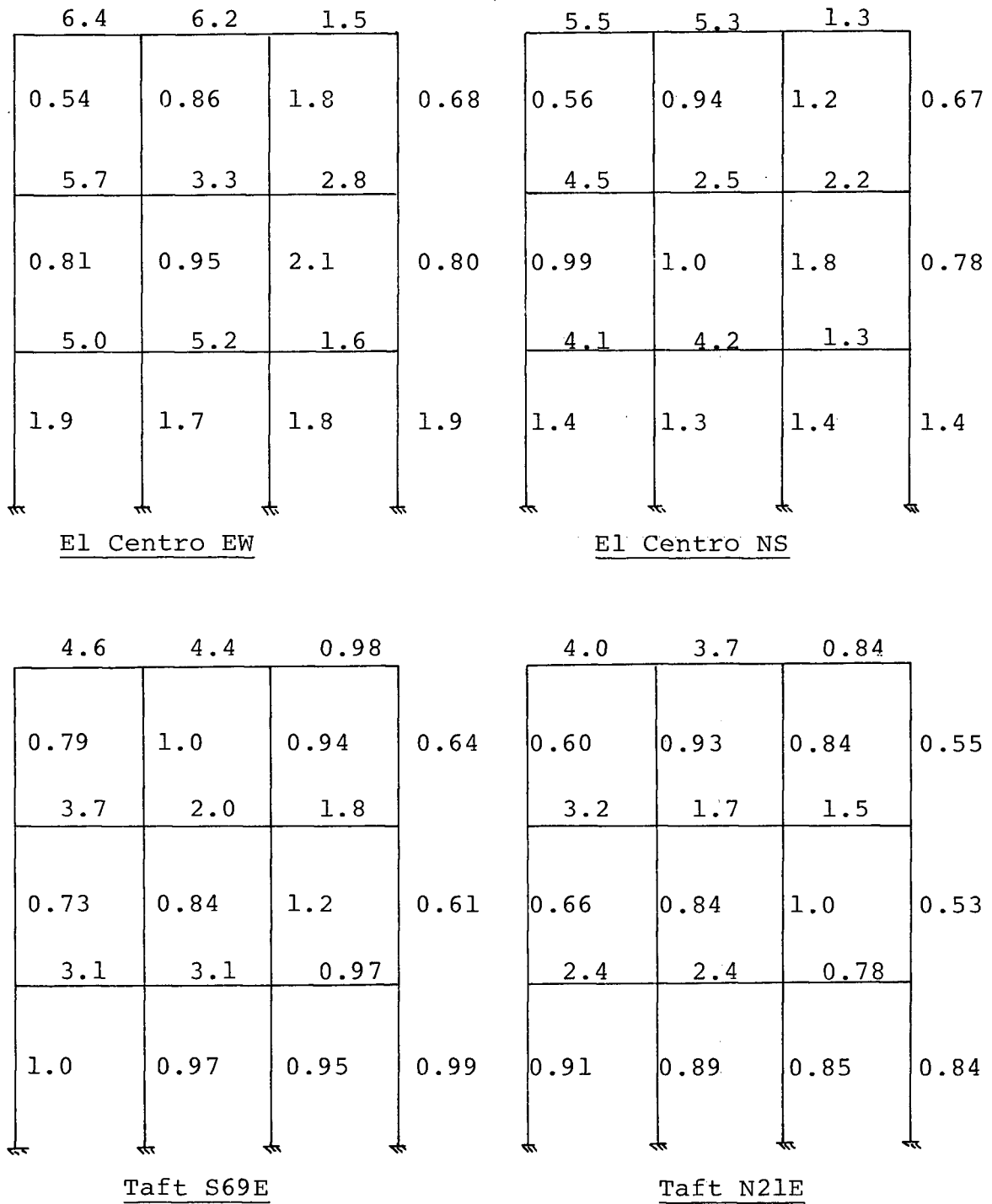


Fig. 4.6 3-Bay, 3-Story Frame - Damage Ratios for Individual Earthquakes

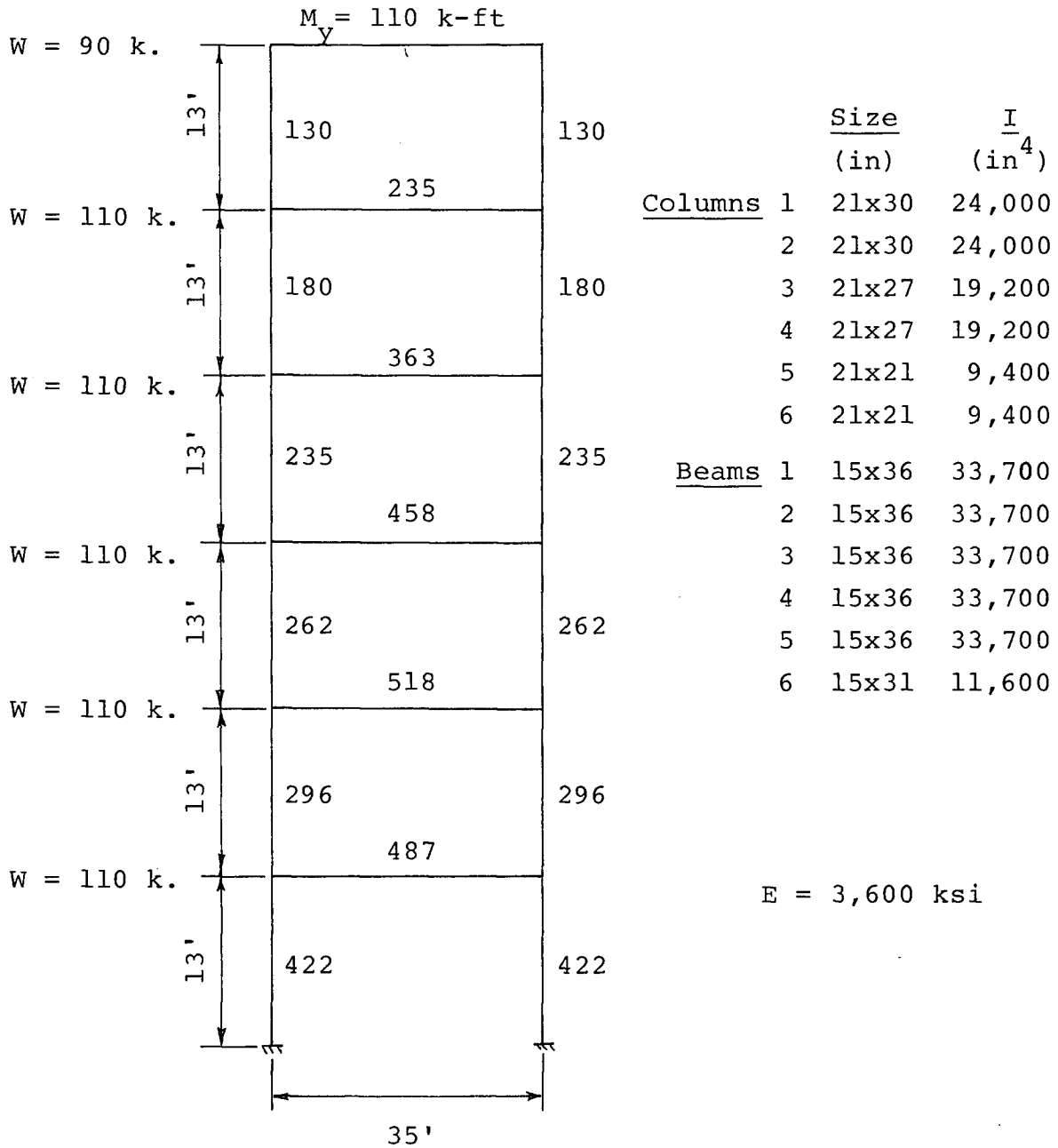


Fig. 4.7 1-Bay, 6-Story Frame - Member Properties and Yield Moments

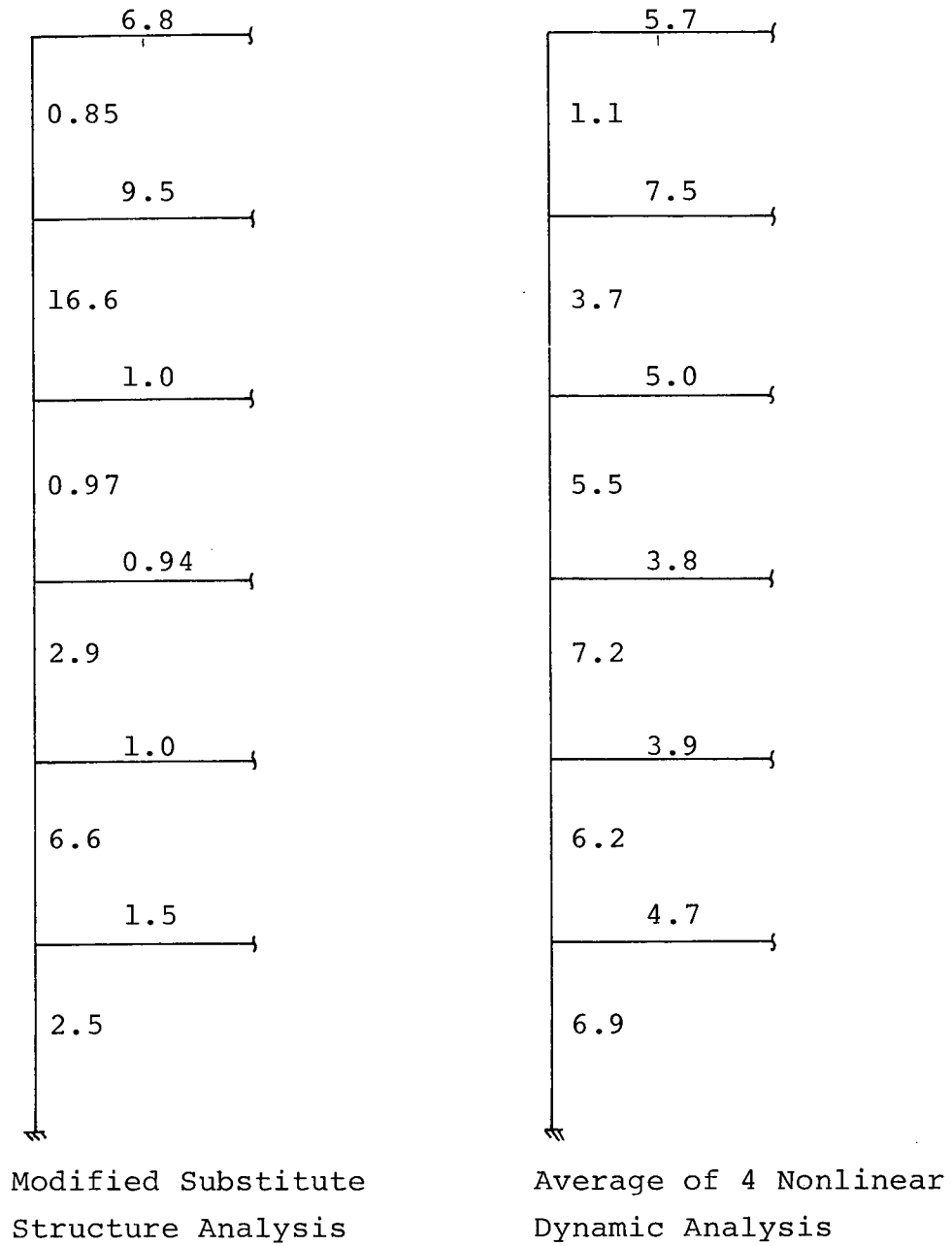


Fig. 4.8 1-Bay, 6-Story Frame - Damage Ratios

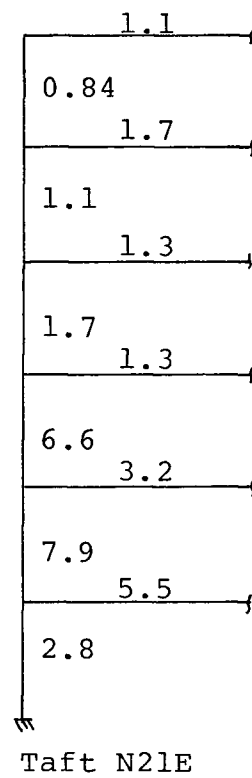
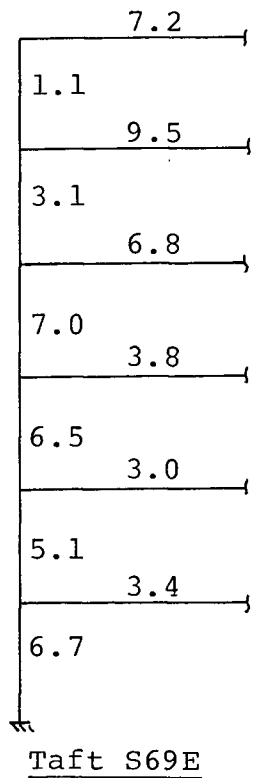
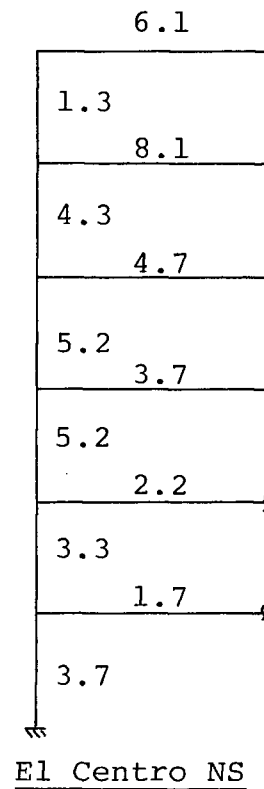
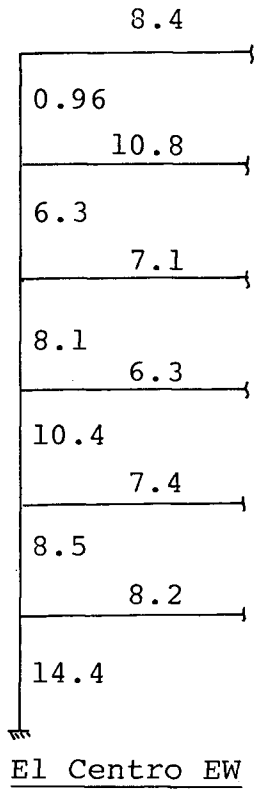
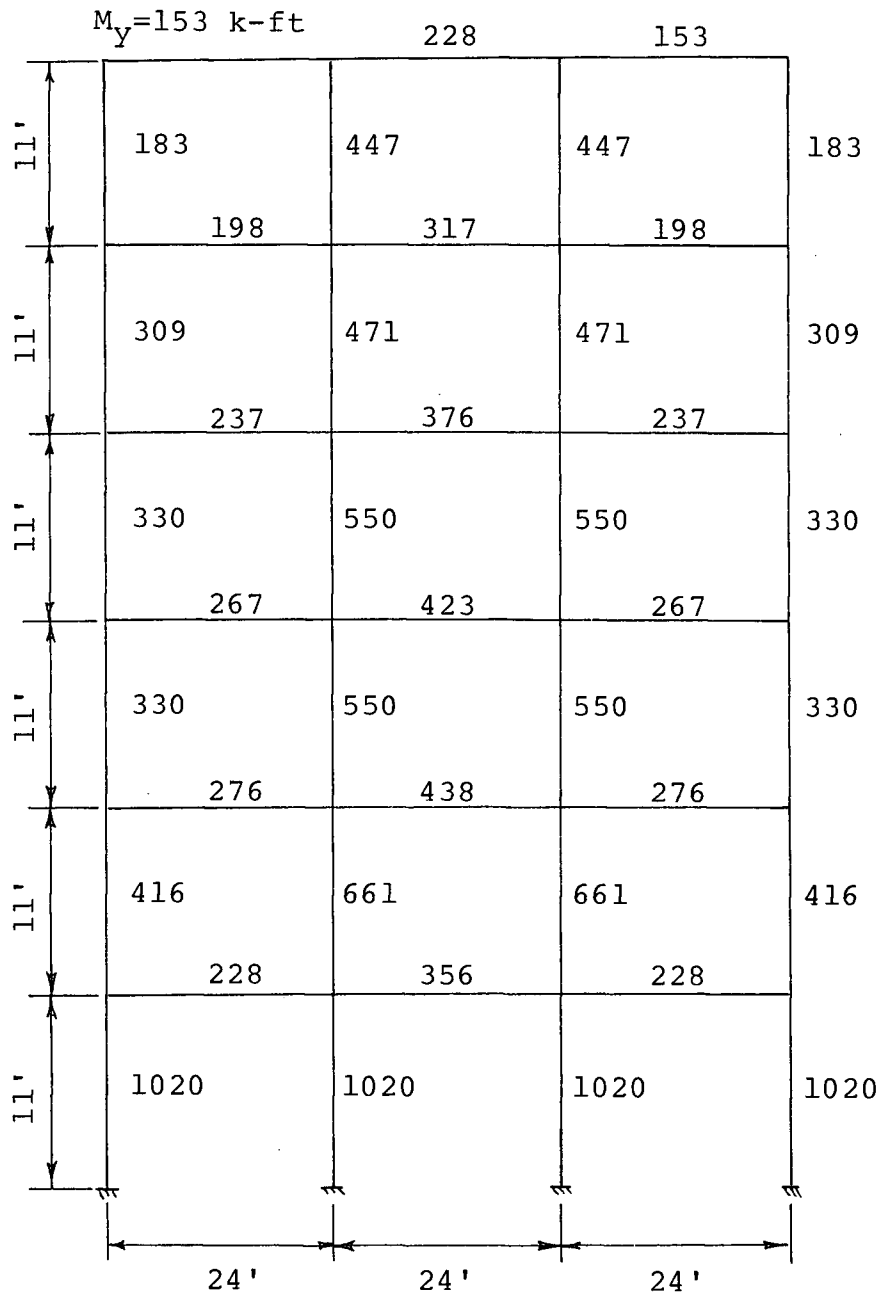


Fig. 4.9 1-Bay, 6-Story Frame - Damage Ratios for Individual Earthquakes



	Size	I	
Columns	24" x 24"	13,824 in ⁴	$E = 3,600 \text{ ksi}$
Beams	18" x 30"	13,500 in ⁴	Floor weight is
			200 kips at all levels

Fig. 4.10 3-Bay, 6-Story frame - Member Properties and Yield Moments

3.5	2.0
0.84	0.83
3.9	2.3
0.81	0.83
4.2	2.5
0.78	0.80
4.3	2.6
0.80	0.83
4.5	2.7
0.77	0.79
4.5	2.7
0.72	0.78

Modified Substitute
Structure Analysis

1.7	0.95
0.86	0.70
2.7	1.6
1.1	0.91
3.6	2.2
1.0	0.88
4.3	2.4
1.1	0.93
4.7	3.0
0.70	0.75
5.2	3.3
0.81	0.88

Average of 4 Nonlinear
Dynamic Analyses

Fig. 4.11 3-Bay, 6-Story Frame - Damage Ratios

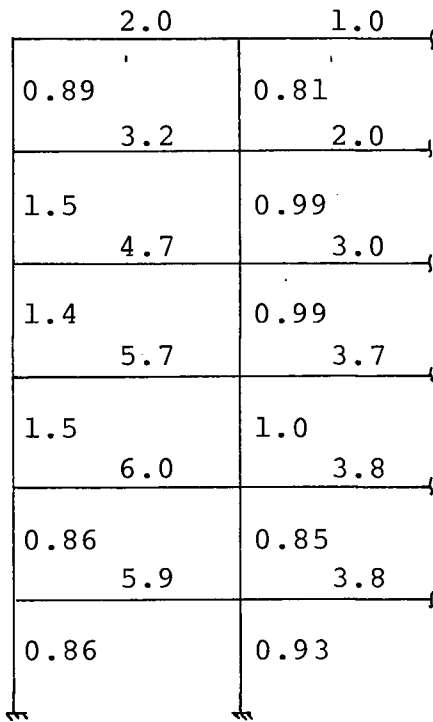
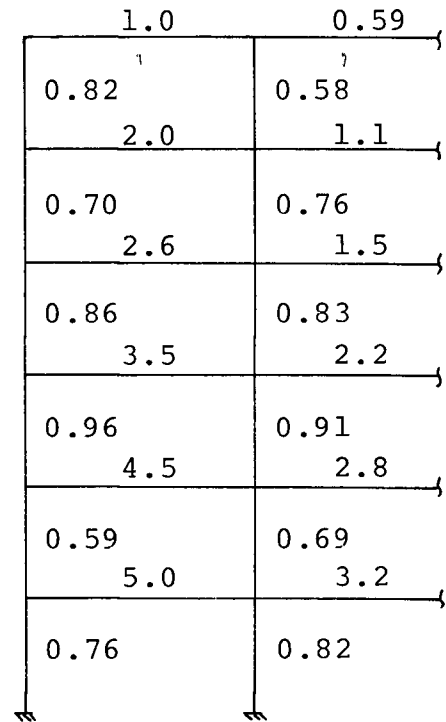
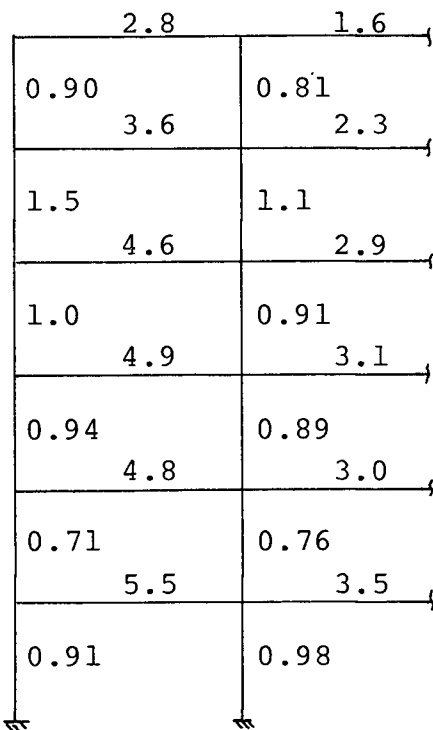
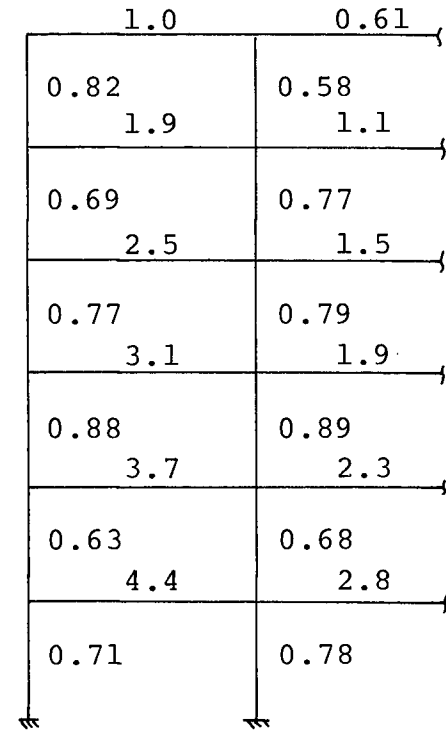
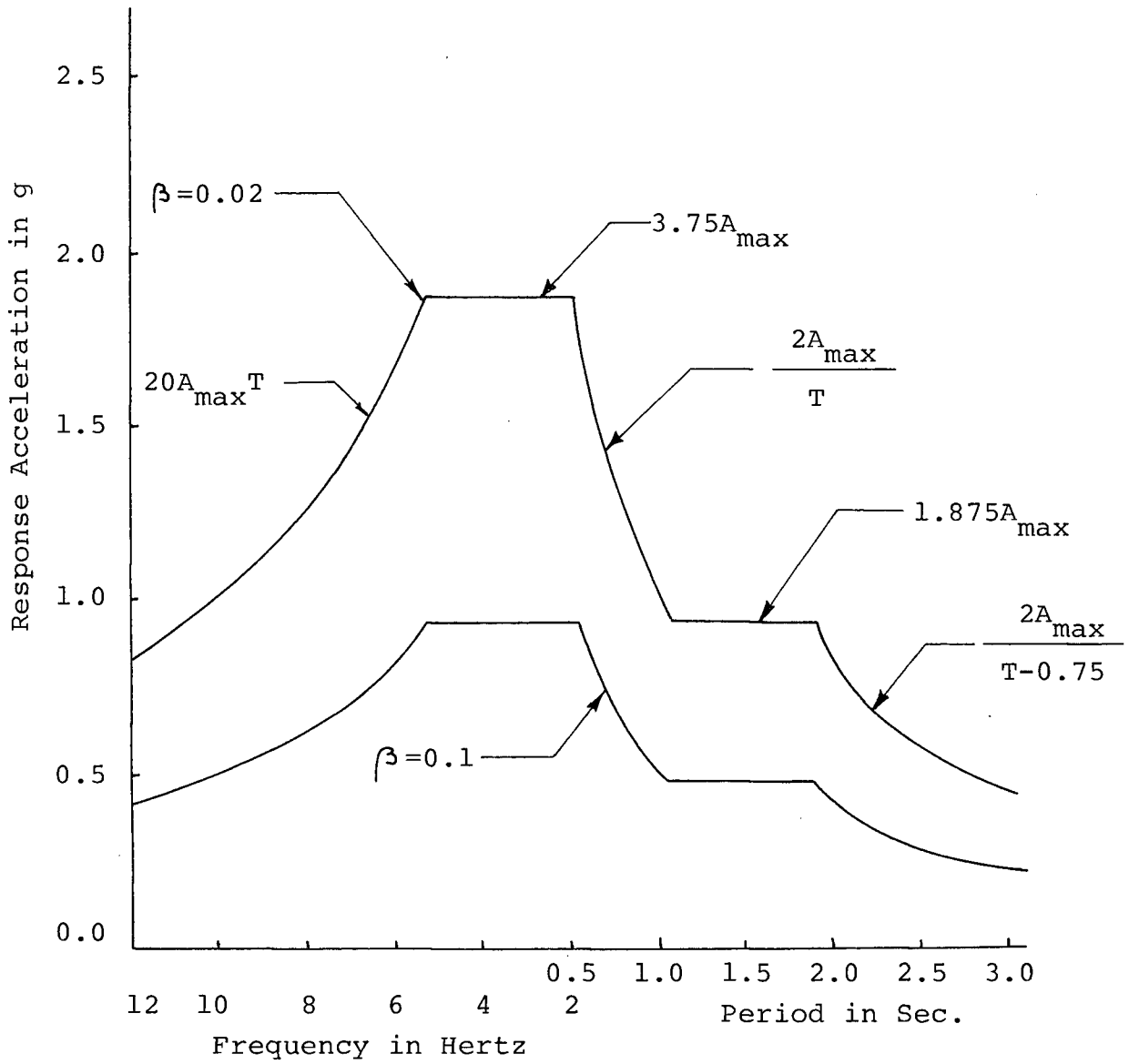
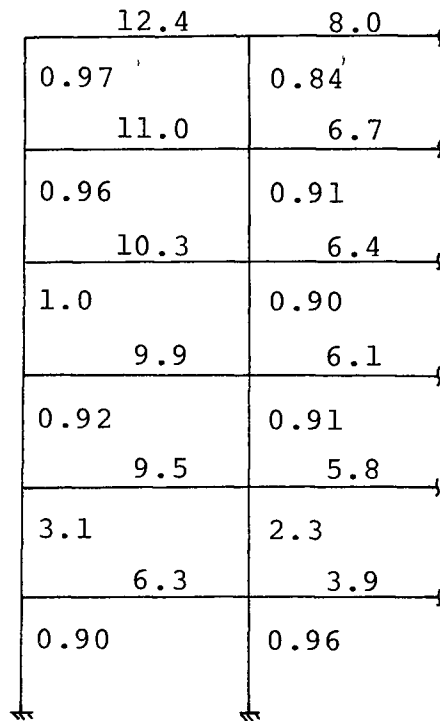
El Centro EWEl Centro NSTaft S69ETaft N21E

Fig. 4.12 3-Bay, 6-Story Frame - Damage Ratios for Individual Earthquakes



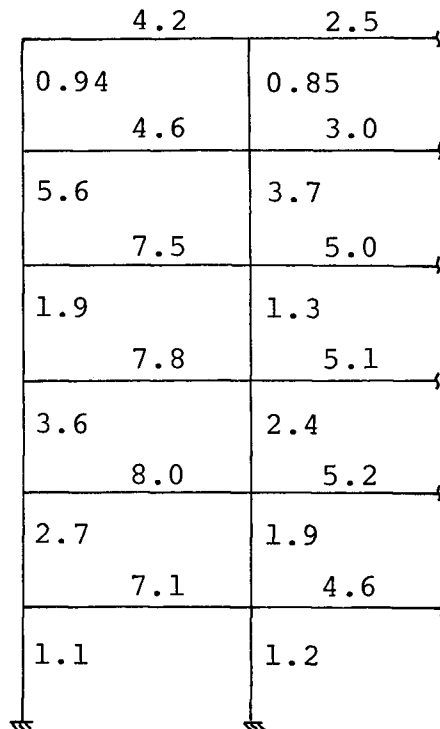
$$\frac{\text{Response Acceleration for } \beta}{\text{Response Acceleration for } \beta=0.02} = \frac{8}{6 + 100\beta}$$

Fig. 5.1 Smoothed Response Spectrum - Design Spectrum B



Modified Substitute
Structure Analysis
(Spectrum B)

W = 200 kips/floor



Nonlinear Dynamic
Analysis
(8244 Orion 1971)

Fig. 5.2 3-Bay, 6-Story Frame A - Damage Ratios

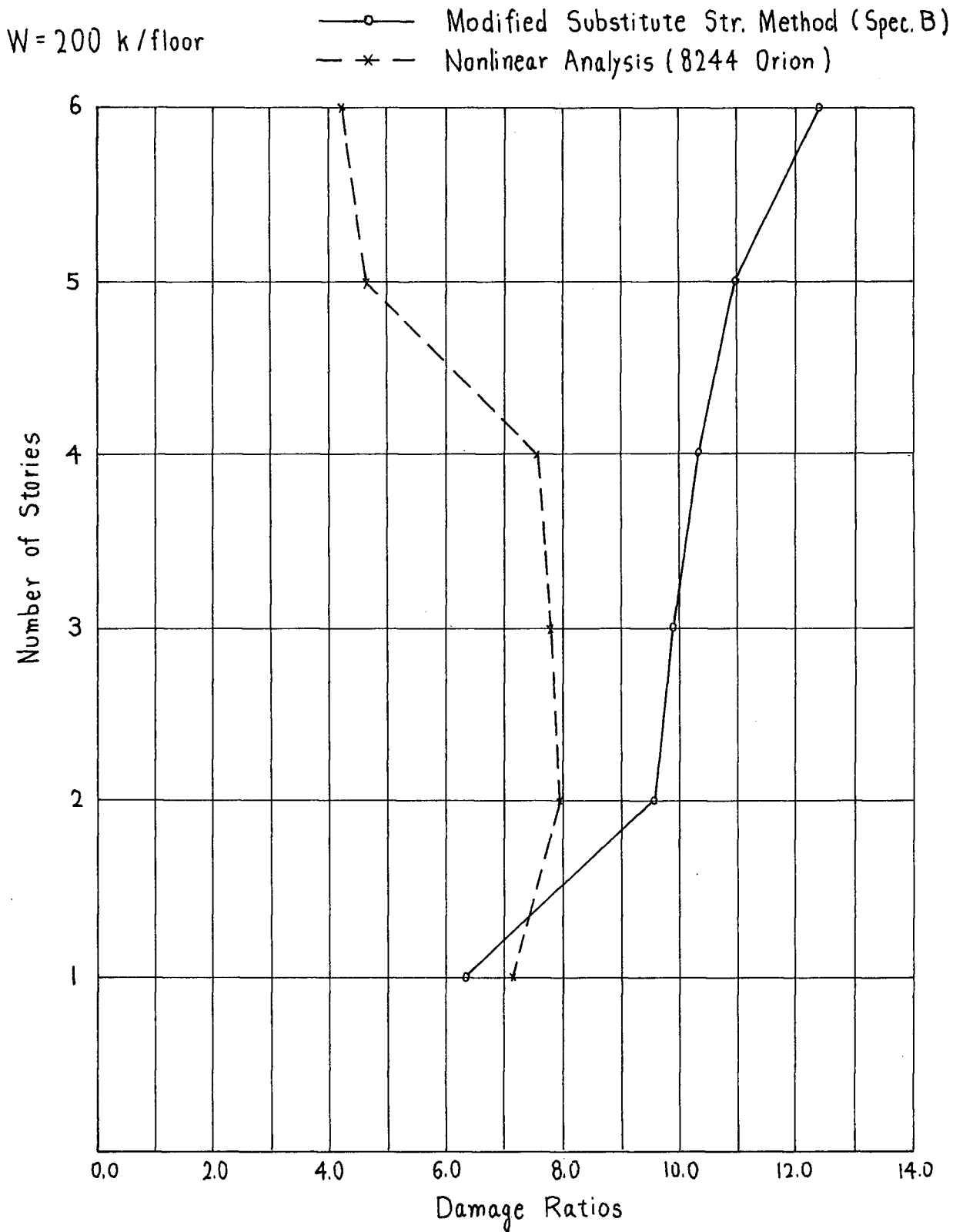


Fig. 5.3 3-Bay, 6-Story Frame A - Plot of Damage Ratios for Beams in the Exterior Bay

2.1	1.1
0.85	0.82
3.1	1.9
0.91	0.91
4.1	2.4
0.87	0.88
4.6	2.8
0.82	0.87
4.8	2.9
0.84	0.85
4.7	2.9
0.75	0.82

Modified Substitute
Structure Analysis
(Spectrum B)

W = 130 kips/floor

1.7	0.84
0.90	0.73
2.9	1.8
1.5	1.1
4.6	2.9
1.2	0.95
5.4	3.4
0.92	0.89
5.6	3.5
0.78	0.80
5.6	3.6
0.80	0.81

Nonlinear Dynamic
Analysis
(8244 Orion 1971)

Fig. 5.4 3-Bay, 6-Story Frame B - Damage Ratios

$W = 130 \text{ k/floor}$

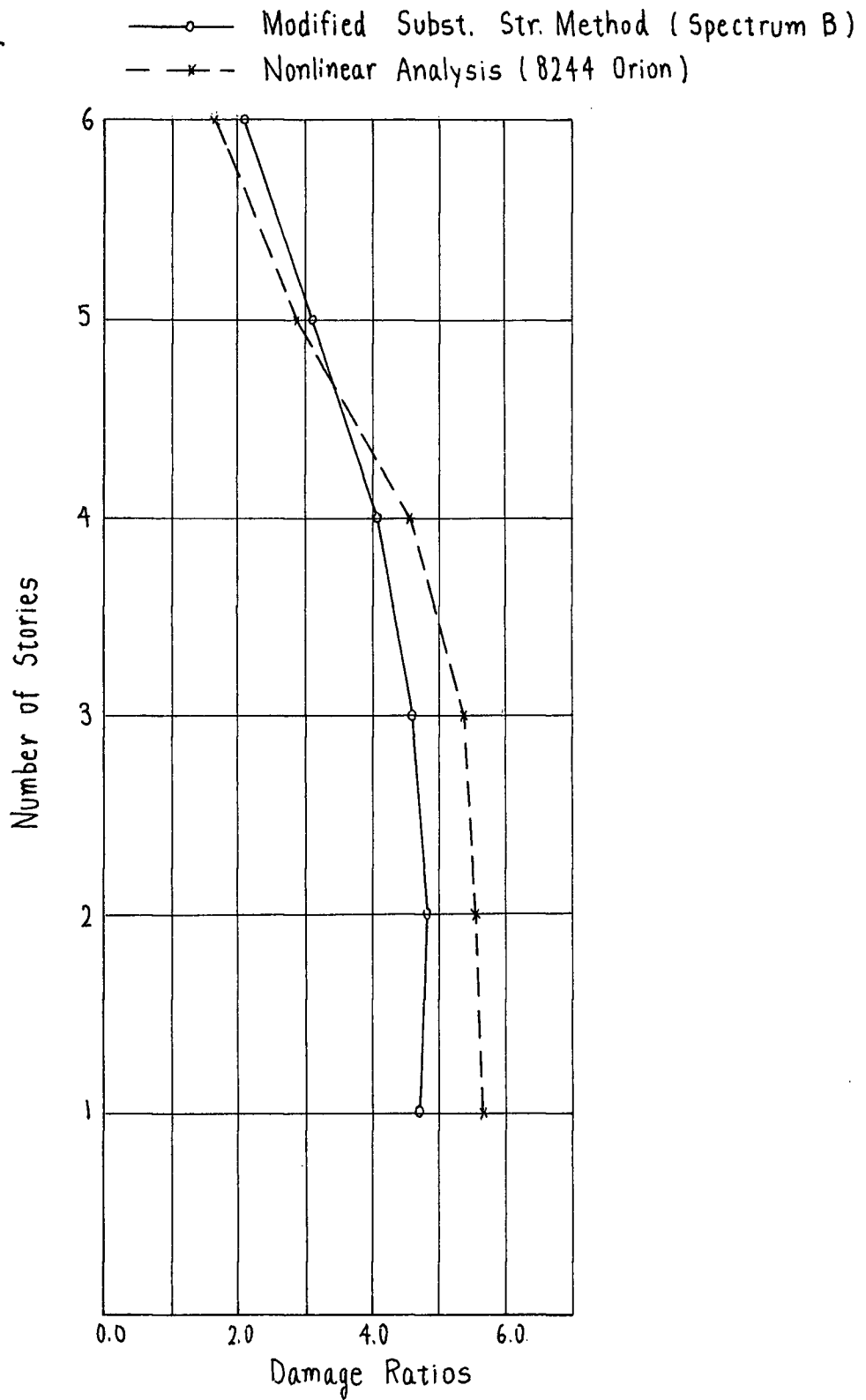


Fig. 5.5 3-Bay, 6-Story Frame B - Plot of Damage Ratios for Beams in the Exterior Bay

	1.3	0.71
0.84		0.67
2.1		1.2
0.75		0.83
2.8		1.7
0.75		0.79
3.2		1.9
0.76		0.83
3.6		2.1
0.67		0.74
3.8		2.3
0.64		0.71

Modified Substitute
Structure Analysis
(Spectrum A)

W = 130 kips/floor

	0.87	0.52
0.73		0.51
1.8		1.0
0.78		0.83
3.0		1.8
0.94		0.83
3.9		2.4
0.90		0.87
4.6		2.9
0.63		0.70
5.0		3.2
0.75		0.82

Average of 4 Nonlinear
Dynamic Analyses

Fig. 5.6 3-Bay, 6-Story Frame B - Damage Ratios

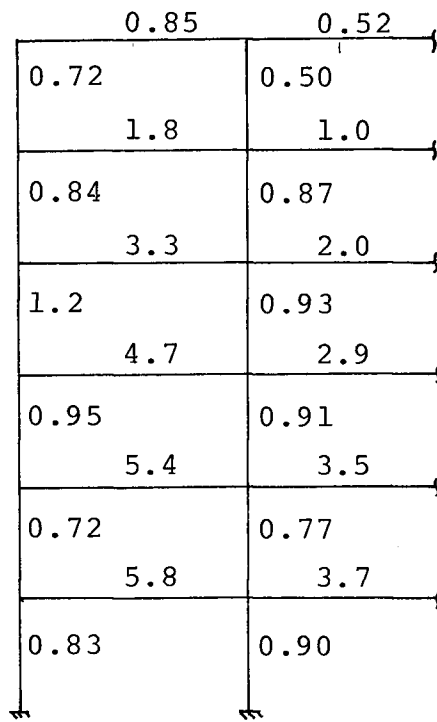
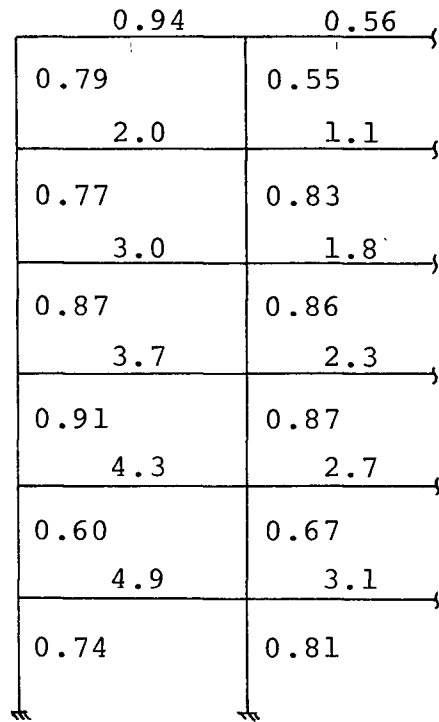
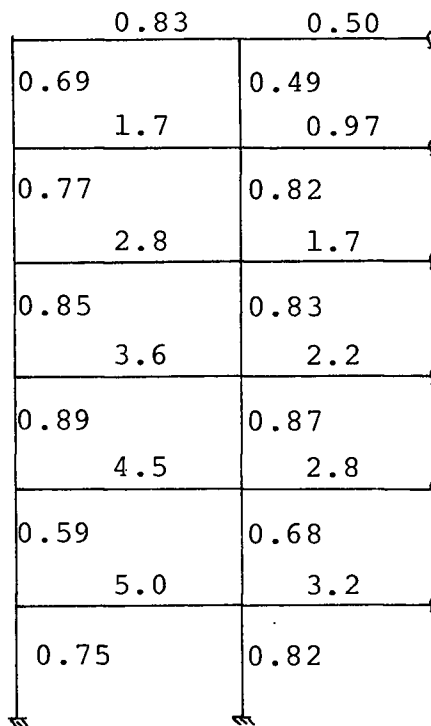
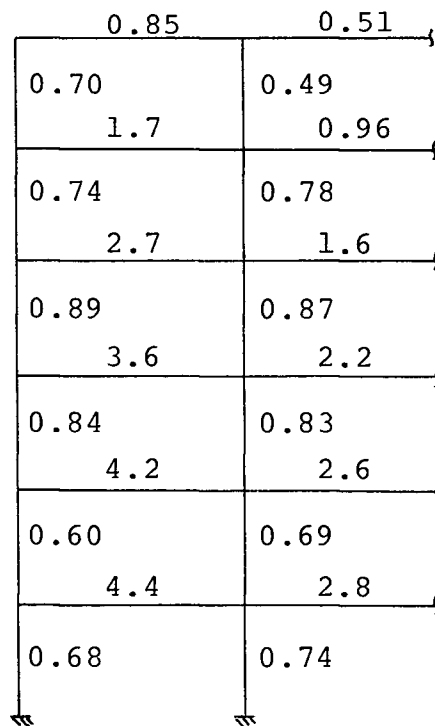
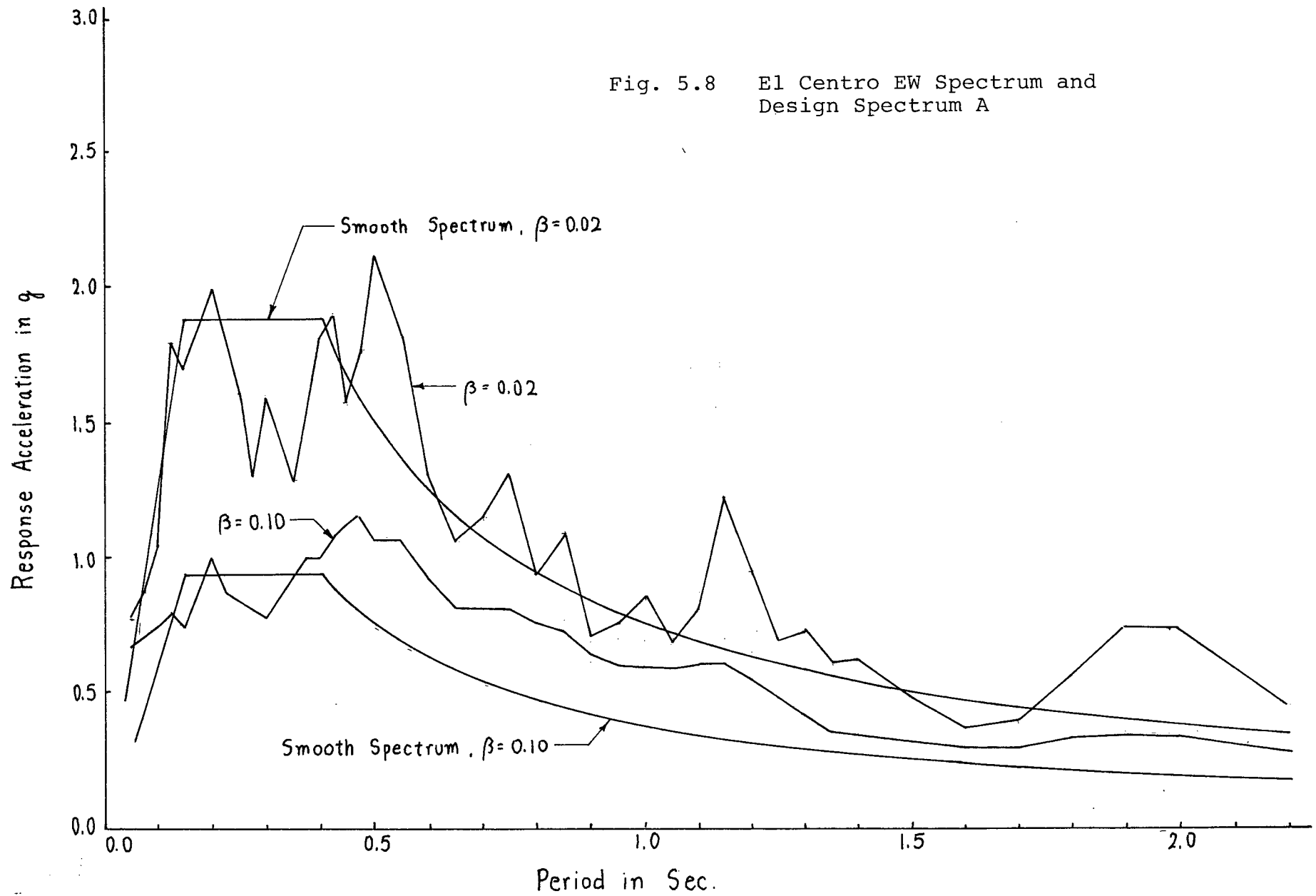
El Centro EWEl Centro NSTaft S69ETaft N21E

Fig. 5.7 3-Bay, 6-Story Frame B - Damage Ratios for Individual Earthquakes

Fig. 5.8 El Centro EW Spectrum and
Design Spectrum A



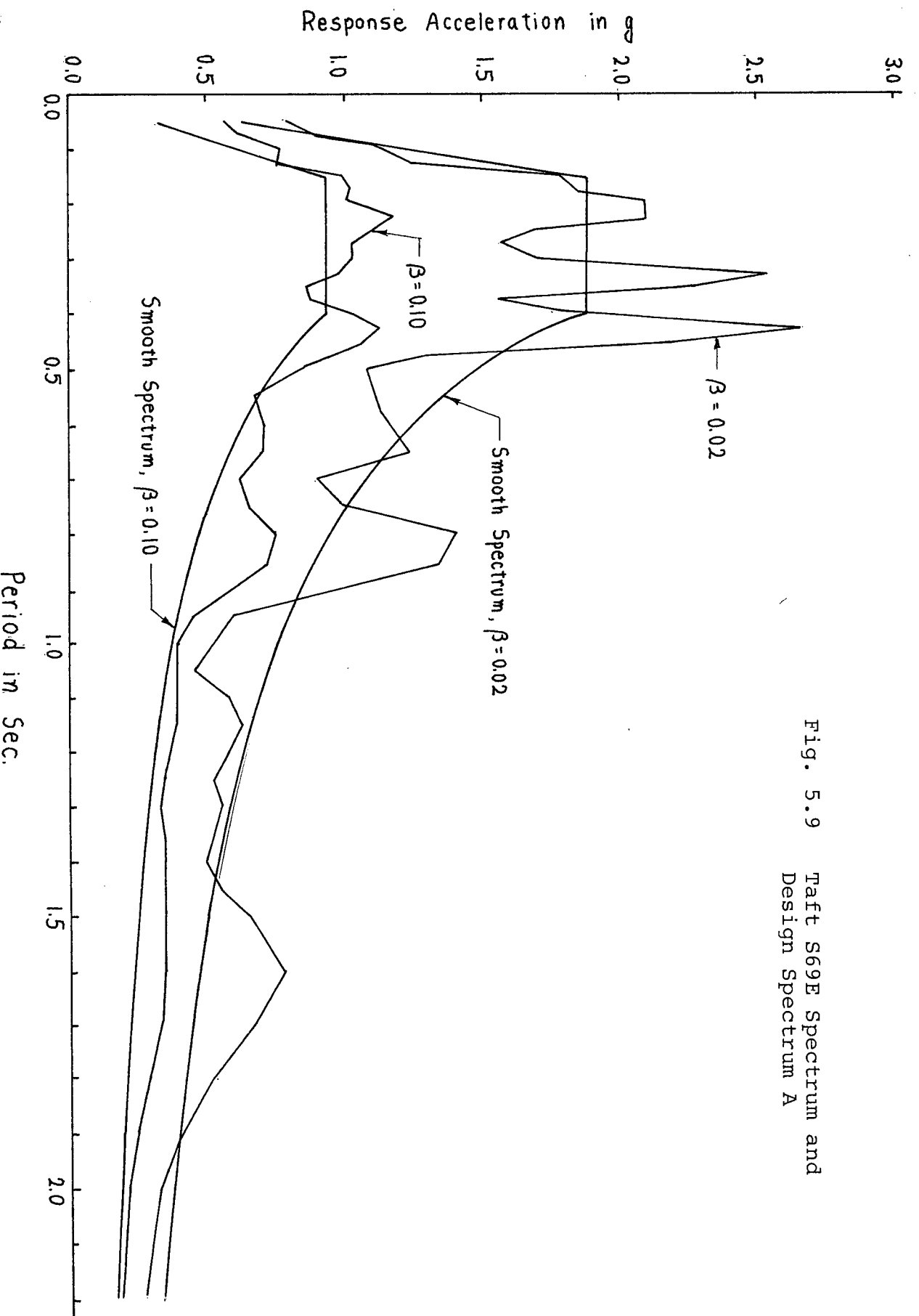
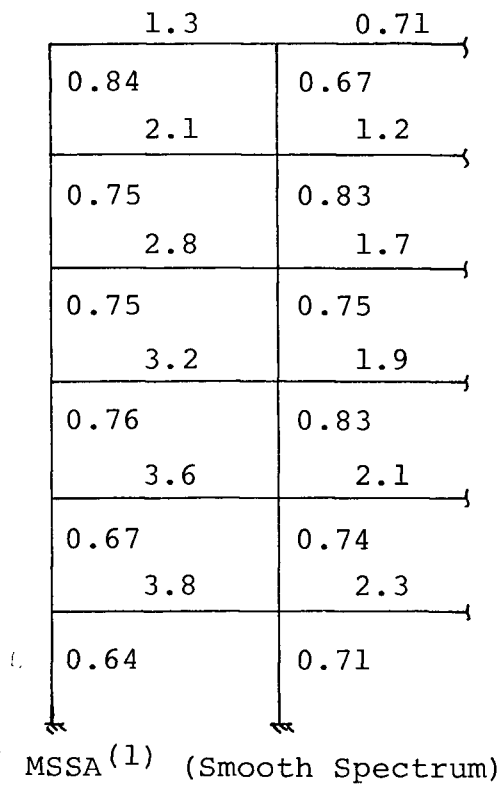
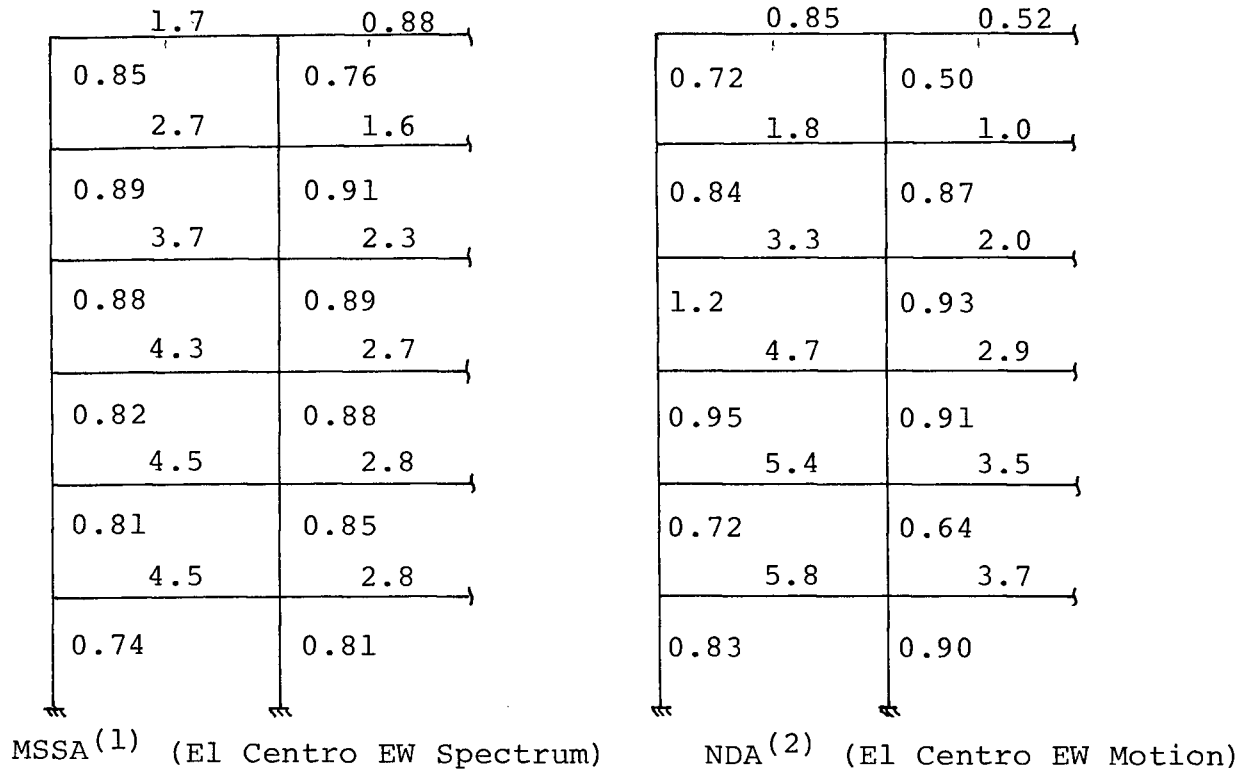


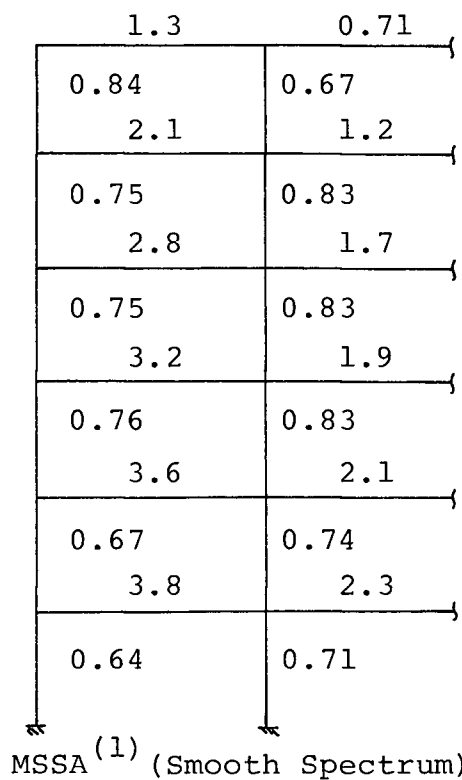
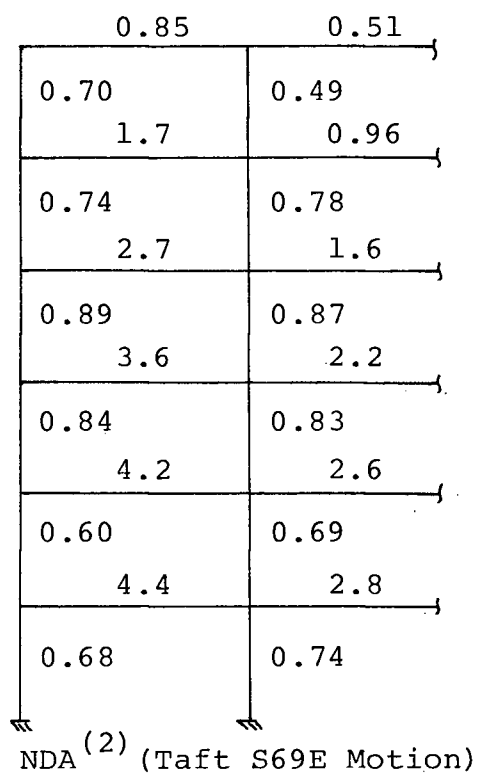
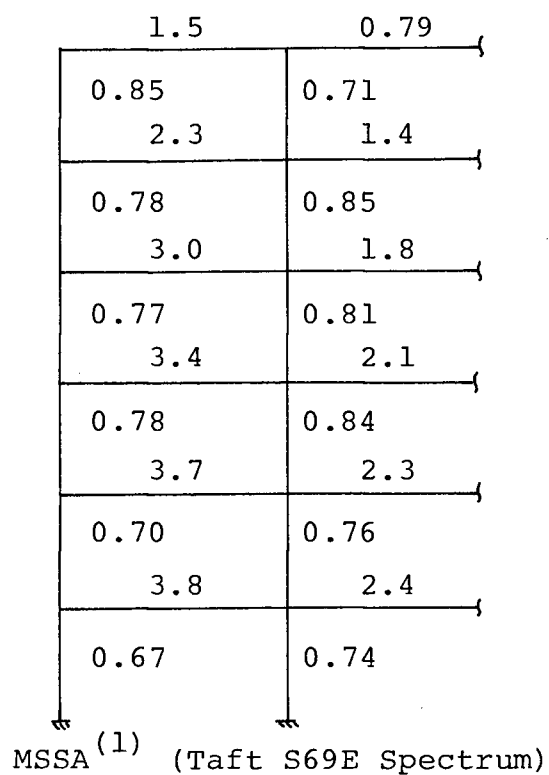
Fig. 5.9 Taft S69E Spectrum and Design Spectrum A



W = 130 kips/floor

- (1) Modified Substitute Structure Analysis
- (2) Nonlinear Dynamic Analysis

Fig. 5.10 3-Bay, 6-Story Frame B - Damage Ratios

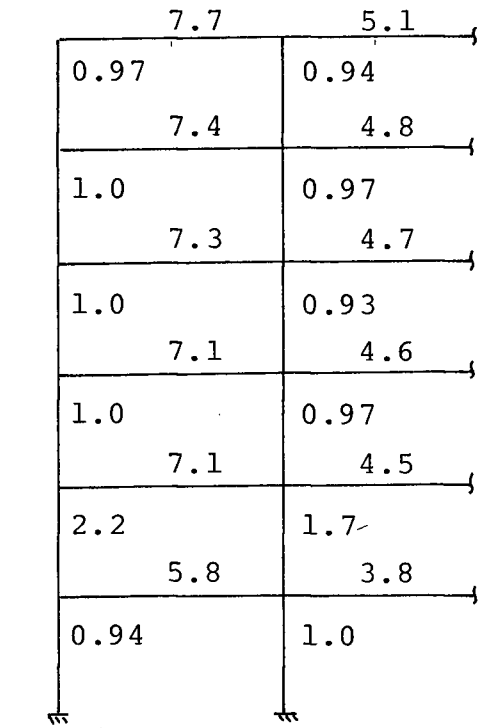
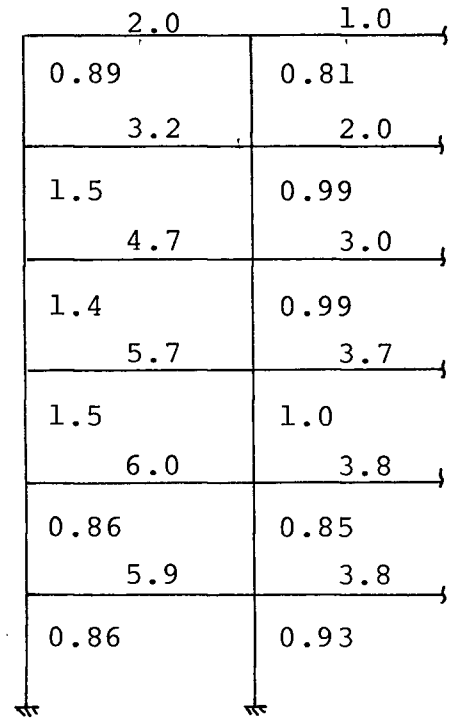
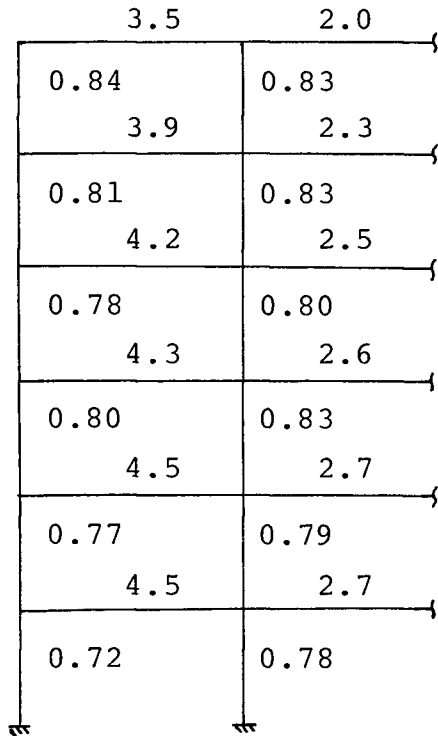


W = 130 kips/floor

(1) Modified Substitute
Structure Analysis

(2) Nonlinear Dynamic Analysis

Fig. 5.11 3-Bay, 6-Story Frame B - Damage Ratios

MSSA⁽¹⁾ (El Centro EW Spectrum)NDA⁽²⁾ (El Centro EW Motion)MSSA⁽¹⁾ (Smooth Spectrum)

W = 200 kips/floor

- (1) Modified Substitute Structure Analysis
- (2) Nonlinear Dynamic Analysis

Fig. 5.12 3-Bay, 6-Story Frame A - Damage Ratios

	4.7	2.9	
0.90		0.88	
5.0		3.1	
0.97		0.95	
5.4		3.4	
0.95		0.92	
5.6		3.6	
0.87		0.89	
5.6		3.6	
1.0		0.96	
5.3		3.4	
0.86		0.93	
MSSA ⁽¹⁾ (Taft S69E Spectrum)			

	2.8	1.6	
0.90		0.81	
3.6		2.3	
1.5		1.1	
4.6		2.9	
1.0		0.91	
4.9		3.1	
0.94		0.89	
4.8		3.0	
0.71		0.76	
5.5		3.5	
0.91		0.98	
NDA ⁽²⁾ (Taft S69E Motion)			

	3.5	2.0	
0.84		0.83	
3.9		2.3	
0.81		0.83	
4.2		2.5	
0.78		0.80	
4.3		2.6	
0.80		0.83	
4.5		2.7	
0.77		0.79	
4.5		2.7	
0.72		0.78	
MSSA ⁽¹⁾ (Smooth Spectrum)			

W = 200 kips/floor

- (1) Modified Substitute
Structure Analysis
(2) Nonlinear Dynamic
Analysis

Fig 5.13 3-Bay, 6-Story Frame A - Damage Ratios

BIBLIOGRAPHY

1. Associate Committee on the National Building Code 1975, Supplement No. 4 to the National Building Code of Canada, National Research Council of Canada, Ottawa, Ontario, 1975.
2. Applied Technology Council, "Tentative Provisions for the Development of Seismic Regulations for Buildings", ATC 3-06 NSF 78-8, Applied Technology Council, Palo Alto, California, June, 1978.
3. Okada, T. and Bresler, B., "Strength and Ductility Evaluation of Existing Low-Rise Reinforced Concrete Buildings - Screening Method", EERC 76-1, Earthquake Engineering Research Center, University of California, Berkeley, California, February, 1976.
4. Freeman, S. A., Nicoletti, J. P., and Tyrrell, J. V., "Evaluation of Existing Buildings for Seismic Risk -- A Case Study of Puget Sound Naval Shipyard, Bremerton, Washington", Proceedings of the U. S. National Conference on Earthquake Engineering, Ann Arbor, Illinois, June, 1975, pp. 113-122.
5. Shibata, A. and Sozen, M. A., "Substitute-Structure Method for Seismic Design in R/C", Journal of the Structural Division, ASCE, Vol. 102, No. ST1, January, 1976, pp.1-18.
6. Clough, R. W. and Penzien, J., Dynamics of Structures, McGraw-Hill, New York, 1975, pp. 545-610.
7. Hudson, D. E., "Some Problems in the Application of Spectrum Technique to Strong-Motion Earthquake Analysis", Bulletin

- of the Seismological Society of America, Vol. 52, No. 2, April, 1962, pp. 417-430.
8. Gulkan, P. and Sozen, M. A., "Inelastic Response of Reinforced Concrete Structures to Earthquake Motions", Journal of the American Concrete Institute, Vol. 71, No. 12, December, 1974, pp. 604-610.
 9. Takeda, T., Sozen, M. A., and Nielsen, N. N., "Reinforced Concrete Response to Simulated Earthquakes", Journal of Structural Division, ASCE, Vol. 96, No. ST12, December, 1970, pp. 2557-2573.
 10. Jennings, P. C., "Equivalent Viscous Damping for Yielding Structures", Journal of the Engineering Mechanics Division, ASCE, Vol. 94, No. EM1, February, 1968, pp. 103-116.
 11. Blume, J. A., Newmark, N. M., and Corning, L. H., Design of Multistory Reinforced Concrete Buildings for Earthquake Motions, Portland Cement Association, Chicago, 1961, pp. 73-86.
 12. Otani, S., "SAKE. A Computer Program for Inelastic Response of R/C Frames to Earthquakes", Structural Research Series No. 413, Civil Engineering Studies, University of Illinois, Urbana, Illinois, November, 1974.
 13. Otani, S. and Sozen, M. A., "Behaviour of Multistory Reinforced Concrete Frames during Earthquakes", Structural Research Series No. 392, Civil Engineering Studies, University of Illinois, Urbana, Illinois, November, 1972.
 14. Nigam, N. C. and Jennings, P. C., "Digital Calculation of Response Spectra from Strong Motion Earthquake Records", Earthquake Engineering Research Laboratory, California Institute of Technology, Pasadena, California, June, 1968.

Appendix A Modification of Damage Ratio - Strain Hardening Case

Consider the bilinear moment-rotation curve shown in

Fig. A.1.

Let k = initial stiffness,

s = ratio of stiffness after yield to initial stiffness,

μ_n = damage ratio used in n th iteration,

μ_{n+1} = damage ratio to be used in $n+1$ th iteration,

M_Y = yield moment,

M_n = computed moment in n th iteration,

ϕ_Y = yield rotation,

and ϕ_n = rotation corresponding to M_n on line OC.

M'_n and ϕ'_n are the moment and rotation at B, which is an intersection of lines OC and AC'.

Assume that the damage ratio, μ_n , used in the n th iteration was too small; point C is off the bilinear curve. Therefore, the damage ratio must be increased in the next iteration. It is assumed that the rotation, ϕ_n , is correct and that the slope of line OC' is used as the new stiffness. The new damage ratio, μ_{n+1} , is derived in a following manner.

$$\text{Slope of line OC':} \quad \frac{k}{\mu_{n+1}} = \frac{M_{n+1}}{\phi_n} \quad (\text{A.1})$$

$$\text{Slope of line OC:} \quad \frac{M_n}{\phi_n} = \mu_n \left(\frac{M_n}{k} \right) \quad (\text{A.2})$$

$$\text{From (A.2),} \quad \phi_n = \mu_n \left(\frac{M_n}{k} \right) \quad (\text{A.3})$$

Substitute equation (A.3) into (A.1).

$$\frac{k}{\mu_{n+1}} = \frac{M_{n+1}}{\mu_n \left(\frac{M_n}{k} \right)} = \frac{k}{\mu_n \left(\frac{M_{n+1}}{M_n} \right)}$$

$$\therefore \mu_{n+1} = \mu_n \left(\frac{M_n}{M_{n+1}} \right) \quad (\text{A.4})$$

Solve for M_{n+1} in terms of M_y and μ_n .

$$\begin{aligned} M_{n+1} &= M'_n + s \cdot k \cdot (\phi_n - \phi'_n) \\ &= M'_n + s \cdot k \cdot \left(\frac{M_n}{k/\mu_n} - \frac{M'_n}{k/\mu_n} \right) \\ &= M'_n + s M_n \mu_n - s M'_n \mu_n \\ \therefore M_{n+1} &= M'_n (1 - s \mu_n) + M'_n \cdot s \mu_n \end{aligned} \quad (\text{A.5})$$

Now solve for M'_n .

$$\begin{aligned} M'_n &= M_y + s \cdot k \cdot (\phi'_n - \phi_y) \\ &= M_y + s \cdot k \cdot \left(\frac{M'_n}{k/\mu_n} - \frac{M_y}{k} \right) \\ &= M_y (1 - s) + M'_n \cdot s \mu_n \end{aligned}$$

$$\therefore M'_n = M_Y \left(\frac{1 - s}{1 - s \mu_n} \right) \quad (\text{A.6})$$

Substitute equation (A.6) into (A.5)

$$M_{n+1} = M_Y \left(\frac{1 - s}{1 - s \mu_n} \right) (1 - s \mu_n) + s \mu_n M_n$$

$$\therefore M_{n+1} = M_Y (1 - s) + s \mu_n M_n \quad (\text{A.7})$$

Substitute equation (A.7) into (A.4).

$$\mu_{n+1} = \frac{\mu_n M_n}{M_Y (1 - s) + s \mu_n M_n} \quad (3.4)$$

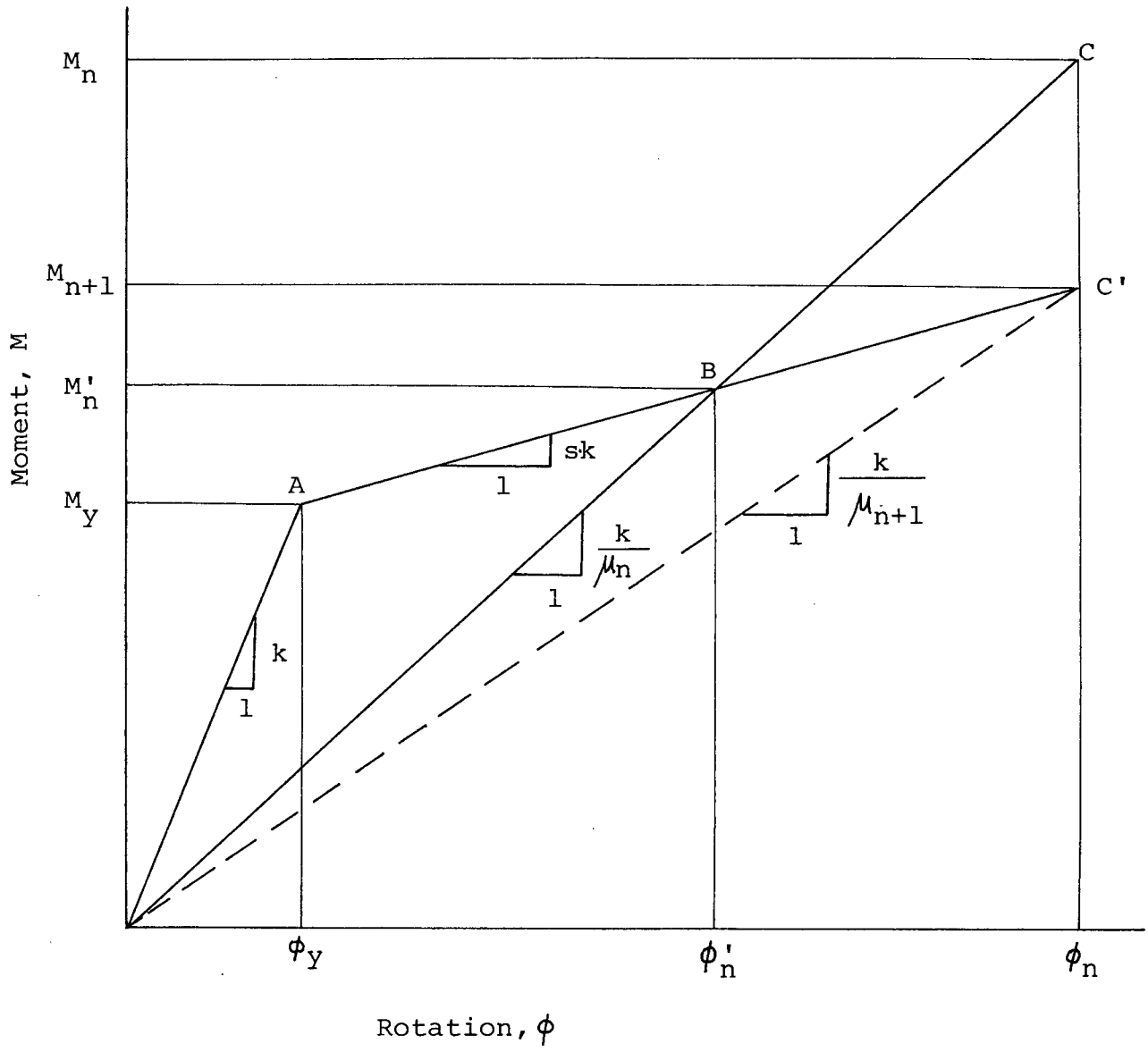


Fig. A.1 Moment-Rotation Curve

Appendix B Computer Program

The FORTRAN IV program for the modified substitute structure method is listed in the following in this appendix. The subroutine, MOD3, is written for an elasto-plastic case. Important variables are explained in each subroutine.

```

      DIMENSION KL(50),KG(50),AREA(50),CRMOM(50),BMCAP(100),
      1DAMRAT(50),ND(3,50),NP(6,50),XM(50),YM(50),DM(50),S(500)

```

```

      2F(100),TITLE(20),SDAMP(50),AV(50)
      DIMENSION I1(300)
      DIMENSION AMASS(50),EVAL(20),EVEC(50,20)

```

```

      C
      C
      C      SAMPLE MAIN PROGRAM

```

```

      IUNIT=7
      CALL CONTRL(TITLE,NRJ,NRM,E,G,7)
      CALL SETUP(NRJ,NRM,E,G,XM,YM,DM,ND,NP,AREA,CRMOM,DAMRAT,
      AV,KL,KG,
      1NU,NB,SDAMP,BMCAP,IUNIT,0)
      NMODES=10
      ICOUNT=0
      AMAX=.5
      IFLAG=0
      CALL MASS(NU,ND,AMASS,IUNIT,NRJ)
      IUNIT=6
      IMAX=200
      IM=IMAX-1
      I=0
      BETA=0.
      ERROR=1.E-3
      10 CONTINUE
      I=I+1
      CALL BUILD(NU,NB,XM,YM,DM,NP,AREA,CRMOM,AV,E,G,DAMRAT,KL
      ,KG,NRM,S,
      1500)
      CALL EIGEN(NU,NB,S,500,AMASS,EVAL,EVEC,NMODES,IUNIT)
      IF(I .GE. 10) BETA=.95
      CALL MOD3(ICOUNT,2,NRJ,NRM,NU,NB,NMODES,S,500,ND,NP,XM,Y
      M,DM,AREA,
      1CRMOM,DAMRAT,KL,KG,SDAMP,BMCAP,E,AMASS,EVEC,EVAL,AMAX,IS
      IGN,
      2IUNIT,BETA,ERROR,1)
      I1(I)=ISIGN
      WRITE(8,201) (DAMRAT(II),II=1,NRM)
      201 FORMAT(' ',15F8.3)
      IF(IFLAG.EQ.1 .AND. I.EQ.IMAX) GO TO 40
      IF(IFLAG.EQ.1) GO TO 20
      IF(I.EQ.1 .AND. ISIGN.EQ.0) GO TO 46
      IF(I.EQ.IM .OR. ISIGN.EQ.0) GO TO 35
      GO TO 10
      35 CONTINUE
      IFLAG=1
      IUNIT=7
      GO TO 10
      20 CONTINUE
      WRITE(IUNIT,30) I
      30 FORMAT(' ',5X,'NO. OF ITERATIONS = ',I5//)
      GO TO 50
      40 CONTINUE
      WRITE(IUNIT,45) I
      45 FORMAT(' ',5X,'DOES NOT CONVERGE AFTER ',I5,' ITERATION

```

S'///)

```

      GO TO 50
46  CONTINUE
      ICOUNT=0
      IFLAG=1
      IUNIT=7
      WRITE(IUNIT,48)
48  FORMAT('-',5X,'MEMBERS DO NOT YIELD '///)
      GO TO 10
50  CONTINUE
      WRITE(IUNIT,60) BETA,ERROR
60  FORMAT('-',5X,'BETA =',F5.3,///5X,'ERROR =',F8.6///)
      JJJ=I-1
      WRITE(7,200) (I1(IJ),IJ=1,JJJ)
200  FORMAT(' ',20I6)
      STOP
      END

```



```
SUBROUTINE CONTRL (TITLE, NRJ, NRM, E, G, IUNIT)
DIMENSION TITLE(20)
```

```
C
C
C
```

```
READ IN TITLE
```

```
READ (5,1) (TITLE(I), I=1,20)
```

```
C
C
C
C
C
C
C
```

```
READ IN NRJ, NRM, E, G
```

```
NRJ = NUMBER OF JOINTS
```

```
NRM = NUMBER OF MEMBERS
```

```
E = ELASTIC MODULUS IN KSI
```

```
G = SHEAR MODULUS IN KSI
```

```
READ (5,2) NRJ, NRM, E, G
```

```
WRITE (IUNIT,3) (TITLE(I), I=1,20)
```

```
WRITE (IUNIT,4) E, G
```

```
WRITE (IUNIT,5)
```

```
WRITE (IUNIT,6) NRJ, NRM
```

```
RETURN
```

```
1 FORMAT(20A4)
```

```
2 FORMAT(2I5,2F10.0)
```

```
3 FORMAT('1',20A4)
```

```
4 FORMAT('-',5X,'E =',F8.3,5X,'G =',F8.3)
```

```
5 FORMAT(///110('*'))
```

```
6 FORMAT('-', 'NO. OF JOINTS', ' = ', I5, 10X, 'NO. OF MEMBERS = ', I5)
```

```
END
```

SUBROUTINE SETUP (NRJ, NRM, E, G, XM, YM, DM, ND, NP, AREA, CRMOM, D
AMRAT, AV,

1 KL, KG, NU, NB, SDAMP, BMCAP, IUNIT, IFLAG)

C
C SET UP THE FRAME DATA FOR MODIFIED SUBSTITUTE
C STRUCTURE METHOD
C

DIMENSION KL (NRM), KG (NRM), AREA (NRM), CRMOM (NRM), SDAMP
(NRM),
1 DAMRAT (NRM), AV (NRM), ND (3, NRJ), NP (6, NRM), XM
(NRM),
2 YN (NRM), DM (NRM)
DIMENSION X (100), Y (100), JNL (100), JNG (100), BMCAP (NRM)

C
C JN = JOINT NUMBER
C ND (1, JN) = JOINT DEGREE OF FREEDOM IN X-DIRECTION
C ND (2, JN) = JOINT DEGREE OF FREEDOM IN Y-DIRECTION
C ND (3, JN) = JOINT DEGREE OF FREEDOM IN ROTATION
C X (JN) = X-COORDINATE OF JN IN FEET
C Y (JN) = Y-COORDINATE OF JN IN FEET
C MN = MEMBER NUMBER
C JNL (MN) = LESSER JOINT NUMBER
C JNG (MN) = GREATER JOINT NUMBER
C KL (MN) = MEMBER TYPE AT LESSER JOINT
C KG (MN) = MEMBER TYPE AT GREATER JOINT
C AREA (MN) = AREA IN IN**2
C CRMOM (MN) = MOMENT OF INERTIA IN IN**4
C DAMRAT (MN) = DAMAGE RATIO FOR MN
C AV (MN) = SHEAR AREA IN IN**2
C BMCAP (MN) = YIELD MOMENT IN K-FT
C
C XM (MN) = MEMBER LENGTH IN X-DIRECTION
C YM (MN) = MEMBER LENGTH IN Y-DIRECTION
C DM (MN) = MEMBER LENGTH
C SDAMP (MN) = SUBSTITUTE DAMPING RATIO FOR MN
C NP (I, MN) = MEMBER DEGREE OF FREEDOM
C NU = NUMBER OF UNKNOWNNS
C NB = HALF BANDWIDTH
C

WRITE (IUNIT, 1)
WRITE (IUNIT, 2)

C
C READ IN JOINT DATA AND COMPUTE NO. OF DEGREES OF FREEDOM
C
C NU=1

C
DO 50 I=1, NRJ
READ (5, 3) JN, ND (1, I), ND (2, I), ND (3, I), X (I), Y (I)

)
C
DO 40 K=1, 3
IF (ND (K, I) - 1) 30, 10, 20
10 ND (K, I) = NU
NU = NU + 1
GO TO 40
20 JNN = ND (K, I)

```

      ND(K,I)=ND(K,JNN)
      GO TO 40
30      CONTINUE
      ND(K,I)=0
40      CONTINUE

C
C      PRINT JOINT DATA
C
      WRITE (IUNIT,4) I, X(I), Y(I), ND(1,I), ND(2,I), ND
(3,I)
50      CONTINUE

C
      NU=NU-1
      WRITE (IUNIT,5)
      WRITE (IUNIT,6)
      WRITE (IUNIT,7)

C
C      READ IN MEMBER DATA AND COMPUTE THE HALF BANDWIDTH
C
      NB=0

C
      DO 180 I=1,NRM
        READ (5,8) MN, JNL(I), JNG(I), KL(I), KG(I), AREA(I
),
1          CRMOM(I), DAMRAT(I), AV(I), BMCAP(I)
        IF(IFLAG.NE.1) GO TO 70
        IF(DAMRAT(I).NE.0.) GO TO 60
        DAMRAT(I)=1.
60      GO TO 80
70      DAMRAT(I)=1.
80      CONTINUE
        JL=JNL(I)
        JG=JNG(I)
        XM(I)=X(JG)-X(JL)
        YM(I)=Y(JG)-Y(JL)
        DM(I)=SQRT((XM(I))**2+(YM(I))**2)
        DAMAGE=DAMRAT(I)
        ROOT=SQRT(DAMAGE)
        SDAMP(I)=0.02+0.2*(1.-1./ROOT)
        NP(1,I)=ND(1,JL)
        NP(2,I)=ND(2,JL)
        NP(3,I)=ND(3,JL)
        NP(4,I)=ND(1,JG)
        NP(5,I)=ND(2,JG)
        NP(6,I)=ND(3,JG)
        MAX=0

C
        DO 110 K=1,6
          IF(NP(K,I)-MAX) 100,100,90
90          MAX=NP(K,I)
100         CONTINUE
110        CONTINUE

C
        MIN=1000

C
        DO 150 K=1,6

```

```

      IF (NP(K,I)) 140,140,120
120      IF (NP(K,I)-MIN) 130,140,140
130      MIN=NP(K,I)
140      CONTINUE
150      CONTINUE
C
      NBB=MAX-MIN+1
      IF (NBB-NB) 170,170,160
160      NB=NBB
170      CONTINUE
C
C      PRINT MEMBER DATA
C
      WRITE (IUNIT,9) I, JNL(I), JNG(I), DM(I), XM(I), YM
(I),
      1      NP(1,I), NP(2,I), NP(3,I), NP(4,I), NP(5,I),
NP(6,I),
      2      AREA(I), CRMON(I), DAMRAT(I), AV(I), BMCAP(I)
, KL(I),
      3      KG(I)
C      CHANGE THE LENGTHS FROM FEET TO INCHES
      XM(I)=XM(I)*12.
      YM(I)=YM(I)*12.
      DM(I)=DM(I)*12.
180 CONTINUE
C
C      PRINT THE NO. OF DEGREES OF FREEDOM AND THE HALF BANDWID
TH
C
      WRITE (IUNIT,11) NU
      WRITE (IUNIT,12) NB
      RETURN
      1 FORMAT('-.','JOINT DATA')
      2 FORMAT('0',7X,'JN',3X,'X(FEET)',3X,'Y(FEET)',4X,'NDX',2X
,'NDY',
      1      2X,'NDR')
      3 FORMAT(4I5,2F10.5)
      4 FORMAT(' ',5X,I4,2F10.3,2X,3I5)
      5 FORMAT('-.','MEMBER DATA')
      6 FORMAT('0',7X,'MN JNL JNG LENGTH XM(FT) YM(FT) NP1 NP
2 NP3 NP4
      1NP5 NP6 AREA I(CRACKED) DAMAGE AV',4X,'MOMENT ',
      2      4X,'KL',3X,'KG')
      7 FORMAT(' ',19X,'(FEET)',41X,'(SQ.IN)',2X,'(IN**4)',6X,'R
ATIO',
      1      2X,'(SQ.IN)', 'CAPACITY')
      8 FORMAT(5I5,5F10.5)
      9 FORMAT(' ',5X,3I4,3F8.2,6I4,F8.1,F12.1,2F8.3,F10.2,2I5)
11 FORMAT('-.','NO.OF DEGREES OF FREEDOM OF STRUCTURE =',I5)
12 FORMAT('0','HALF BANDWIDTH OF STIFFNESS MATRIX =',I5)
      END

```

SUBROUTINE MASS (NU,ND,AMASS,IUNIT,NRJ)

THIS SUBROUTINE SETS UP THE MASS MATRIX

ND(J,I)=DEGREES OF FREEDOM OF I TH JOINT

WTX,WTY,WTR=X-MASS,Y-MASS,ROT.MASS IN FORCE UNITS (KIPS OR IN-KIPS)

AMASS(I)=MASS MATRIX

NMASS=NO.OF MASS POINTS

MASSSES ARE LUMPED AT NODES. THE MASS MATRIX IS DIAGONALIZED.

DIMENSION ND(3,NRJ), AMASS(NU)

READ IN NO. OF NODES WITH MASS

READ (5,1) NMASS

WRITE (IUNIT,2)

WRITE (IUNIT,3) NMASS

WRITE (IUNIT,4)

WRITE (IUNIT,5)

ZERO MASS MATRIX

DO 10 I=1,NU

AMASS(I)=0.

10 CONTINUE

READ IN X-MASS,Y-MASS AND ROT. MASS (IN UNITS OF WEIGHT

DO 50 I=1,NMASS

READ (5,6) JN, WTX, WTY, WTR

WRITE (IUNIT,7) JN, WTX, WTY, WTR

N1=ND(1,JN)

N2=ND(2,JN)

N3=ND(3,JN)

IF(N1.EQ.0) GO TO 20

AMASS(N1)=AMASS(N1)+(WTX/386.4)

20 IF(N2.EQ.0) GO TO 30

AMASS(N2)=AMASS(N2)+(WTY/386.4)

30 IF(N3.EQ.0) GO TO 40

AMASS(N3)=AMASS(N3)+(WTR/386.4)

40 CONTINUE

50 CONTINUE

RETURN

1 FORMAT(I5)

2 FORMAT(///110('*'))

3 FORMAT(' ','NO. OF NODES WITH MASS', ' ',I5)

4 FORMAT('0',7X,'JN',3X,'X-MASS',4X,'Y-MASS',2X,'ROT.MASS'

5 FORMAT(' ',12X,' (KIPS) ',4X,' (KIPS) ',2X,' (IN-KIPS) ')

6 FORMAT(I5,3F10.0)

7 FORMAT(' ',5X,I4,3F10.3)

END

```

SUBROUTINE BUILD (NU, NB, XM, YM, DM, NP, AREA, CRMOM, AV, E, G, DAM
RAT,
1      KL, KG, NRM, S, IDIM)
C
C      THIS SUBROUTINE CALCULATES THE STIFFNESS MATRIX OF EACH
C      MEMBER AND ADDS IT INTO THE STRUCTURE STIFFNESS MATRIX.
C      FLEXURAL STIFFNESSES OF MEMBERS ARE MODIFIED
C      ACCORDING TO THE DAMAGE RATIOS.
C      THE FINAL STIFFNESS MATRIX S IS RETURNED.
C
C      DAMRAT (I) = DAMAGE RATIO FOR I TH MEMBER
C      S (I)      = STRUCTURE STIFFNESS MATRIX
C      SM (I)     = MEMBER STIFFNESS MATRIX
C
C      DIMENSION XM (NRM), YM (NRM), DM (NRM), NP (6, NRM), AREA (NRM
),
1      CRMOM (NRM), AV (NRM), DAMRAT (NRM), KL (NRM), KG (
NRM)
C      DIMENSION S (IDIM), SM (21)
C
C      ZERO STRUCTURE STIFFNESS MATRIX
C
C      DO 10 I=1, IDIM
C          S (I) = 0.
10  CONTINUE
C
C      BEGIN MEMBER LOOP
C
C      DO 200 I=1, NRM
C
C      ZERO MEMBER STIFFNESS NATRIX
C
C          DO 20 J=1, 21
C              SM (J) = 0.
20  CONTINUE
C
C          DM2=DM (I) *DM (I)
C          XM2=XM (I) *XM (I)
C          YM2=YM (I) *YM (I)
C          XMYM=XM (I) *YM (I)
C          F=AREA (I) *E / (DM (I) *DM2)
C          H=0.
C          IF (AV (I) .EQ. 0. .OR. G .EQ. 0.) GO TO 30
C          H=12. *E*CRMOM (I) / (AV (I) *G*DM2)
30  XM2F=XM2*F
C          YM2F=YM2*F
C          XMYMF=XMYM*F
C
C      FILL IN PIN-PIN SECTION OF MEMBER STIFFNESS MATRIX
C
C          SM (1)=XM2F
C          SM (2)=XMYMF
C          SM (4)=-XM2F
C          SM (5)=-XMYMF
C          SM (7)=YM2F
C          SM (9)=-XMYMF

```

```

SM(10)=-YM2F
SM(16)=XM2F
SM(17)=XMYMF
SM(19)=YM2F
IF(KL(I)+KG(I)-1) 100,40,50
40  F=3.*E*CRNOM(I)/(DM2*DM2*DM(I)*(1.+H/4.))/DAMRAT(I)
GO TO 60
50  F=12.*E*CRNOM(I)/(DM2*DM2*DM(I)*(1.+H))/DAMRAT(I)

C
C  FILL IN TERMS WHICH ARE COMMON TO PIN-FIX, FIX-PIN, AND
C  FIX-FIX MEMBERS
C
60  XM2F=XM2*F
    YM2F=YM2*F
    XMYMF=XMYM*F
    DM2F=DM2*F
    SM(1)=SM(1)+YM2F
    SM(2)=SM(2)-XMYMF
    SM(4)=SM(4)-YM2F
    SM(5)=SM(5)+XMYMF
    SM(7)=SM(7)+XM2F
    SM(9)=SM(9)+XMYMF
    SM(10)=SM(10)-XM2F
    SM(16)=SM(16)+YM2F
    SM(17)=SM(17)-XMYMF
    SM(19)=SM(19)+XM2F
    IF(KL(I)-KG(I)) 70,80,90

C
C  FILL IN REMAINING PIN-FIX TERMS
C
70  SM(6)=-YM(I)*DM2F
    SM(11)=XM(I)*DM2F
    SM(18)=-SM(6)
    SM(20)=-SM(11)
    SM(21)=DM2*DM2F
    GO TO 100

C
C  FILL IN REMAINING FIX-FIX TERMS
C
80  SM(3)=-YM(I)*DM2F*.5
    SM(6)=SM(3)
    SM(8)=XM(I)*DM2F*.5
    SM(11)=SM(8)
    SM(12)=DM2*DM2F*(4.+H)/12.
    SM(13)=-SM(3)
    SM(14)=-SM(8)
    SM(15)=DM2*DM2F*(2.-H)/12.
    SM(18)=-SM(3)
    SM(20)=-SM(8)
    SM(21)=SM(12)
    GO TO 100

C
C  FILL IN REMAINING FIX-PIN TERMS
C
90  SM(3)=-YM(I)*DM2F
    SM(8)=XM(I)*DM2F

```



```

      SM(12)=DM2*DM2F
      SM(13)=-SM(3)
      SM(14)=-SM(8)
100    CONTINUE
C
C      ADD THE MEMBER STIFFNESS MATRIX SM INTO THE STRUCTURE
C      STIFFNESS MATRIX S.
C
      NB1=NB-1
C
      DO 190 J=1,6
        IF (NP(J,I)) 190,190,110
110      J1=(J-1)*(12-J)/2
C
        DO 180 L=J,6
          IF (NP(L,I)) 180,180,120
120          IF (NP(J,I)-NP(L,I)) 150,130,160
130          IF (L-J) 140,150,140
140          K=(NP(L,I)-1)*NB1+NP(J,I)
            N=J1+L
            S(K)=S(K)+2.*SM(N)
            GO TO 180
150          K=(NP(J,I)-1)*NB1+NP(L,I)
            GO TO 170
160          K=(NP(L,I)-1)*NB1+NP(J,I)
170          N=J1+L
            S(K)=S(K)+SM(N)
180        CONTINUE
C
190      CONTINUE
C
200 CONTINUE
C
      RETURN
      END

```

```

SUBROUTINE EIGEN (NU, NB, S, IDIM, AMASS, EVAL, EVEC, NMODES, IUN
IT)
C
C THIS SUBROUTINE COMPUTES A SPECIFIED NO. OF NATURAL FREQ
UENCIES
C AND ASSOCIATED MODE SHAPES
C
C NU=NO. OF DEGREES OF FREEDOM
C NB=HALF BANDWIDTH
C NMODES=NO. OF MODE SHAPES TO BE COMPUTED
C AMASS(I)=MASS MATRIX M=RANK OF MASS MATRIX
C S(I)=STIFFNESS MATRIX STORED BY COLUMNS
C EVAL(I)=NATURAL FREQUENCIES
C EVEC(I,J)=MODE SHAPES
C
C DIMENSION S(IDIM), AMASS(NU), EVAL(NMODES), EVEC(50,20),
1 SCR(900)
C DIMENSION CMASS(100), SS(500)
C
C COMPUTE THE RANK OF MASS MATRIX
C
C M=0
C
C DO 10 I=1, NU
C CMASS(I)=AMASS(I)
C IF (AMASS(I).EQ.0.) GO TO 10
C M=M+1
10 CONTINUE
C
C IF (NMODES.GT.M) NMODES=M
C IF (NMODES.EQ.0) NMODES=M
C WRITE (IUNIT,1) NMODES
C
C CALL RVPOW TO COMPUTE EIGENVALUES AND EIGENVECTORS
C
C DO 20 I=1, 500
C SS(I)=S(I)
20 CONTINUE
C
C EPS=0.
C EPSV=0.
C CALL RVPOWR(SS, CMASS, NU, NB, EVEC, 50, EVAL, NMODES, EPS, EPSV,
100, 1, SCR, M)
C
C PRINT EIGENVALUES AND EIGENVECTORS (MODE SHAPES)
C
C WRITE (IUNIT,2)
C WRITE (IUNIT,3)
C WRITE (IUNIT,4)
C
C DO 30 I=1, NMODES
C EVAL1=EVAL(I)
C EVAL(I)=SQRT(EVAL1)
C FREQ=EVAL(I)/6.283185308
C PERIOD=6.283185308/EVAL(I)

```

```

      WRITE (IUNIT,5) I, EVAL1, EVAL(I), FREQ, PERIOD
30 CONTINUE
C
      WRITE (IUNIT,6) NMODES
      WRITE (IUNIT,7) (I,I=1,NMODES)
C
      DO 40 I=1,M
        WRITE (IUNIT,8) (EVEC (I,J) ,J=1,NMODES)
40 CONTINUE
C
      RETURN
1 FORMAT('-', 'NO. OF MODES TO BE ANALYZED =', I5///110('*')
///)
2 FORMAT(///110('*'))
3 FORMAT('0',5X,'MODES',4X,'EIGENVALUES',6X,'NATURAL FREQU
ENCIES',
1      13X,'PERIODS')
4 FORMAT(' ',30X,' (RAD/SEC)',5X,' (CYCS/SEC)',8X,' (SECS)')
5 FORMAT(' ',5X,I5,4F15.4)
6 FORMAT('0',5X,'MODE SHAPES CORRESPONDING TO FIRST',I5,'
FREQUENCIE
1S')
7 FORMAT('0',10I12)
8 FORMAT(' ',10F12.6)
      END

```

```

      SUBROUTINE MOD3(ICOUNT,ISPEC,NRJ,NRM,NU,NB,NMODES,S,IDIM
,ND,NP,XM,
      1          YN,DM,AREA,CRMOM,DAMRAT,KL,KG,SDAMP,BMCAP,E,A
MASS,EVEC,
      2          EVAL,AMAX,ISIGN,IUNIT,BETA,ERROR,IBASE)
C
C      MODIFIED SUBSTITUTE STRUCTURE METHOD
C      THIS SUBROUTINE COMPUTES JOINT DISPLACEMENTS AND MEMBER
FORCES
C      NEW DAMAGE RATIOS WILL BE CALCULATED AND RETURNED.
C
C      ICOUNT = 0 IF DAMPING IS SET AT 10% AND ELASTIC
              ANALYSIS IS TO BE CARRIED OUT
C      ISPEC = 1 FOR SPECTRUM A, 2 FOR B, AND 3 FOR C
C      IDIM = DIMENSION OF S(I)
C      ISIGN = NUMBER OF MEMBERS FOR WHICH DAMAGE RATIOS
              ARE MODIFIED
C      IUNIT = OUTPUT DEVICE UNIT
C      BETA = CONSTANT FOR ACCELERATED CONVERGENCE
C      ERROR = CONSTANT FOR CONVERGENCE CRITERION
C      IBASE = 1 IF BASE SHEAR IS TO BE PRINTED
C
C      DIMENSION ND(3,NRJ), NP(6,NRM), XM(NRM), YN(NRM), DM(NRM
),
      1          AREA(NRM), CRMOM(NRM), DAMRAT(NRM), KL(NRM), K
G(NRM),
      2          AMASS(NRM), EVEC(50,20), EVAL(NMODES), S(IDIM)
,
      3          SDAMP(NRM), ZETA(10), PI(100)
      DIMENSION BMASS(40), IDOF(100), ALPHA(20), RMS(7,100),
      1          F(100), D(6)
      DIMENSION BMCAP(1)
C
C      CALCULATE THE MODAL PARTICIPATION FACTOR
C
      JJ=1
C
      DO 10 I=1,NU
          IF(AMASS(I).EQ.0.) GO TO 10
          BMASS(JJ)=AMASS(I)
          IDOF(JJ)=I
          JJ=JJ+1
      10 CONTINUE
C
      JJ=JJ-1
C
      DO 30 I=1,NMODES
          AMT=0.
          AMB=0.
          ALPHA(I)=0.
C
          DO 20 J=1,JJ
              AMT=AMT+BMASS(I)*EVEC(J,I)
              AMB=AMB+BMASS(I)*EVEC(J,I)**2
      20 CONTINUE

```

```

C      ALPHA(I)=AMT/AMB
30 CONTINUE
C      WRITE (IUNIT,1)
C      DO 40 I=1,NMODES
        WRITE (IUNIT,2) I, ALPHA(I)
40 CONTINUE
C
C      WHEN KK=1, MODAL FORCES FOR UNDAMPED SUBSTITUTE STRUCTUR
E ARE
C      COMPUTED. THEY ARE USED TO COMPUTE 'SMEARED' DAMPING VA
LUES,
C      WHICH ARE USED TO CALCULATE THE ACTUAL RESPONSE OF THE S
UBSTITUTE
C      STRUCTURE
C      INDEX=1
C
C      DO 420 KK=1,2
        IF(ICOUNT-1) 400,70,50
50      CONTINUE
        IF(KK.NE.1) GO TO 70
C
        DO 60 K=1,NMODES
          ZETA(K)=0.
60      CONTINUE
C
70      CONTINUE
        SHRMS=0.
C
C      ZERO ABSO(J,I) AND RMS(J,I)
C
        DO 90 I=1,100
C
          DO 80 J=1,7
            RMS(J,I)=0.
80      CONTINUE
C
90      CONTINUE
C
C      CALCULATE THE MODAL DISPLACEMENT VECTOR
C
        DO 290 K=1,NMODES
C
C      CALCULATE NATURAL PERIOD AND CALL SPECTA
C
        WN=6.283185308/EVAL(K)
        DAMP=ZETA(K)
        CALL SPECTR(ISPEC,DAMP,WN,AMAX,SA)
C
C      ZERO LOAD VECTOR
C
        DO 100 J=1,NU
          F(J)=0.

```

```

100      CONTINUE
C
      FF=0.
C
C      COMPUTE LOAD VECTOR
C
      FAC=SA*ALPHA (K) *386.4
C
      DO 110 J=1,JJ
        I1=IDOF (J)
        F (I1)=EVEC (J,K) *FAC*AMASS (I1)
        FF=FF+F (I1)
110      CONTINUE
C
C      CALCULATE THE BASE SHEAR
C
      IF (KK.NE.2) GO TO 120
      SHRMS=SHRMS+FF**2
      IF (K.LT.NMODES) GO TO 120
      SHRMS=SQRT (SHRMS)
120      CONTINUE
C
C      COMPUTE DEFLECTIONS
C
C      CALL SUBROUTINE FBAND
C
      RATIO=1.E-7
      CALL FBAND (S,F,NU,NB,INDEX,RATIO,DET,JEXP,0,0,0.)
      INDEX=INDEX+1
C
      DO 160 I=1,NRJ
        DX=0.
        DY=0.
        DR=0.
        N1=ND (1,I)
        N2=ND (2,I)
        N3=ND (3,I)
        IF (N1.EQ.0) GO TO 130
        DX=F (N1)
        RMS (1,I)=RMS (1,I) +DX**2
130      CONTINUE
        IF (N2.EQ.0) GO TO 140
        DY=F (N2)
        RMS (2,I)=RMS (2,I) +DY**2
140      CONTINUE
        IF (N3.EQ.0) GO TO 150
        DR=F (N3)
        RMS (3,I)=RMS (3,I) +DR**2
150      CONTINUE
160      CONTINUE
C
C      COMPUTE MEMBER FORCES
C
      SIGPI=0.
C

```

```

DO 260 I=1,NRM
C
      DO 200 J=1,6
        N1=NP(J,I)
        IF(N1) 180,180,170
170      D(J)=F(N1)
        GO TO 190
180      D(J)=0.
190      CONTINUE
200      CONTINUE
C
      XL=XM(I)
      YL=YM(I)
      DL=DM(I)
      AXIAL=(AREA(I)*E/DL**2)*(D(4)*XL+D(5)*YL-D(1)*X
L-D(2)*YL)
      IF(KL(I).EQ.0 .AND. KG(I).EQ.0) GO TO 230
      DV=(D(2)*XL-D(1)*YL+D(4)*YL-D(5)*XL)/DL
      AK=CRMOM(I)*E/DL/DAMRAT(I)
      BML=-AK*(6.*DV/DL+4.*D(3)+2.*D(6))/12.
      SHEAR=AK*6.*(2.*DV/DL+D(3)+D(6))/DL
      BMG=BML+SHEAR*DL/12.
      IF(KL(I)-KG(I)) 210,240,220
210      BMG=BMG+BML*.5
      SHEAR=SHEAR+1.5*BML/(DL/12.)
      BML=0.
      GO TO 240
220      BML=BML+BMG*.5
      SHEAR=SHEAR-1.5*BMG/(DL/12.)
      BMG=0.
      GO TO 240
230      BMG=0.
      BML=0.
      SHEAR=0.
240      CONTINUE
C
C      COMPUTE THE RELATIVE FLEXURAL STRAIN ENERGY
C
      IF(KK.NE.1) GO TO 250
      PI(I)=(BML**2+BMG**2+BML*BMG)/6./AK
      SIGPI=SIGPI+PI(I)
250      CONTINUE
C
C      ACCUMULATE ABSOLUTE SUM AND RMS SUM
C
      RMS(4,I)=RMS(4,I)+AXIAL**2
      RMS(5,I)=RMS(5,I)+SHEAR**2
      RMS(6,I)=RMS(6,I)+BML**2
      RMS(7,I)=RMS(7,I)+BMG**2
260      CONTINUE
C
C      COMPUTE THE SHEARED DAMPING FOR EACH MODE
C
      IF(KK.NE.1) GO TO 280
C
      DO 270 I=1,NRM

```

```

      ZETA(K)=ZETA(K)+PI(I)*SDAMP(I)
270  CONTINUE
C
      ZETA(K)=ZETA(K)/SIGPI
280  CONTINUE
290  CONTINUE
C
      IF(KK.EQ.1) GO TO 420
C
C  PRINT RMS DISPLACEMENTS AND FORCES
C
      WRITE (IUNIT,4)
      WRITE (IUNIT,5)
      WRITE (IUNIT,3)
C
      DO 310 I=1,NRJ
C
          DO 300 J=1,3
              SCRAT=RMS(J,I)
              RMS(J,I)=SQRT(SCRAT)
300  CONTINUE
C
          WRITE (IUNIT,6) I, (RMS(J,I),J=1,3)
310  CONTINUE
C
C  MODIFY DAMAGE RATIOS
C
      WRITE (IUNIT,7)
      IF(IBASE.NE.1) GO TO 320
      WRITE (IUNIT,8) SHRMS
320  CONTINUE
      WRITE (IUNIT,9)
      ISIGN=0
C
      DO 390 I=1,NRM
          IF(RMS(6,I)-RMS(7,I)) 330,330,340
330  BIG=RMS(7,I)
          GO TO 350
340  BIG=RMS(6,I)
350  CONTINUE
          BM=SQRT(BIG)
          DAMOLD=DAMRAT(I)
          DAMRAT(I)=BM/BMCAP(I)*DAMRAT(I)
          DAMRAT(I)=DAMRAT(I)+BETA*(DAMRAT(I)-DAMOLD)
          IF(DAMRAT(I).LT.1.0) GO TO 360
          CHECK=ABS(BM-BMCAP(I))/BMCAP(I)
          IF(CHECK.GT.ERROR) ISIGN=ISIGN+1
          GO TO 370
360  CONTINUE
          DAMRAT(I)=1.
370  CONTINUE
          SDAMP(I)=0.02+0.2*(1.-1./SQRT(DAMRAT(I)))
C
          DO 380 J=4,7
              RMS(J,I)=SQRT(RMS(J,I))
380  CONTINUE

```



```

C
      WRITE (IUNIT,11) I, (RMS(J,I),J=4,7), BNCAP(I), D
AMRAT(I)
390      CONTINUE
C
      GO TO 420
400      CONTINUE
C
      DO 410 I=1,NMODES
      ZETA(I) = .1
410      CONTINUE
C
      ICOUNT=ICOUNT+1
      WRITE (IUNIT,12)
420 CONTINUE
C
      ICOUNT=ICOUNT+1
      RETURN
1  FORMAT('-', 'MODAL PARTICIPATION FACTOR', '/')
2  FORMAT(' ', 5X, 'MODE', I5, 5X, F10.5)
3  FORMAT('-', 7X, 'JOINT NO.', 10X, 'X-DISP(IN)', 10X, 'Y-DISP(I
N)', 7X,
1      'ROTATION (RAD)')
4  FORMAT('-', 110(' '))
5  FORMAT('-', 'ROOT MEAN SQUARE DISPLACEMENTS')
6  FORMAT(' ', 6X, I10, 3F20.4)
7  FORMAT('-', 'ROOT MEAN SQUARE FORCES')
8  FORMAT(1H0, 7X, 'RSS BASE SHEAR =', F10.3)
9  FORMAT('-', 8X, 'MN', 10X, 'AXIAL', 10X, 'SHEAR', 11X, 'BML', 12X
, 'BMG',
1      9X, 'MOMENT', 10X, 'DAMAGE'/21X, 'KIPS', 12X, 'KIPS', 2(
9X, ' (K-FT)
2'), 8X, 'CAPACITY', 9X, 'RATIO')
11 FORMAT(' ', 5X, I5, 6F15.3)
12 FORMAT('-', 110(' '))
      END

```

SUBROUTINE SPECTR (ISPEC,DAMP,WN,AMAX,SA)

```

C
C   ISPEC=1 IF SPECTRUM A IS USED
C       =2 IF SPECTRUM B IS USED
C       =3 IF SPECTRUM C IS USED
C   DAMP=DAMPING FACTOR (FRACTION OF CRITICAL DAMPING)
C   WN  =NATURAL PERIOD IN SECONDS
C   AMAX=MAXIMUM GROUND ACCELERATION (FRACTION OF G)
C   SA  =RESPONSE ACCELERATION (FRACTION OF G)
C
C   IF (ISPEC.EQ.2) GO TO 10
C   IF (ISPEC.EQ.3) GO TO 60
C
C   SPECTRUM A
C
C   IF (WN.LT.0.15) SA=25.*AMAX*WN
C   IF (WN.GE.0.15 .AND. WN.LT.0.4) SA=3.75*AMAX
C   IF (WN.GT.0.4) SA=1.5*AMAX/WN
C   GO TO 90
C
C   SPECTRUM B
C
10  CONTINUE
C   IF (WN.LT.0.1875) GO TO 20
C   IF (WN.LT.0.53333333) GO TO 30
C   IF (WN.LT.1.6666667) GO TO 40
C   IF (WN.LT.1.8166667) GO TO 50
C   SA=2.*AMAX/(WN-0.75)
C   GO TO 90
C   20 SA=20.*AMAX*WN
C   GO TO 90
C   30 SA=3.75*AMAX
C   GO TO 90
C   40 SA=2.*AMAX/WN
C   GO TO 90
C   50 SA=1.875*AMAX
C   GO TO 90
C
C   SPECTRUM C
C
60  CONTINUE
C   IF (WN.LT.0.15) GO TO 70
C   IF (WN.LT.0.38333333) GO TO 80
C   SA=0.5*AMAX/(WN-0.25)
C   GO TO 90
C   70 SA=25.*AMAX*WN
C   GO TO 90
C   80 SA=3.75*AMAX
C   90 CONTINUE
C   SA=SA*8./(6.+100.*DAMP)
C   RETURN
C   END

```